Mathematical modeling of vector-borne diseases with an additional host-to-host transmission

Arsha Sherly

Vom Fachbereich Mathematik der Rheinland-Pfälzischen
Technischen Universität Kaiserslautern-Landau
zur Verleihung des akademischen Grades
Doktor der Naturwissenschaften (Doctor rerum naturalium,
Dr. rer. nat.) genehmigte Dissertation

Gutachter:
Prof. Dr. Axel Klar, RPTU Kaiserslautern-Landau
Prof. Dr. Thomas Goetz, Universität Koblenz.Landau

Datum der Disputation 20 März 2023
DE-386

Declaration

I hereby declare that except where specific reference is made to the work of others, the contents of this dissertation are original and have not been submitted in whole or in part for consideration for any other degree or qualification in this, or any other university. This dissertation is my own work and contains nothing which is the outcome of work done in collaboration with others, except as specified in the text and Acknowledgements. Parts of this work have been submitted to and published in peer-reviewed journals, appropriately noted in the corresponding chapters. A detailed list of these publications can be found on the next page.

Arsha Sherly
20 März 2023

Journal articles

The following articles, which were published in peer-reviewed journals, were used in this thesis:

[46] A. SHERLY **and** W. BOCK. *Multipatch ZIKV Model and Simulations*. **in**: *Mathematics in Industry*. Springer International Publishing, 2022. 433–438 DOI: 10.1007/978-3-031-11818-0_56

Acknowledgements

I would like to extend my sincere gratitude towards Prof. Dr. Axel Klar, the Graduate School of Mathematics at TU Kaiserslautern, and DAAD Germany for their collective decision to offer me this opportunity to be a beneficiary of the program named Mathematics in Industry and Commerce(MIC). During this program I was funded with the DAAD post doctorate scholarship to complete my Ph.D in the Department of Mathematics, TU Kaiserslautern. Firstly, I extend my thanks to Prof. Dr. Axel Klar for offering me the opportunity to be a Ph.D student under him. For all the help and guidance during these years, I would specially thank Dr. Wolfgang Bock along with Prof. Dr. Axel Klar. During the tough times of my Ph.D, especially towards the last year, the helpful and understanding nature of Prof. Dr. Axel Klar and Dr. Wolfgang Bock has helped me a lot. At this point, I would extend my gratitude to Prof. Dr. Thomas Goetz for his initiative to be my second reviewer. Next, I would like to thank the graduate school of Mathematics, TU Kaiserslautern, especially Dr. Falk Triebsch who had been motivating and helpful through out my studies in TU Kaiserslautern. At the same time, I cannot forget Ms. Jessica Borsche and Ms. Claudia Korb for the help and support they offered during my Ph.D. I would like to gratefully acknowledge DAAD for the financial help they have granted and specially Ms. Parisa Asemi-Rauber, my contact person from DAAD, for all her help. I am sincerely grateful to the department of mathematics, TU Kaiserslautern for offering the Ph.D. scholarship to finish the thesis. I whole-heartedly extend my thanks to Dr. Satyananda Panda, my Professor in NIT Calicut for being the light and driving force of my academic journey in Germany. I would also like to thank Dr. Sudarsan Tiwari, for his support and advises which helped me in many ways. Outside the academic world there were many people who have supported me in a lot of ways. Firstly, I would like to thank my family, Mrs. Sherly and Mr. Ramesan who stood like my pillar of strength through out the walk of my life. I am indebted to all the good deeds that they have ever done for me, which directed me until now. On this regard, I would like to thank Ashfaq, my better half, for being a constant support and standing by me through out this journey. My dearest friends whom I met in Germany, who were more like family to me also helped me to survive the hard times. Considering the direct contribution of some people in the successful completion of my thesis I would like to specially mention my gratitude towards Deepthy Maria, Bichu Bhaskar, Aiswarya Nair, Jithmi Jannidi and Parveena Shamim. All of them have helped me in one way or the other, from motivating me to strive through some tough phases to proof-reading the thesis and their help had a profound impact on my Ph.D journey. I would also like to thank my friends and relatives who were away from me, in different parts of the world, who extended their support in all ways possible.

Abstract

Mechanistic disease spread models for different vector borne diseases have been studied from the 19th century. The relevance of mathematical modeling and numerical simulation of disease spread is increasing nowadays. This thesis focuses on the compartmental models of the vector-borne diseases that are also transmitted directly among humans. An example of such an arboviral disease that falls under this category is the Zika Virus disease. The study begins with a compartmental *SIRUV* model and its mathematical analysis. The non-trivial relationship between the basic reproduction number obtained through two methods have been discussed. The analytical results that are mathematically proven for this model are numerically verified. Another *SIRUV* model is presented by considering a different formulation of the model parameters and the newly obtained model is shown to be clearly incorporating the dependence on the ratio of mosquito population size to human population size in the disease spread. In order to incorporate the spatial as well as temporal dynamics of the disease spread, a meta-population model based on the *SIRUV* model was developed. The space domain under consideration are divided into patches which may denote mutually exclusive spatial entities like administrative areas, districts, provinces, cities, states or even countries. The research focused only on the short term movements or commuting behavior of humans across the patches. This is incorportated in the multi-patch meta-population model using a matrix of residence time fractions of humans in each patches. Mathematically simplified analytical results are deduced by which it is shown that, for an exemplary scenario that is numerically studied, the multi-patch model also admits the threshold properties that the single patch *SIRUV* model holds. The relevance of commuting behavior of humans in the disease spread has been presented using the numerical results from this model. The local and non-local commuting are incorporated into the meta-population model in a numerical example. Later, a PDE model is developed from the multi-patch model.

Abstrakt

Mechanistische Ausbreitungsmodelle für verschiedene vektorübertragene Krankheiten werden seit dem 19. Jahrhundert untersucht. Die Bedeutung der mathematischen Modellierung und numerischen Simulation der Krankheitsausbreitung nimmt heutzutage zu. Diese Arbeit konzentriert sich auf die Kompartimentmodelle für vektorübertragene Krankheiten, die auch direkt auf den Menschen übertragen werden. Ein Beispiel für eine solche arbovirale Krankheit ist das Zika-Virus. Die Studie beginnt mit einem kompartimentellen *SIRUV*-Modell und seiner mathematischen Analyse. Die nicht-triviale Beziehung Reproduktionszahl zur Ausbreitung, die mit zwei Methoden ermittelt wurde, wird diskutiert. Die analytischen Ergebnisse, die für dieses Modell mathematisch bewiesen sind, werden numerisch verifiziert. Ein weiteres *SIRUV*-Modell wird unter Berücksichtigung einer anderen Formulierung der Modellparameter vorgestellt, und es wird gezeigt, dass das neu gewonnene Modell die Abhängigkeit vom Verhältnis zwischen der Größe der Mückenpopulation und der Größe der menschlichen Bevölkerung bei der Krankheitsausbreitung deutlich berücksichtigt. Um sowohl die räumliche als auch die zeitliche Dynamik der Krankheitsausbreitung zu berücksichtigen, wurde ein Meta-Populationsmodell auf der Grundlage des *SIRUV*-Modells entwickelt. Das betrachtete Gebiet ist in Patches unterteilt, die sich gegenseitig ausschließende räumliche Einheiten wie Verwaltungsgebiete, Bezirke, Provinzen, Städte, Staaten oder sogar Länder bezeichnen können. Die Forschung konzentrierte sich nur auf die kurzfristigen Bewegungen oder das Pendelverhalten von Menschen in den Patches. Dies wird in das Meta-Populationsmodell für mehrere Gebiete aufgenommen, indem eine Matrix der Aufenthaltszeitanteile der Menschen in den einzelnen Gebieten erstellt wird. Es werden mathematisch vereinfachte analytische Ergebnisse abgeleitet, mit denen gezeigt wird, dass für ein beispielhaftes Szenario, das numerisch untersucht wird, das Multi-Patch-Modell ebenfalls die Schwellenwerteigenschaften aufweist, die das Single-Patch-*SIRUV*-Modell besitzt. Die Bedeutung des Pendelverhaltens von Menschen für die Krankheitsausbreitung wurde anhand der numerischen Ergebnisse dieses Modells dargestellt. Das lokale und nicht-lokale Pendeln wird in einem numerischen Beispiel in das Meta-Populationsmodell einbezogen. Später wird aus dem Multi-Patch-Modell ein PDE-Modell entwickelt.

Contents

1 Introduction

Mathematical modeling of disease dynamics is of increasing relevance nowadays. This thesis mainly discusses the modeling of the spread of diseases that involve direct transmission between humans, along with incidences through mosquitoes. Zika Virus(ZIKV) illness or Zika fever is an important disease that falls under this category. ZIKV belongs to the genus *Flavivirus*[52] and it causes an arboviral disease in humans. An arboviral disease is a term used for infections caused by a group of viruses spread to people by the bite of infected arthropods(insects). Other arboviruses that fall under the genus *Flavivirus* are West Nile Virus, Dengue Virus, yellow fever Virus, etc. The major arthropods involved in the transmission of ZIKV are mosquitoes of the Culicidea family and of the *Aedes* genus, including *Aedes Aegypti*[34]. There is also evidence for the sexual transmission of ZIKV among humans[25, 43]. Zika can also be transmitted from the mother to the fetus and there is evidence of perinatal transmission from an outbreak in French Polynesia[8]. In those cases where the virus got transmitted through the placenta, it is suspected that this increases the risk of stillbirth and microcephaly in newborn babies[42]. In most cases of ZIKV infection, the symptoms are reportedly mild, ranging from rashes and fever to headache and conjunctivitis. The symptoms last for 2-7 days. Most people develop no symptoms of a Zika infection and for these reasons, most cases go unreported. At the same time, a major concern is proposed in association with the correlation of the illness to some neurological and auto-immune disorders like Gullian Barre syndrome[7].

Zika Virus was first isolated in the Zika forest of Uganda in April 1947, from a rhesus monkey[17] and later was identified in humans in 1952, in an antibody survey held in Uganda(see [16]). Later on, it was spread across the countries and continents until a major outbreak was reported in 2007 where 73% of the population in Yap Island was infected[22]. Further, in 2015, a major ZIKV outbreak occurred in the Americas, starting with Brazil. During this outbreak, there was evidence that ZIKV traces were found in the specimens of *Aedes Aegepti* mosquitoes collected from Rio de Janeiro[13]. Favorable climatic conditions for the vectors to breed, as well as human mobility, played a key role in this outbreak. Further from Brazil, the disease was transmitted to different other countries within the Americas in the following months. Currently, ZIKV can be detected using a real-time PCR rapid test (see [23]). During the ZIKA outbreak in Brazil, studies show that it is highly probable that many cases of this infection go undetected due to reasons like the asymptomatic nature of the disease, serological cross-reaction of ZIKV with other flaviviruses that leads to false-positive or uninterpretable ZIKV serology results, etc. which collectively might have resulted in severe under-reporting[38]. A further detailed overview of the outbreak of ZIKV in Brazil can be found in the literature(see for eg. [40]). There is also no specific treatment protocol for curing the disease, thereby the only possible treatment is to address the symptoms and treat them.

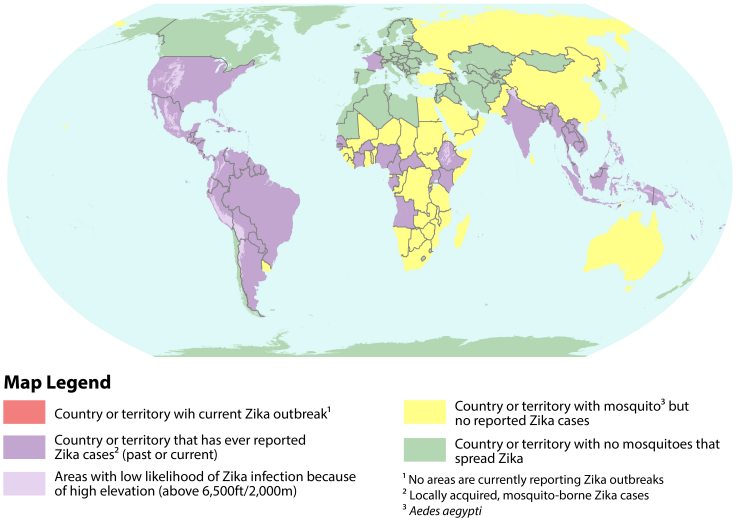

Figure 1.1 – The areas that are at risk of a Zika Virus outbreak according to a CDC report dated 22 July 2022 are shown in the figure. Source: https://wwwnc.cdc.gov/travel/files/zika-areas-of-risk.pdf

At present, no vaccine to prevent ZIKV is developed. Therefore, non-pharmaceutical interventions can only help in the prevention and control of the disease. Zika risk areas have been reported and often it is advised that pregnant women should refrain from traveling to these areas. A schematic map of the risk areas of Zika is given in Figure 1.1. By examining this map itself we can identify that the virus has been transmitted even across continents.

Mathematical modeling is a tool in epidemiology that helps in analyzing a disease outbreak, forecasting, policy making, qualitative analysis of control measures, etc. Remarkably, mathematical epidemiological tools help in simulating experiments that are unethical to be done in reality or are too expensive to be conducted, thereby finding cost-effective mitigation strategies to control the spread of infectious diseases. The modeling techniques in mathematical epidemiology can be broadly classified into statistical, mechanistic, and machine learning based according to Siettos et. al [48]. An important set of deterministic models that can be classified under mechanistic techniques, is the compartmental dynamics transmission models. These models divide the population under consideration into mutually disjoint groups called compartments according to their epidemiological status and study the temporal dynamics of the population size or proportion of these groups. The classical *SIR* model proposed by Kermack and McKendrick is a major simplistic foundation for compartmental models. This model basically considers only three compartments, namely, susceptible, infected, and removed. There are other complex versions of compartmental models that are developed by adding new compartments like exposed, hospitalized, vaccinated, quarantined, etc. An example of an extension is the *SEIR* model given in [27] where the infected compartment is divided into asymptomatic, symptomatic, and severe categories. Another extension also can be seen in the same article where the quarantine compartment is incorporated. Similarly, there are many such extensions to the classical *SIR* model to be seen in the literature, for example [1, 6, 24]. Another im-

provement to a compartmental model is incorporating a time-dependent parameter(see for eg: [26]) or incorporating randomness to the compartmental models to obtain a continuous time Markov chain or stochastic differential equation(see for eg: [2]). Stochastic models are relevant when the number of infectious individuals is small or when the dependence of the parameters involved in the disease spread process on time impacts the epidemic. A compartmental model can also be extended to obtain multi-group models, like age-structured[44] and meta-population models. In standard and simple epidemiological models, we always assume that the population is homogeneously mixed. Taking spatial heterogeneity in populations into consideration, meta-population disease spread models are proposed, which involve sub-populations of the same species and a matrix that describes the interaction between these sub-populations. This can also be viewed as the adjacency matrix of a directed graph, where the sub- populations form the nodes of the graph and the weights of each edge is the rate at which these sub-populations mix among each other. The meta-population models are further divided into two types: Lagrangian and Eulerian models. The Lagrangian models deal with the short-term movements of the sub populations among each other and the Eulerian approach deals with long-term movements like migration[15]. The compartmental modeling of vector-borne diseases mostly considers two populations of different species- the humans or hosts and the vectors or mosquitoes. The dynamical models concerning vector population age back to the early twentieth century's Ross-MacDonald models and their variations. In a historical review, D.L Smith et al. present the different models of vector-borne diseases on the basis of the idea of Ross and MacDonald[49]. A remarkable version of the Ross-Macdonald model is given by Anderson and May[4] where the ratio of population sizes of mosquitoes to humans appears in the model. These models are widely used for simulating and studying the spread of vector-borne diseases like dengue, Chikungunya, Malaria, etc. A simple and intuitive model for simulating the spread of vector-borne diseases is the *SIRUV* model, where S, I, R in this term represents the susceptible, infected, and recovered compartments of the host species and U, V represent the susceptible and infected compartments of the vector species respectively.

In this thesis, Chapter 3 discusses the *SIRUV* model for diseases like Zika fever which has both vector-host and host-host pathogen transmission. This model can be seen as an extension of the *SIRUV* Dengue model discussed in the literature[35, 45]. A system of ordinary differential equations involving the different compartments from the human and mosquito species that describe the evolution of the disease is presented and analyzed mathematically. The equilibrium points and their local stability through the variational formulation are discussed in detail. In connection with this, a significant threshold value, namely reproduction number, is discussed. The two methods of finding reproduction numbers are presented and their relations are established. Later the global asymptotic stability of the two equilibrium points are discussed, which concludes the mathematical analysis of the model. Numerical simulations are done and exemplary scenarios to exhibit the stability of the equilibrium points and the relation with the reproduction numbers are provided. The dependence of the reproduction number on the different parameters is also discussed through examples. In Chapter 4 a different scaling is incorporated into the *SIRUV* by redefining the

parameters from a different perspective. Structurally, the model presented in this chapter is the same as that of the model in Chapter 3. The involvement of the ratio of the population size of mosquitoes to the population size of humans is one important concept that is discussed in this chapter. Mathematical analysis is almost the same as that of the model in Chapter 3. The numerical simulations are done to present comparative results of the two *SIRUV* models. The endemic equilibrium for both models is numerically shown to be distinct and the influence of the ratio of population sizes of the human and mosquito species in both models and its impact on the disease dynamics is shown through exemplary scenarios, by varying the initial conditions. There are certain assumptions that are assumed for the models discussed in Chapters 3 and 4, which might be slightly unrealistic. The host and vector populations are assumed to have constant birth and death rates. The population sizes of humans and mosquitoes are assumed to remain constant throughout the period under consideration. The models discussed in Chapters 3 and 4 are both ignoring the incubation period and latency period of the pathogen in mosquitoes and humans. Majorly, the populations of both species are assumed to be homogeneously mixed within each other. To address the issue of spatially heterogeneous populations, we should incorporate spatial heterogeneity in the population under consideration.

In Chapter 5, a meta-population model is proposed as an extension to the single-patch *SIRUV* model presented in Chapter 4. To involve spatial heterogeneity, the space domain under consideration is divided into multiple smaller domains called patches and the dynamics of the disease within these patches are modeled using a single patch *SIRUV* model corresponding to the intrinsic population and the disease compartments of the intrinsic population of these patches. The heterogeneous spread among the distinct patches is modeled using the residence time budgeting matrix. Unlike the usual meta-population models that take into account the sub-populations of the same species, here we let the species of hosts and vectors from different patches form sub populations and each sub-population is divided into mutually exclusive compartments. The interaction of these sub-populations through short-term movements between these patches is described using the residence time budgeting matrix. The movement is restricted to the sub-population of hosts, as we assume that vectors are not moving across the patches. This assumption is made by referring to the papers [32, 53], by which we assumed that the mosquitoes were only moving across a few hundred meters in their lifetime. Therefore, we assume that the mosquitoes are confined within each patch and are considered the intrinsic mosquito population that interacts with the other patches only through the humans visiting them. A general mathematical expression has been derived for simplifying the quest of finding the endemic equilibrium. Similarly, a simplified mathematical expression to find the reproduction number has been found. Using these expressions numerical results for a two-patch model in an exemplary scenario have been presented which shows the relationship between the value of the reproduction number and the stability of the equilibrium points of the model. Further, we have shown different examples where the relevance of a multi-patch model has been studied and results are presented showing how does the infection rate changes from the single-patch model with the choice of different residence time budgeting matrices. In another numerical study, two examples are given for which the influence of nearest neighboring commuting and non-local commuting are

exhibited using respective residence time budgeting matrices.
In Chapter 6, a PDE model is derived from the multi-patch model for a residence time budgeting matrix that exhibits an orthogonal movement to the nearest neighbors. In Chapter 7 we conclude the research done for the completion of this dissertation.

2 Preliminaries

In this chapter, we give a brief introduction to the underlying concepts that are required for the understanding of this research. The basic definitions and theoretical knowledge of dynamical systems and the concept of stability, underlying numerical tools used in simulations, etc are described in this chapter.

2.1 Dynamical Systems

A collection of n interrelated equations of real variables $x_1, x_2, \cdots, x_n$ that involves ordinary derivates of the form,

$$\begin{aligned}
\frac{dx_1}{dt} &= f_1(t, x_1, x_2, \cdots, x_n) \\
\frac{dx_2}{dt} &= f_2(t, x_1, x_2, \cdots, x_n) \\
&\cdots \\
\frac{dx_n}{dt} &= f_n(t, x_1, x_2, \cdots, x_n)
\end{aligned}$$

is called a *system of ordinary differential equations*. The variables x_i are the dependent variables and t is the independent variable. Each equation tells us how the variable x_i is varying with respect to t. Note that the change is not random but is related to the other variables as well through f_i which are real-valued functions of the $n+1$ variables x_1, x_2, $\cdots$, x_n, and t. We may also denote this in the vector form as follows,

$$X'(t) = F(t, X(t));$$

where

$$F(t, X(t)) = \begin{pmatrix} f_1(t, x_1, x_2, \cdots, x_n) \\ f_2(t, x_1, x_2, \cdots, x_n) \\ \vdots \\ f_n(t, x_1, x_2, \cdots, x_n) \end{pmatrix}$$

and $X'(t) = \left(\frac{dx_1}{dt}, \frac{dx_2}{dt}, \cdots, \frac{dx_n}{dt}\right)^T$. Here the $'$ denotes nothing but $\frac{d}{dt}$.

A system is said to be *linear* if all functions f_i involve terms of x_j containing the power of 1 for all $1 \leq j \leq n$. If it contains non-linear terms like x_i^2, $x_i x_j$, or other transcendental functions of x_j's for eg: $sin(x_2)$ or $log(x_4)$, the system is called *non-linear*.

An initial condition is an expression of the form $X(t_0) = X_0$, where t_0 denotes the starting point of the independent variable t. Usually, we take $t_0 = 0$. A system of differential equations for which the initial condition is specified is called an *initial value problem*(IVP).

Theorem 2.1 [31] Consider the initial value problem

$$X' = F(X), \qquad X(t_0) = X_0,$$

where $X_0 \in \mathbb{R}^n$. Suppose that $F : \mathbb{R}^n \to \mathbb{R}^n$ is continuously differentiable. Then, first, there exists a solution to this initial value problem, and second, this is the only such solution. More precisely, there exists an $a > 0$ and a unique solution,

$$X : (t_0 - a, t_0 + a) \to \mathbb{R}^n,$$

of this differential equation satisfying the initial condition $X(t_0) = X_0$.

Definition 2.2 [31] A *smooth dynamical system* on $\mathbb{R}^n$ is a continuously differentiable function $\phi : \mathbb{R} \times \mathbb{R}^n \to \mathbb{R}^n$, where $\phi(t, X) = \phi_t(X)$ satisfies

- $\phi_0 : \mathbb{R}^n \to \mathbb{R}^n$ is the identity function, $\phi_0(X_0) = X_0$.
- The composition $\phi_t \circ \phi_s = \phi_{t+s}$ for each $t, s \in \mathbb{R}$.

Note that in the definition of a dynamical system, the independent variable t is nothing but time. For an initial value problem given by the linear system of ODEs

$$X' = AX$$

and an initial condition $X(0) = X_0$, where A is an $n \times n$ real-valued matrix, the solution of this IVP forms a smooth dynamical system on $\mathbb{R}^n$ given by the function $\phi_t(X_0) = exp(tA)X_0$.

Definition 2.3 — Equilibrium point. Let $X' = F(X)$ represent a system of differential equations in $\mathbb{R}^n$, a vector X^* for which $F(X^*) = 0$ is called an equilibrium point for the system.

2.1.1 Stability Analysis

Definition 2.4 — Stability. Suppose $X^* \in \mathbb{R}^n$ is an equilibrium point for the differential equation

$$X' = F(X).$$

- X^* is a stable equilibrium if, for every neighbourhood $\mathscr{O}$ of X^* in $\mathbb{R}^n$, there is a neighbourhood $\mathscr{O}_1$ of X^* in $\mathscr{O}$ such that every solution $X(t)$ with $X(0) = X_0$ in $\mathscr{O}_1$ is defined and remains in $\mathscr{O}$ for all $t > 0$.
- If $\mathscr{O}_1$ can be chosen so that, in addition to the properties for stability, we have $lim_{t\to\infty} X(t) =$

X^*, then we say that X^* is asymptotically stable.

- If an equilibrium X^* is not stable, it is called an unstable equilibrium point.

Let $L : \mathscr{O} \to \mathbb{R}$ be a differentiable function defined on an open set $\mathscr{O} \in \mathbb{R}^n$ that contains an equilibrium point X^* of the system $X' = F(X)$. Consider the function

$$\dot{L}(X) = DL_X(F(X)).$$

Theorem 2.5 — Lyapunov stability. [31] Let X^* be an equilibrium point of $X' = F(X)$. Let $L : \mathscr{O} \to \mathbb{R}$ be a differentiable function defined on an open set $\mathscr{O}$ containing X^*. Suppose further that

(a) $L(X^*) = 0$ and $L(X) > 0$ if $X \neq X^*$

(b) $\dot{L} \leq 0$ in $\mathscr{O} - X^*$
Then X^* is stable. Furthermore, if L also satisfies

(c) $\dot{L} < 0$ in $\mathscr{O} - X^*$
then X^* is asymptotically stable.

Definition 2.6 — Lyapunov function. A function L satisfying (a) and (b) is called a Lyapunov function of the equilibrium point X^*. If additionally, (c) holds, we call L a strict Lyapunov function.

There is no standard method to find Lyapunov functions. Generally, an educated guess is what gives us a Lyapunov function. If we have a strict Lyapunov function, the corresponding equilibrium point is asymptotically stable. But in some cases even if we could only find a Lyapunov function we can prove the asymptotic stability using the following theorem.

Theorem 2.7 — Lasalle's Invariance Principle. [31] Let X^* be an equilibrium point for $X' = F(X)$ and let $L : \mathscr{U} \to \mathbb{R}$ be a Lyapunov function for X^*, where $\mathscr{U}$ is an open set containing X^*. Let $\mathscr{P} \subset \mathscr{U}$ be a neighbourhood of X^* that is closed. Suppose that $\mathscr{P}$ is positively invariant and that there is no entire solution in $\mathscr{P} - X^*$ on which L is constant. Then X^* is asymptotically stable, and $\mathscr{P}$ is contained in the basin of attraction of X^*

Definition 2.8 — Basin of attraction. The set of all initial conditions with solution that tend to the equilibrium point of a system $X' = F(X)$ is called the *basin of attraction* of that equilibrium point

2.1.2 Bifurcation

In a dynamical system, a bifurcation is said to occur if the qualitative structure of the flow is changed depending upon the variation in the value of a parameter. By qualitative change, it means,

the number of fixed points gets increased or decreased, or the stability of some fixed points gets changed, etc. Saddle node bifurcation is a basic type of bifurcation where the fixed points are created or destroyed with a change in the value of the bifurcation parameter. For example, consider the ordinary differential equation given by

$$x' = a + x^2$$

where a is the parameter under consideration.

- When $a < 0$, there are two equilibrium points namely $x^* = -\sqrt{(r)}$ and $x^* = sqrt(r)$.
- When $a = 0$, there is only one equilibrium point $x = 0$.
- When $a > 0$, there are no equilibrium points.

Another type of bifurcation that we will discuss in this thesis is transcritical bifurcation.

Definition 2.9 A transcritical bifurcation is said to occur at a bifurcation point ω, if an exchange of stability has occurred at ω[20, 55]

2.1.3 Reproduction Number

The basic reproduction number is a crucial threshold value in population dynamics models. In epidemiology, this threshold value of a disease outbreak is defined as the number of secondary infections produced by one infective individual in its entire period of infectivity, when introduced to an entirely susceptible population. in classical epidemiological models, the basic reproduction number can be deduced as a combination of parameters and usually, we can establish a relationship between the value of the basic reproduction number and the stability of the underlying equilibrium points of the system that governs the disease dynamics, which equivalently answers whether the disease prevails in the population or if it dies out. Mathematically, a combination of parameters R_0, for which $R_0 < 1$ resulting in the disease dying out and $R_0 > 1$ resulting in the disease pertaining, is called the basic reproduction number of a disease spread model. Finding an analytical expression for this threshold value and understanding the bifurcation of the model around this value is crucial in mechanistic disease spread models. There are different methods available in the literature that help in finding the reproduction number. In Chapter 3, we discuss two methods namely, Jacobian and next generation method[20, 21] for finding an analytical expression for the basic reproduction number of those models in which disease spread has two cycles namely, host-host and host-vector and show that the reproduction numbers derived using the Jacobian and next generation matrix are not equal and the relationship between them is not so obvious such that an equivalence in the threshold condition is satisfied by both. But we prove that these methods give us two expressions, both of which hold the threshold condition that is required in the mathematical definition of the basic reproduction number.

2.1.4 Numerical Methods

It is not always easy to find an analytical expression for the solution of a system of differential equations. In complex non-linear systems, we may use numerical methods to find approximate solutions. In this thesis, we are dealing with first-order non-linear systems given as in $X' = F(X)$. Each numerical method approximates the value of $X(t_k)$ in an iterative process where we find a sequence of approximations given by X_k at each discrete time-point t_k. Generally, t_k's are obtained by starting at the initial step t_0, and incrementing by small step sizes Δt. There are different methods available for finding the approximate solution of first-order differential equations. A very basic numerical one-step method used in solving initial value problems involving a system of ordinary differential equations is the Explicit-Euler method. Given an initial value of a problem, we may iteratively obtain the solution values at the consecutive time points by the following equation.

$$X_{n+1} = X_n + \Delta t F(t_n, X_n)$$

This can be seen as updating the new point by climbing across a line with a slope given by $F(t_n, X_n)$. An efficient numerical method in this regard can be defined as the one that approximates a solution which is really close to the real solution. Mathematically, the efficiency of numerical methods is measured using the convergence errors. The consistency or local error is defined as the error occurring in one step whereas convergence error is the collective error propagated by the local errors of all the previous steps. The order of these errors is used as a measure of the efficiency of these numerical methods. A slightly different version of the explicit-Euler method is the implicit-Euler method which uses the following iterative process to obtain the approximate solution.

$$X_{n+1} = X_n + \Delta t F(t_{n+1}, X_{n+1}).$$

A modified method to find the numerical solution of a system of ordinary differential equations is the Classical Runge-Kutta method. A general set of equations that define a Runge-Kutta method of s stages, is as follows.

$$X_{n+1} = X_n + \Delta t \sum_{i=1}^{s} b_i k_i$$

where

$$\begin{aligned} k_1 &= F(t_n, X_n) \\ k_2 &= F(t_n + c_2 \Delta t, X_n + a_{21} k_1 \Delta t) \\ &\vdots \\ k_s &= F(t_n + c_s \Delta t, X_n + (\sum_{i=1}^{s-1} a_{si} k_i) \Delta t) \end{aligned}$$

where $\sum_{i=1}^{s} b_i = 1$ and $\sum_{j=1}^{i-1} a_{ij} = c_i$ for $i = 2, \cdots, s$ Runge-Kutta methods are modified to obtain adaptive step-size methods or embedded Runge-Kutta methods. These methods use two Runge-Kutta methods of order p and $p-1$ simultaneously and adapt the step size to make sure the error is below a certain threshold value and that the step size is not too small to save computational cost.

We are using such an adaptive step size method given in MATLAB by the name 'ode45' throughout this thesis to obtain the numerical solution of ODEs wherever it applies. 'ode45' uses an embedded Runge-Kutta method called Dormand-Prince method[18].

3 SIRUV model with Vector-Host and Host-Host prevalence

3.1 Introduction to Compartmental Disease Models

Mathematical modeling of infectious disease has been useful in studying the dynamics of infectious disease spread to make predictions about a disease outbreak and additionally to study the effect of mitigation strategies and measures taken during the course of an outbreak. Out of different mathematical modeling techniques to model disease spread, the most simpler one is compartmental modeling, where a given population under consideration is divided into different compartments and the transition dynamics between them due to events related to disease spread is the core of this modeling approach. The standard model using this approach is the *SIR* model [3, 29] which was initially proposed by W. O. Kermack and A. G McKendrick[36]. This also is a reason to refer to this model with the name Kermack-McKendrick model. The population is divided into compartments namely Susceptible(S), Infected(I), and Removed(R)(or Recovered). The classical *SIR* model which is also known as the SIR-epidemic model[29] is given by the IVP,

$$\begin{aligned} \frac{dS}{dt} &= -\frac{\beta}{N} IS \\ \frac{dI}{dt} &= \frac{\beta}{N} IS - \gamma I \\ \frac{dR}{dt} &= \gamma I \end{aligned} \tag{3.1}$$

provided an initial condition $((S(0), I(0), R(0))) = (S_0, I_0, R_0)$ such that $S_0, I_0, R_0 \geq 0$. The unknown variables are given by,

- $S(t)$ is the number of susceptibles in the population at time t,
- $I(t)$ is the number of infected in the population at time t,
- $R(t)$ is the number of removed/recovered in the population at time t.

The total population size is given by $N = S + I + R$. For ease of analysis, we assume that the total population size is constant throughout the epidemic period in all the epidemiological models within this and the coming chapters. One may notice that this is a direct consequence of the sum of the equations in the system given in 3.1. We also assume that the coefficients β and γ are constants that returns the SIR model to be an autonomous IVP.

Remark 3.1 If we have assumed that the coefficients β and/or γ are time-varying then the SIR model given by 3.1 turns to be non-autonomous.

In the Kermack-McKendrick model, a disease spread process is defined with the assumption that the infectivity rate varies at different stages of an infected individual. The classical SIR model is a special case where the infectivity rate is constant for every stage of an infected individual. Another major outlook from Hethcote[29] that has been useful in understanding the term $\frac{\beta}{N}IS$ and why is this used instead of the mass action law for disease spread which uses ηSV, where the term η has a problem with its biological description. In Hethcote[29] they have discussed evidence too by which they have concluded that $\eta = \frac{\beta}{\mathscr{N}}$ is more realistic than its alternative($\eta = \beta$) where $\mathscr{N}$ is the total size of the population that is being affected. The parameter β denotes the average number of adequate contacts per person in unit time. βS is the average number of adequate contacts of all susceptibles in unit time, out of which $\frac{\beta}{N}IS$ represents the infectious contacts that happen between infected and susceptible people in unit time. The dimension of β is $[\text{number of people}]^{-1}[\text{time}]^{-1}$. The rate of removal is given by γ. The total number of people removed either due to recovery or death is represented by γI. To incorporate vital transitions within the compartments another version of the *SIR* model is also widely used in the literature. As per Hethcote[29], we refer to this model as the endemic-*SIR* model. In this case, we may call R as the recovered compartment, as removal due to death is incorporated through other terms. This model is given by the IVP,

$$\begin{aligned} \frac{dS}{dt} &= \mu(N-S) - \frac{\beta}{N}IS \\ \frac{dI}{dt} &= \frac{\beta}{N}IS - \gamma I - \mu I \\ \frac{dR}{dt} &= \gamma I - \mu R \end{aligned} \tag{3.2}$$

with a positive initial condition as in model 3.1, where μN and μS in the first equation denote the birth and death of susceptibles, and the terms μI and μR in the other two equations denote the removal from infected and recovered compartments due to death, under the assumption that μ denotes the birth and death rate in unit time. Here γI is the transition due to recovery. Another basic compartmental model is the *SI* model. This is nothing but the *SIR* model without the removed/recovered compartment in the population. The *SI* model with vital transition is given by the following IVP

$$\begin{aligned} \frac{dS}{dt} &= \mu(N-S) - \frac{\beta}{N}IS \\ \frac{dI}{dt} &= \frac{\beta}{N}IS - \mu I \end{aligned} \tag{3.3}$$

Remark 3.2 The birth and death rates are assumed to be equal which is an assumption far from reality. Another assumption made in system 3.1 is that death due to infections are not taken into

account as a separate entity. This is also a simplification of the model that is against the real disease scenario. In the coming models as well we are making these two assumptions.

3.1.1 Modeling vector-borne diseases

The prevalence of vector-borne diseases is of increasing importance in the present day. In epidemiology, a vector is the transmitting agent of a different species other than the hosts, that spreads the pathogen to the host species. In many cases, the vectors can be mosquitoes, for example in diseases like Malaria, Chikungunya, West Nile Virus, Dengue, and Zika Virus. Most of these diseases are purely vector-borne, which means that the disease prevails only due to the transmission of the pathogen from vectors to susceptible hosts. At the same time, in the case of the Zika Virus, the disease prevalence is due to vector-host as well as host-host transmissions. The SIRUV model[45] describes the dynamics of disease spread in purely vector-borne diseases. It is deduced by combining the endemic-*SIR* and endemic-*SI* models. The model is as follows

$$\begin{aligned}
\frac{dS}{dt} &= \mu(N-S) - \frac{\alpha}{M}VS \\
\frac{dI}{dt} &= \frac{\alpha}{M}VS - \gamma I - \mu I \\
\frac{dR}{dt} &= \gamma I - \mu R \\
\frac{dU}{dt} &= \nu(M-U) - \frac{\vartheta}{N}IU \\
\frac{dV}{dt} &= \frac{\vartheta}{N}IU - \nu V
\end{aligned} \tag{3.4}$$

where the compartments involved are S, I, and R denoting the susceptible, infected, and recovered classes of the host population. Similarly, the vector population is assumed to be comprised of the susceptible and infected compartments, denoted by U and V respectively. Considering the short life-span of mosquitoes the state of recovery is not considered. The incidence terms are as follows.

- $\frac{\alpha}{M}VS$: vector to host infection. The parameter α denotes the average number of adequate contacts one host is having with vectors in unit time. αS is the total adequate contacts between the susceptible host population and vectors in unit time, out of which, only $\frac{\alpha}{M}VS$ is the number of cases that lead to vector to host infection.

- $\frac{\vartheta}{N}IU$: host to vector infection. The parameter ϑ denotes the average number of adequate contacts one vector is having with hosts in unit time. ϑU is the total adequate contacts between the susceptible vector population and hosts in unit time, out of which, only $\frac{\vartheta}{N}IU$ is the number of cases that lead to vector to host infection.

The vital dynamics in the vector population is given by the term $\nu(M-U)$, where ν is the birth/death rate of the vectors and M is the size of the vector population. For reference, we call this the *SIRUV*-vector model, for the reason that this model is used for purely vector-borne diseases.

3.2 Vector-host SIRUV model

The prevalence of Zika Virus is not only due to mosquitoes but humans themselves too. We are considering a mechanistic modeling approach initially to get a set of ordinary differential equations that describe the dynamics of different compartments that are involved in the disease spread. The compartments are the same as in the case of the *SIRUV*-vector model. From this section, we denote the population size in each compartment as s, i, r, u, and v. The total number of hosts is given ba N and that of vectors is M. The vector-host *SIRUV* model is nothing but a combination of endemic-*SIR* and *SIRUV*-vector models. The parameters involved are specified in the following table

parameter	number of adequate contacts per unit time
α	per susceptible host with vectors
β	per susceptible host with hosts
ϑ	per susceptible vector with hosts

The disease spread between hosts and vectors is described by terms like $\frac{\alpha}{M}vs$ and $\frac{\vartheta}{N}iu$. Additionally in this model, we have an incidence from hosts to hosts which is described in the term $\frac{\beta}{N}is$. We consider the vital dynamics due to birth and death as well in this model and make an assumption that the populations under consideration have constant birth and death rates. For the host population, we assume that after being infected they recovered permanently and entered into the compartment r at a constant rate γ. In diseases like ZIKV, which is vector-borne with host prevalence, the dynamics is thereby described by the following *SIRUV* model.

$$\begin{aligned}
\frac{ds}{dt} &= \mu(N-s) - \frac{\alpha}{M}vs - \frac{\beta}{N}is \\
\frac{di}{dt} &= \frac{\alpha}{M}vs + \frac{\beta}{N}is - \gamma I - \mu I \\
\frac{dr}{dt} &= \gamma i - \mu r \\
\frac{du}{dt} &= \nu(M-u) - \frac{\vartheta}{N}iu \\
\frac{dv}{dt} &= \frac{\vartheta}{N}iu - \nu v
\end{aligned} \tag{3.5}$$

Remark 3.3 As in the model given by the system of equations 3.1, here also we have that the total population size of hosts and vectors, respectively M and N, remains constant and this can be seen as a direct consequence of the system of equations 3.5.

This system of equations can be normalized by defining new variables as given in the following table

S	I	R	U	V
$\frac{s}{N}$	$\frac{i}{N}$	$\frac{r}{N}$	$\frac{u}{M}$	$\frac{v}{M}$

Note that in this case $S+I+R=1$ and $U+V=1$. A host or human who goes through the infection cycle shall pass the different stages namely susceptible, infected, and recovered. The same is the case with vectors. A person(or vector) in a population can be at different stages of infection throughout their lifetime. We are considering the population as a whole and the proportion of people(vectors) at the different stages of infection collectively. In model 3.5 we are considering the number of people at these different stages and now we consider the ratios of people who are susceptible, infected, recovered, etc at a given time. We are modelling the evolution of these entities as variables that change continuously with respect to time. An example is given below by considering the first equation in 3.5, which shows the derivation of the first equation in the normalised system.

$$\begin{aligned}\frac{dS}{dt} &= \frac{1}{N}\frac{ds}{dt}\\ &= \frac{1}{N}\left[\mu(N-s)-\frac{\alpha}{M}vs-\frac{\beta}{N}is\right]\\ &= \mu(1-S)-\alpha VS-\beta IS\end{aligned}$$

In a similar way, we can deduce the normalised system, which will be referred to as the *SIRUV* model in the rest of the text unless mentioned otherwise. The analysis of the normalized system is equivalent to the standard model. The *SIRUV*-model is given as follows.

$$\begin{aligned}\frac{dS}{dt} &= \mu(1-S)-\alpha VS-\beta IS\\ \frac{dI}{dt} &= \alpha VS+\beta IS-(\gamma+\mu)I\\ \frac{dR}{dt} &= \gamma I-\mu R\\ \frac{dU}{dt} &= \nu(1-U)-\vartheta IU\\ \frac{dV}{dt} &= \vartheta IU-\nu V\end{aligned} \tag{3.6}$$

Theorem 3.4 The region given by

$$\Gamma=\{X=(S,I,R,U,V);0\leq S,I,R,U,V\leq 1, S+I+R=1, U+V=1\}$$

is a positively invariant set for system 3.6 where the trajectory of an IVP involving system 3.6 and an initial condition from Γ will remain in this region for all points of time.

Proof. Let us assume that system 3.6 with a non-negative initial condition has solution X where one or more components of $X(t)$ hits zero for the first time at $t=t_0$. We shall prove that the gradient of all such components with respect to time is non-negative at $t=t_0$. As soon as the value of the i^{th} component of X hits zero, for the next time steps the value of these components will either remain zero or becomes positive. For examining this, let us assume that $S(t_0)=0$.

$$\frac{dS}{dt}|_{t=t_0}=\mu\geq 0$$

Now if $I(t_0) = 0$ then

$$\frac{dI}{dt}|_{t=t_0} = \alpha SV \geq 0$$

which is due to our assumptions about t_0 that results in $S(t_0)$ and $V(t_0)$ being non-negative. Similarly, we can prove that the gradient of each compartment value is non-negative at t_0 which proves that the component values are always non-negative. We may use a similar argument to prove that the component values will always be less than 1. Let us assume that t_1 is the point where any of the components X_i meet the plane $X_i = 1$. We shall prove that for all the components such a scenario will lead to a situation where the gradient of X_i is non-negative. We will consider the cases for two components namely $X_1 = S$ and $X_2 = I$. For all other components, the condition is held and can be proven in a similar way. Let $S(t_1) = 1$, all other compartmental values are then belonging to $[0,1)$.

$$\frac{dS}{dt}|_{t=t_1} = -\alpha V - \beta I \leq 0$$

Now if in case $I(t_1) = 1$ and all other compartmental values are belonging to $[0,1)$, then

$$\frac{dI}{dt}|_{t=t_1} = -(\gamma+\mu) + \alpha SV + \beta S$$

We have the characteristic for compartments S, I, R that $S+I+R = 1$ for all points in time. If $I(t_1) = 1$, then $S(t_1)+R(t_1) = 0$ which in turn gives us that $S(t_1) = R(t_1) = 0$. Using this criterion we can deduce that

$$\frac{dI}{dt}|_{t=t_1} = -(\gamma+\mu) \leq 0$$

A similar approach would show that the remaining components also hold this property and collectively we see that Γ is positively invariant. ■

Even though we need to get the values of all compartments we need not use all the equations in model 3.6 to find out the values. As we have the properties $S+I+R = 1$ and $U+V = 1$ we need to find the values of S, I and V to get the solution for model 3.6. Also, we may notice that if we add up the first and second equations in 3.6 we get the third equation. Similarly, equations 4 and 5 are simply negations of each other. The sufficient and necessary equations form the new system

$$\begin{aligned} \frac{dS}{dt} &= \mu(1-S) - \alpha VS - \beta IS \\ \frac{dI}{dt} &= -(\gamma+\mu)I + \alpha VS + \beta IS \\ \frac{dV}{dt} &= -\nu V + \vartheta I(1-V) \end{aligned} \tag{3.7}$$

The set of deterministic equations in 3.7 forms a dynamical system. So we may also use 3.7 instead of 3.6 and obtain the other variables like R and U using equations $R = 1-(S+I)$ and $U = 1-V$.

3.2.1 Equilibrium points

Asymptotically, disease dynamics behaves in two ways, the first case is when the disease dies out and the second case is when the disease pertains. As $t \to \infty$, if the proportion of infected people

in the population $I(t)$ tends to 0 and the solution of the system $X(t)$ tends to $(1,0,0,1,0)$ we say that the system asymptotically reached the disease-free equilibrium(DFE). Another situation is that the disease pertains i.e., $I(t) \to I^* > 0$ as $t \to \infty$. In this case, the solution of the system $X(t) \to X^*$ which is called the endemic equilibrium.

Theorem 3.5 There exists an endemic equilibrium for the one patch model 3.6, which is of the form

$$(S^*, I^*, R^*, U^*, V^*) = (1 - \frac{(\gamma+\mu)}{\mu} I^*, I^*, \frac{\gamma}{\mu} I^*, \frac{\nu}{\nu + \vartheta I^*}, \frac{\vartheta I^*}{\nu + \vartheta I^*}),$$

where I^* is a solution of the quadratic polynomial in the unknown x given by $ax^2 + bx + c = 0$, for,

$$\begin{aligned} a =& \beta \frac{\vartheta(\gamma+\mu)}{\mu} \\ b =& -(\beta\vartheta - \frac{\beta\nu(\gamma+\mu)}{\mu} - \frac{\alpha\vartheta(\gamma+\mu)}{\mu} - (\gamma+\mu)\vartheta) \\ c =& \nu(\gamma+\mu-\beta) - \alpha\vartheta, \end{aligned}$$

provided $c < 0$

Proof. Let $X^* = (S^*, I^*, R^*, U^*, V^*)$ be an endemic equilibrium of the one-patch model 3.6. We require to find the vector X^* with $I^* > 0$ so that

$$\lim_{t\to\infty} X(t) = X^*,$$

for the solution of the initial value problem involving the system of equations 3.6 and some given initial condition $X(0) = X_0$. At endemic equilibrium, the system of equations 3.6 gives $X' = 0$ when $X = X^*$ which shall be expanded as follows.

$$\mu(1 - S^*) - \alpha V^* S^* - \beta I^* S^* = 0 \tag{3.8a}$$

$$-(\gamma+\mu) I^* + \alpha V^* S^* + \beta I^* S^* = 0 \tag{3.8b}$$

$$\gamma I^* - \mu R^* = 0 \tag{3.8c}$$

$$\nu(1 - U^*) - \vartheta I^* U^* = 0 \tag{3.8d}$$

$$-\nu V^* + \vartheta I^* U^* = 0 \tag{3.8e}$$

Using 3.8c we can deduce that $R^* = \frac{\gamma}{\mu} I^*$. Adding equations 3.8a and 3.8b we get the following relation between S^* and I^*.

$$S^* = 1 - \frac{\gamma+\mu}{\mu} I^*$$

From equations 3.8d and 3.8e we get

$$U^* = \frac{\nu}{\nu + \vartheta I^*}$$

and

$$V^* = \frac{\vartheta I^*}{\nu + \vartheta I^*}$$

respectively. Using these expressions for S^* and V^* in 3.8b we get

$$(\gamma+\mu)I^* - \alpha\left(\frac{\vartheta I^*}{\nu+\vartheta I^*}\right)\left(1-\frac{(\gamma+\mu)I^*}{\mu}\right) - \beta I^*\left(1-\frac{(\gamma+\mu)I^*}{\mu}\right)$$

Multiplying this expression by $\frac{\nu+\vartheta I^*}{I^*}$ and simplifying gives the required quadratic polynomial in $ax^2+bx+c=0$. It is clear that $a >= 0$.

$$c = \nu(\gamma+\mu-\beta) - \alpha\vartheta < 0. \tag{3.9}$$

Since $a > 0$, when $c < 0$, we have

1. the discriminant $b^2-4ac > 0$ which is equivalent to having real roots.
2. $\frac{c}{a} < 0 \iff$ The two roots both have different signs.

There exists one positive root $I*$ which gives us an endemic equilibrium lying in the feasible region Γ. We can conclude that the endemic equilibrium exists if it is given that

$$c = \nu(\gamma+\mu-\beta) - \alpha\vartheta < 0.$$

■

Corollary 3.6 The endemic equilibrium is unique provided

$$c = \nu(\gamma+\mu-\beta) - \alpha\vartheta < 0$$

Proof. As $c < 0$ and $a = \beta\frac{\vartheta(\gamma+\mu)}{\mu} > 0$ we have

$$b^2-4ac > b^2 > 0 \tag{3.10}$$

$$\sqrt{b^2-4ac} > |b| \tag{3.11}$$

We get two distinct real roots for the polynomial $aI^2+bI+c=0$. But the solution which is feasible requires that it should be positive. We will take two possible cases.

- If $b >= 0$
  Clearly $-b-\sqrt{b^2-4ac} < 0$. In this case $|b| = b$ and 3.11 implies that $-b+\sqrt{b^2-4ac} > 0$.
- If $b < 0$
  Again $-b+\sqrt{b^2-4ac} > 0$. Here $|b| = -b$ and 3.11 implies that $-b-\sqrt{b^2-4ac} < 0$.

Simultaneously both roots will not be positive or negative. In all cases $I^* = \frac{-b+\sqrt{b^2-4ac}}{2a}$ is the feasible solution ■

The behaviour of the non-linear system at an equilibrium point can also be understood from analysing the linearised system at that equilibrium state(See pp: 151, 152 in [50] for a 2-dimensional analogue of this statement with derivation). Let $X(t) = (S(t), I(t), R(t), U(t), V(t))^T$ be the 5-dimensional variable whose change with respect to time is represented by the system of equations 3.6, which can be simply written as

$$X' = F(X(t)) = \begin{pmatrix} \mu(1-S) - \alpha VS - \beta IS \\ -(\gamma+\mu)I + \alpha VS + \beta IS \\ \gamma I - \mu R \\ \nu(1-U) - \vartheta IU \\ -\nu V + \vartheta IU \end{pmatrix} \tag{3.12}$$

where X' denotes $\frac{d}{dt}X$. The variational equation along the solution of 3.12 with initial state X_0 being the DFE, is an autonomous linear system[31] given by

$$W' = DF_{X_0}W$$

where DF_{X_0} denotes the Jacobian matrix of F evaluated at X_0 and $W = X - X_0$. This system is called the linearised system at the disease-free equilibrium.

Definition 3.7 — Hyperbolic Equlibrium Point. An equilibrium point X_0 of a nonlinear system is hyperbolic if all of the eigen values of DF_{X_0} have nonzero real parts

We will discuss the hyperbolicity of the disease-free equilibrium of the system of equations 3.12 in the next section. The linearisation theorem in [31] states that the nonlinear flow of an n-dimensional system $X' = F(X)$ is conjugate to the flow of the linearised system in a neighbourhood of a hyperbolic equilibrium point X_0 of the system. Two maps are conjugate means, they have equivalent dynamics ie; all topological features should be preserved when the homeomorphism transforms one map to another. A definition of conjugacy in the two-dimensional scenario is given in Chapter 4 of [31].

3.2.2 Basic Reproduction Number

A crucial threshold value in connection with population dynamics models is the basic reproduction number. In epidemiology, whether the disease dies out or if it pertains can be deduced from this threshold value. Reproduction number is the value of a combination of parameters which gives us the secondary cases that one infected individual produces in a completely susceptible population.

- The reproduction number can be found using the Jacobian approach and next-generation matrix method

Jacobian approach

We take the flux part of the normalised system given as follows

$$F(X) = \begin{pmatrix} \mu(1-S) - \alpha VS - \beta IS \\ -(\gamma+\mu)I + \alpha VS + \beta IS \\ \gamma I - \mu R \\ \nu(1-U) - \vartheta IU \\ -\nu V + \vartheta IU \end{pmatrix}$$

The jacobian of this vector-valued function at the disease-free equilibrium(DFE) is given by

$$J = \frac{\partial F}{\partial X}|_{(1,0,0,1,0)} = \begin{pmatrix} -\mu & -\beta & 0 & 0 & -\alpha \\ 0 & -(\gamma+\mu)+\beta & 0 & 0 & \alpha \\ 0 & \gamma & -\mu & 0 & 0 \\ 0 & -\vartheta & 0 & -\nu & 0 \\ 0 & \vartheta & 0 & 0 & -\nu \end{pmatrix} \tag{3.13}$$

We want this matrix to have all eigenvalues negative in order to make sure that the DFE is locally asymptotically stable. The characteristic polynomial given by $|J - \lambda I| = 0$ is expressed as

$$[-\mu-\lambda][-\mu-\lambda][-\nu-\lambda][\lambda^2 + \lambda(\nu+\gamma+\mu-\beta) + \nu(\gamma+\mu-\beta) - \alpha\vartheta] = 0$$

The first three eigenvalues of J are μ,μ and ν. The rest of the eigenvalues are the roots of the polynomial

$$[\lambda^2 + \lambda(\nu+\gamma+\mu-\beta) + \nu(\gamma+\mu-\beta) - \alpha\vartheta] = 0 \tag{3.14}$$

Theorem 3.8 (Routh-Hurwitz Criterion)[41] Consider the nth- degree polynomial with real coefficients

$$P(\lambda) = \lambda^n + a_1\lambda^{n-1} + \cdots + a_{n-1}\lambda + a_n.$$

Define n Hurwitz matrices using the coefficients a_i of the characteristic polynomial:

$$H_1 = (a_1) \quad H_2 = \begin{pmatrix} a_1 & 1 \\ a_3 & a_2 \end{pmatrix} \quad H_3 = \begin{pmatrix} a_1 & 1 & 0 \\ a_3 & a_2 & a_1 \\ a_5 & a_4 & a_3 \end{pmatrix}$$

and

$$H_n = \begin{pmatrix} a_1 & 1 & 0 & 0 & \dots & 0 \\ a_3 & a_2 & a_1 & 1 & \dots & 0 \\ a_5 & a_4 & a_3 & a_2 & \dots & 0 \\ \vdots & \vdots & \vdots & \vdots & \dots & \vdots \\ 0 & 0 & 0 & 0 & \dots & a_n \end{pmatrix}$$

where $a_j = 0$ if $j > n$. All roots of the polynomial $P(\lambda)$ are negative or have a negative real part if and only if the determinants of all Hurwitz matrices are positive:

$$detH_j > 0, \quad j = 1, \cdots, n.$$

By Routh-Hurwitz criteria the roots of the quadratic polynomial 3.14 are both negative if the coefficients a_1 and a_2 are both positive following which we get two conditions,

$$\nu + \gamma + \mu - \beta > 0 \tag{3.15}$$

$$\nu(\gamma + \mu - \beta) - \alpha\vartheta > 0 \tag{3.16}$$

Theorem 3.9 The condition 3.16, for the set of parameters of the model 3.6 implies condition 3.15.

Proof. Let us assume that

$$\nu(\gamma + \mu - \beta) - \alpha\vartheta > 0$$

As α and ϑ are non-negative we have,

$$\begin{aligned} \nu(\gamma + \mu - \beta) &\geq 0 \\ \Rightarrow \nu(\gamma + \mu - \beta) &> -\nu^2 \\ \Rightarrow \nu(\gamma + \mu - \beta) + \nu^2 &> 0 \end{aligned}$$

which in turn implies condition 3.15 ■

If condition 3.16 is true, it is also equivalent to the following expression

$$\frac{\beta}{\gamma + \mu} + \frac{\alpha\vartheta}{\nu(\gamma + \mu)} < 1$$

This gives us the reproduction number given by

$$\mathcal{R}_0^J = \frac{\beta}{\gamma + \mu} + \frac{\alpha\vartheta}{\nu(\gamma + \mu)} \tag{3.17}$$

so that if $\mathcal{R}_0^J < 1$ it implies both 3.15 and 3.16 are true, which in turn gives us that the eigen values of the Jacobian are all negative. This guarantees that the disease-free equilibrium is locally asymptotically stable when $\mathcal{R}_0^J < 1$. In this expression, $R_{H_H} = \frac{\beta}{\gamma+\mu}$ can be defined as the secondary infections in the susceptible host population due to the infective host introduced. This is also the product of infection rate and death-adjusted infectious period that is given as the reproduction number for the endemic *SIR* model, which is nothing but a *SIR* model with vital dynamics (See pp. 607-608 in [29]). The second term is the combination of two terms.

- $R_{H_V} = \frac{\vartheta}{\gamma+\mu}$ which is the number of secondary infections one infected host produces in the whole susceptible population of vectors.

– $R_{V_H} = \frac{\alpha}{\nu}$ which is the number of secondary infections one infected vector will produce in an entirely susceptible host population (see also pp. 108-109 in [41]).

So the reproduction number using the Jacobian approach is given by

$$\mathcal{R}_0^J = R_{H_H} + R_{H_V} R_{V_H} \tag{3.18}$$

Additionally, the Jacobian at DFE has all its eigenvalues with non-zero real parts, which in turn guarantees the hyperbolicity of the disease-free equilibrium.

Theorem 3.10 $\mathcal{R}_0^J > 1 \iff \nu(\gamma+\mu-\beta) - \alpha\vartheta < 0$. The endemic equilibrium exists and is unique provided $\mathcal{R}_0^J > 1$

Proof. By the definition of $\mathcal{R}_0^J$, we have that

$$\begin{aligned} & \mathcal{R}_0^J > 1 \\ \iff & \frac{\beta}{\gamma+\mu} + \frac{\alpha\vartheta}{\nu(\gamma+\mu)} > 1 \\ \iff & \nu\beta + \alpha\vartheta > \nu(\gamma+\mu) \\ \iff & \nu(\gamma+\mu-\beta) - \alpha\vartheta < 0 \end{aligned}$$

By theorem 3.5 and corollary 3.6, we can easily deduce that the endemic equilibrium exists and is unique only if $\mathcal{R}_0^J > 1$ ■

The next generation matrix approach(20, 21)

To find the reproduction number using the next generation matrix we have to divide the compartments into disease(x) and non-disease(y) compartments. The flux part of the set of equations involving x is divided into a disease flux($\mathcal{F}$), which includes all terms that define the new infections, and the term $\mathcal{V}$ which represents the transition terms like death, recovery etc.

We choose $x = [I,V]^T$ and $y = [S,R,U]^T$. The terms $\mathcal{F}$ and $\mathcal{V}$ are given below

$$\mathcal{F} = \begin{pmatrix} \alpha VS + \beta IS \\ \vartheta IU \end{pmatrix} \quad \text{and} \quad \mathcal{V} = \begin{pmatrix} (\gamma+\mu)I \\ \nu V \end{pmatrix}$$

In the derivation of the next generation matrix, we consider this idea of analysing the stability of the linearised system at DFE. For this, we rewrite the variable vector as $X = (I,V,S,R,U)^T = (x,y)^T$. The linearised system at DFE is

$$X' = DF_{X_0}(X - X_0)$$

Since X is rewritten, 3.13 is also rearranged as

$$DF_{X_0} = \begin{pmatrix} -(\gamma+\mu)+\beta & \alpha & 0 & 0 & 0 \\ \vartheta & -\nu & 0 & 0 & 0 \\ -\beta & -\alpha & -\mu & 0 & 0 \\ \gamma & 0 & 0 & -\mu & 0 \\ -\vartheta & 0 & 0 & 0 & -\nu \end{pmatrix} \tag{3.19}$$

which is of the block matrix form

$$DF_{X_0} = \begin{pmatrix} \hat{F}-\hat{V} & 0 \\ J_{21} & J_{22} \end{pmatrix}$$

where

$$\hat{F} = \frac{\partial \mathcal{F}}{\partial x}|_{DFE} = \begin{pmatrix} \beta & \alpha \\ \vartheta & 0 \end{pmatrix} \quad \text{and} \quad \hat{V} = \frac{\partial \mathcal{V}}{\partial x}|_{DFE} = \begin{pmatrix} \gamma+\mu & 0 \\ 0 & \nu \end{pmatrix}$$

The disease-free equilibrium is locally asymptotically stable if all the eigenvalues of the Jacobian matrix have negative real parts. The eigenvalues of DF_{X_0} are nothing but the eigenvalues of $\hat{F}-\hat{V}$ and J_{22}. Since J_{22} is clearly a diagonal matrix with negative real numbers as entries we need to only focus on the eigenvalues of $\hat{F}-\hat{V}$. In other words, the linear stability of the linearised system of 3.12 is completely determined by the linear stability of

$$x' = (\hat{F}-\hat{V})x$$

We may notice that the quadratic polynomial deduced in the derivation of the reproduction number using the Jacobian approach is the characteristic polynomial of $\hat{F}-\hat{V}$.

Lemma 3.11 — see Lemma 2 in (20). If F is non-negative and V is a non-singular M-matrix, then $\mathcal{R}_0 = \rho(FV^{-1}) < 1$ if and only if all the eigenvalues of $(F-V)$ have negative real parts.

A proof for this is given in Lemma 2(also see Lemma 1) of [20]. The eigenvalues of $\hat{F}-\hat{V}$ has negative real parts if and only if $\rho(\hat{F}\hat{V}^{-1}) < 1$. By the definition of the basic reproduction number, for a classical epidemic SIR model R_0 can be expressed as the product of the expected duration of the infectious period and the rate at which secondary infections occur(see [29] p. 605) whereas, for the SIR model with vital dynamics, R_0 is the product of contact rate and the death-adjusted infectious period which is given by $\frac{1}{\gamma+\mu}$, where μ is the death rate of the population under consideration(see [29] p. 608). On a general compartmental epidemic model, this heuristic definition is not sufficient. Rather a mathematical explanation in [20] shows that the next generation matrix FV^{-1} is in compliance with the heuristic definition of the process of producing secondary infections due to the presence of one infected individual(see also [21]).

In this case, the next generation matrix is $K = \hat{F}\hat{V}^{-1}$ and the basic reproduction number($\mathcal{R}_0^{NGM}$) is the spectral radius of this matrix. Thereby

$$\mathcal{R}_0^{NGM} = \rho(K) = \frac{\beta}{2(\gamma+\mu)} + \left[\left(\frac{\beta}{2(\gamma+\mu)}\right)^2 + \frac{\alpha\vartheta}{\nu(\gamma+\mu)}\right]^{\frac{1}{2}} \tag{3.20}$$

$$= \frac{R_{H_H}}{2} + \left[\left(\frac{R_{H_H}}{2}\right)^2 + R_{H_V}R_{V_H}\right]^{\frac{1}{2}} \tag{3.21}$$

Though, we failed to interpret this expression as the number of secondary infections, one infectious host individual will produce in a completely susceptible population, as in the case of the threshold value obtained through the Jacobian approach.

3.2.3 Relationship between $\mathcal{R}_0^{NGM}$ and $\mathcal{R}_0^J$

In a similar compartmental model, that describes the dynamics of vector-borne diseases given in [41] they have established an obvious relationship between $\mathcal{R}_0^{NGM}$ and $\mathcal{R}_0^J$ which is that the reproduction number obtained using the Jacobian approach is the square of the reproduction number obtained using the next generation matrix approach. This holds for purely vector-borne(for eg: dengue) disease models. In this case, we are having a human-human spread as well which gives us a relationship with the two threshold values that is not trivial. In this case, we can establish that

$$\mathcal{R}_0^J = \mathcal{R}_0^{NGM^2} + 2a(1-\mathcal{R}_0^{NGM}) \tag{3.22}$$

using 3.17 and 3.20, where $a = \frac{\beta}{2(\gamma+\mu)}$. Even though $\mathcal{R}_0^{NGM}$ could not be interpreted as a reproduction number, both $\mathcal{R}_0^{NGM}$ and $\mathcal{R}_0^J$ hold certain relationships by which it can be proven mathematically that, $R_0 > 1$ implies that the disease pertains(asymptotic stability of Endemic equilibrium) and $R_0 < 1$ implies that the disease dies out ()asymptotic stability of DFE) which is enough for them to be named as reproduction numbers for a disease spread model.

Theorem 3.12 Let $y = x^2 + 2a(1-x)$ where $a, x, y > 0$, for $2a < 1$, we have

(a) $x < 1$ implies $y < 1$

(b) $x > 1$ implies $y > 1$

Proof. (a) Let us assume that $x < 1$. Then we have

$$x^2 < x \tag{3.23}$$

Since it is given that $2a < 1$ and since $1 - x > 0$ we have that

$$2a(1-x) < 1-x \tag{3.24}$$

Adding 3.23 and 3.24 gives us

$$y = x^2 + 2a(1-x) < x + 1 - x = 1$$

(b) Let us assume that $x > 1$ which gives us

$$x^2 > x \tag{3.25}$$

In this case $x-1>0$. Since $2a<1$, we have

$$\begin{aligned} & 2a(x-1) < x-1 \\ \implies & 1 < x-2ax+2a \\ \underset{3.25}{\implies} & 1 < x-2ax+2a < x^2-2ax+2a = y \end{aligned}$$

■

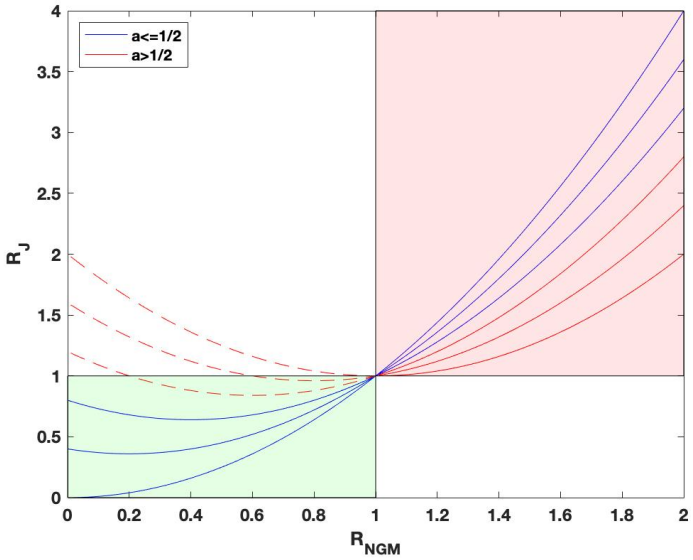

Figure 3.1 – The figure shows $\mathcal{R}_0^J$ as a function of $\mathcal{R}_0^{NGM}$. Here we have used the relation 3.22. The function is plotted for different values of a and it is clearly seen that for $0 < a \leq \frac{1}{2}$ only the required threshold property holds. For $a > \frac{1}{2}$, we may ignore the dashed region, because given a and b are positive, the case of $a > \frac{1}{2}$ and $\mathcal{R}_0^{NGM}$ being less than 1 is not feasible.

Theorem 3.13 For $\mathcal{R}_0^{NGM}$ and $\mathcal{R}_0^J$ we have

(a) $\mathcal{R}_0^{NGM} \leq 1 \iff \mathcal{R}_0^J \leq 1$

(b) $\mathcal{R}_0^{NGM} > 1 \iff \mathcal{R}_0^J > 1$

Proof. For simplicity we may use, $a = \frac{\beta}{2(\gamma+\mu)}$ and $b = \frac{\alpha\vartheta}{\nu(\gamma+\mu)}$. Note that $a > 0$ and $b > 0$ for all parameters being positive. Let $a > \frac{1}{2}$,

$$a^2 > \frac{1}{4} \implies a^2 + b > a^2 > \frac{1}{4}$$

$$\implies (a^2+b)^{\frac{1}{2}} > \frac{1}{2}$$
$$\implies a+(a^2+b)^{\frac{1}{2}} > 1 \implies \mathcal{R}_0^{NGM} > 1$$

Similarly, if $a > \frac{1}{2}$, we have $\mathcal{R}_0^J > 1$. So for $\mathcal{R}_0^{NGM} \leq 1$ or $\mathcal{R}_0^J \leq 1$, due to the positivity of b, $a \leq \frac{1}{2}$ should hold.

(a) If $\mathcal{R}_0^{NGM} \leq 1$ we have $a \leq \frac{1}{2}$ and this implies $\mathcal{R}_0^J \leq 1$ by theorem 3.12 part (a).

On the other hand if $\mathcal{R}_0^J < 1$

$$\implies 2a+b < 1$$
$$\implies b < 1-2a$$
$$\implies a^2+b < 1-2a+a^2$$
$$\underset{1-a>0}{\implies} (a^2+b)^{\frac{1}{2}} < 1-a$$
$$\implies \mathcal{R}_0^{NGM} < 1$$

(b) If $a < \frac{1}{2}$ and $\mathcal{R}_0^J > 1$, a similar argument as above proves that $\mathcal{R}_0^{NGM} > 1$
On the other hand, for $a < \frac{1}{2}$, if $\mathcal{R}_0^{NGM} > 1$ we have $\mathcal{R}_0^J > 1$, by part (b) of theorem 3.12.
For $a < \frac{1}{2}$, we have already shown that both $\mathcal{R}_0^{NGM}$ and $\mathcal{R}_0^J$ are greater than 1.

■

As we have already seen that $\mathcal{R}_0^J < 1$ ensures local asymptotic stability of 3.12, from theorem 3.13, we may conclude that mathematically $\mathcal{R}_0^{NGM}$ also can be seen as the threshold value that determines the stability of DFE.

3.2.4 Global Stability using Lyapunov function

We make use of a matrix-theoretic method suggested in [47] to find out a Lyapunov function at the disease-free equilibrium and the graph-theoretic method to construct a Lyapunov function at the endemic equilibrium

Definition 3.14 (Sharp Threshold Property) A given model satisfies the sharp threshold property if it holds that

the DFE is globally asymptotically stable for $R_0 \leq 1$

- there is a unique endemic equilibrium X^* that is globally asymptotically stable in the interior of the feasible region for $R_0 > 1$

Theorem 3.15 Let

$$Q = \frac{R_0 I}{\alpha} + \frac{V}{\nu},$$

then $Q' \leq 0$ when $R_0 \leq 1$ in $\Gamma = \{X : 0 \leq X(i) \leq 1, S+I+V \leq 1, U+V \leq 1\}$ where $X = (S,I,R,U,V)$,

Proof. We begin the proof by establishing an important result with respect to $\mathcal{R}_0^{NGM}$ which is used further. From the relation 3.22 between $\mathcal{R}_0^{NGM}$ and $\mathcal{R}_0^{J}$, we can deduce that R_0 holds the following equation,

$$R_0 = \frac{\beta}{\gamma+\mu} + \frac{\alpha\vartheta}{\nu(\gamma+\mu)R_0} \tag{3.26}$$

for $R_0 = \mathcal{R}_0^{NGM}$. From the expression of Q, we have that,

$$\begin{aligned}
Q' =& \frac{R_0}{\alpha} I' + \frac{V'}{\nu} \\
=& \frac{R_0}{\alpha}\left(-(\gamma+\mu)I + \alpha VS + \beta IS\right) + \frac{1}{\nu}\left(-\nu V + \vartheta IU\right) \\
=& \left(\frac{R_0}{\alpha}\left(-(\gamma+\mu)I\right) - V\right) + \left(\frac{R_0}{\alpha}\left(\alpha VS + \beta IS\right) + \frac{1}{\nu}\vartheta IU\right) \\
=& \left(\frac{R_0}{\alpha}\left(-(\gamma+\mu)I\right) - V + R_0 V + \frac{R_0}{\alpha\beta} I + \frac{1}{\nu}\vartheta I\right) \\
&+ \left(-R_0 V - \frac{R_0}{\alpha\beta} I - \frac{1}{\nu}\vartheta I + R_0 VS + \frac{R_0}{\alpha\beta} IS + \frac{1}{\nu}\vartheta IU\right) \\
=& \frac{R_0}{\alpha}(\gamma+\mu)I\left(-1 + \frac{\beta}{\gamma+\mu} + \frac{\alpha\vartheta}{\nu(\gamma+\mu)R_0}\right) + (R_0-1)V \\
&- \left(R_0 V(1-S) + \frac{R_0}{\alpha\beta} I(1-S) + \frac{1}{\nu}\vartheta I(1-U)\right)
\end{aligned}$$

Here it is evident that

$$W(S,I,V) = \left(R_0 V(1-S) + \frac{R_0}{\alpha\beta} I(1-S) + \frac{1}{\nu}\vartheta I(1-U)\right) \geq 1$$

on the set Γ. So we have that,

$$\begin{aligned}
Q' \leq& \frac{R_0}{\alpha}(\gamma+\mu)I\left(-1 + \frac{\beta}{\gamma+\mu} + \frac{\alpha\vartheta}{\nu(\gamma+\mu)R_0}\right) + (R_0-1)V \\
\underset{3.26}{=}& \frac{R_0}{\alpha}(\gamma+\mu)I(-1+R_0) + (R_0-1)V \\
=& (R_0-1)\left(\frac{R_0}{\alpha}(\gamma+\mu)I + V\right)
\end{aligned}$$

Since $\left(\frac{R_0}{\alpha}(\gamma+\mu)I + V\right) \geq 0$ we can conclude that

$$Q' \leq 0 \text{ only if } R_0 \leq 1.$$

■

Theorem 3.16 The SIRUV model 3.6 holds the sharp threshold property.

Proof. To prove the first condition of the sharp threshold property we are finding the Lyapunov function corresponding to the DFE. We make use of the theorem 2.1 of [47]. For finding the Lyapunov function we need to find the left eigenvector of $\hat{V}^{-1}\hat{F}$ which is given by

$$w = \begin{pmatrix} \frac{R_0(\gamma+\mu)}{\alpha} \\ 1 \end{pmatrix}$$

The Lyapunov funcion is given by $Q = w^T \hat{V}^{-1} x$

$$Q = \frac{R_0 I}{\alpha} + \frac{V}{\nu}$$

where R_0 here denotes the $\mathcal{R}_0^{NGM}$. We prove in the theorem 3.15 that $Q' \leq 1$ in $\Gamma = \{X : 0 \leq X_i \leq 1, S+I+R \leq 1, U+V \leq 1\}$, where $X = (S,I,R,U,V)$if $R_0 = \mathcal{R}_0^{NGM} \leq 1$, and thus Q is a Lyapunov function for the DFE. Also, the only invariant set where $x = 0$ is a singleton set containing the DFE. So by LaSalle's invariance principle[37], DFE is globally asymptotically stable in Γ. Also by theorem 2.2 of [47], we have that the Lyapunov function Q can also be used to prove the uniform persistence and thus establish the existence of an endemic equilibrium. Therefore theorem 2.2 of [47] gives that if $R_0 > 1$, then the DFE is unstable and that system 3.6 is uniformly persistent and there exists at least one endemic equilibrium.

We have already proven the existence of a unique endemic equilibrium given $\mathcal{R}_0^J > 1$ in 3.10. And since we have that the threshold condition is equivalent for $\mathcal{R}_0^J$ and $\mathcal{R}_0^{NGM}$ by 3.13, it is evident that a unique endemic equilibrium exists also when $R_0 = \mathcal{R}_0^{NGM} < 1$.

Now we prove that when $R_0 > 1$ we have global asymptotic stability of endemic equilibrium. For this, we construct the Lyapunov function for endemic equilibrium using the graph-theoretic method suggested in [47]. Let us define

$$\begin{aligned} D_1 &= S - S^* - S^* ln\frac{S}{S^*} + I - I^* - I^* ln\frac{I}{I^*} \\ D_2 &= \frac{1}{2}(U - U^*)^2 \\ D_3 &= V - V^* - V^* ln\frac{V}{V^*} \end{aligned}$$

We show that there exist constants a_{ij} and functions $G_{ij} : Z \to \mathbb{R}$ for which we can deduce the inequality $D_i' \leq \sum_{j=1}^{n} a_{ij} G_{ij}(z)$ for $z \in Z$ where $Z = int(\Gamma)$, where Γ is the feasible region of model 3.6.

$$\begin{aligned} D_1' &= S' - S^* \left(\frac{S^*}{S}\frac{S'}{S^*}\right) + I' - I^* \left(\frac{I^*}{I}\frac{I'}{I^*}\right) \\ &= \frac{S - S^*}{S} S' + \frac{I - I^*}{I} I' \end{aligned}$$

The first term of this equation can be written as

$$\frac{S - S^*}{S} S' = \frac{S - S^*}{S}(\mu - \mu S - \alpha V S - \beta I S).$$

At endemic equilibrium, precisely by using 3.8a, we have

$$\mu = \mu S^* + \alpha V^* S^* + \beta I^* S^*.$$

Using this we get

$$\begin{aligned}\frac{S-S^*}{S}S' &= \frac{S-S^*}{S}(\mu(S^*-S)+\alpha(V^*S^*-VS)+\beta(I^*S^*-IS)) \\ &\leq \frac{S-S^*}{S}(\alpha(V^*S^*-VS)+\beta(I^*S^*-IS)) \\ &= \alpha V^*S^*(1-\frac{VS}{V^*S^*}-\frac{S^*}{S}+\frac{V}{V^*})+\beta I^*S^*(1-\frac{IS}{I^*S^*}-\frac{S^*}{S}+\frac{I}{I^*})\end{aligned}$$

Now we make use of the inequality $1+x \leq -lnx$ provided $x \geq 0$ to get

$$1-\frac{S^*}{S} \leq -ln\frac{S^*}{S} = -ln\frac{VS}{V^*S^*} - ln\frac{V}{V^*} \tag{3.27}$$

and we make use of the same method to get the inequality (which is used in the second part)

$$1-\frac{S^*}{S} \leq ln\frac{IS}{I^*S^*} - ln\frac{I}{I^*}$$

which together give that

$$\frac{S-S^*}{S}S' \leq \alpha V^*S^*(ln\frac{VS}{V^*S^*}-\frac{VS}{V^*S^*}-ln\frac{V}{V^*}+\frac{V}{V^*})+\beta I^*S^*(ln\frac{IS}{I^*S^*}-\frac{IS}{I^*S^*}-ln\frac{I}{I^*}+\frac{I}{I^*})$$

Again by making use of the logarithmic inequality we get

$$1-\frac{S}{S^*} \leq -ln\frac{S}{S^*} = -ln\frac{SI}{S^*I^*} + ln\frac{I}{I^*}$$

and

$$1-\frac{SV}{S^*V^*}\frac{I^*}{I} \leq -ln\frac{SV}{S^*V^*}\frac{I^*}{I} = -ln\frac{SV}{S^*V^*} + ln\frac{I}{I^*}$$

which in turn gives us the following inequality,

$$\frac{I-I^*}{I}I' \leq \beta I^*S^*(\frac{IS}{I^*S^*}-ln\frac{IS}{I^*S^*}-\frac{I}{I^*}+ln\frac{I}{I^*})+\alpha V^*S^*(\frac{VS}{V^*S^*}-ln\frac{VS}{V^*S^*}+ln\frac{I}{I^*}-\frac{I}{I^*})$$

This collectively gives us

$$D_1' \leq \alpha S^*V^*(-ln\frac{V}{V^*}+\frac{V}{V^*}+ln\frac{I}{I^*}-\frac{I}{I^*}) = a_{13}G_{13} \tag{3.28}$$

By differentiating D_2 and using equation 3.8d we get

$$\begin{aligned}D_2' &= (U-U^*)U' \\ &= (U-U^*)(\nu(U^*-U)+(U-U^*)\vartheta(I^*U^*-IU) \\ &\leq (U-U^*)\vartheta(I^*U^*-IU^*+IU^*-IU) \\ &= (U-U^*)\vartheta U^*(I^*-I)+(U-U^*)\vartheta(U^*-U)I \\ &= (U-U^*)\vartheta U^*(I^*-I)-\vartheta(U-U^*)^2I \\ &\leq \vartheta U^*(U-U^*)(I^*-I)\end{aligned}$$

We could write this inequality because $\vartheta(U-U^*)^2 I$ is positive. We also have that

$$\vartheta(U-U^*) = (V-V^*).$$

By using this we have

$$\begin{aligned} D_2' &\leq \vartheta(V-V^*)(I^*-I) \\ &= a_{23}G_{23} \end{aligned} \tag{3.29}$$

Similarly

$$\begin{aligned} D_3' &= (1-\frac{V^*}{V})V' \\ &= (1-\frac{V^*}{V})(-\nu V + \vartheta I(1-V)) \\ &\underset{3.8e}{=} (1-\frac{V^*}{V})(-\vartheta I^*(1-V^*)\frac{V}{V^*} + \vartheta I(1-V)) \\ &= (1-\frac{V^*}{V})\vartheta(-\frac{I^*V}{V^*} + I^*V + I - VI) \\ &= \vartheta(-\frac{V}{V^*} + 1 + \frac{I}{I^*} - \frac{I}{I^*}\frac{V^*}{V}) + \vartheta I^* V^*(\frac{V}{V^*} - 1 - \frac{VI}{V^*I^*} + \frac{I}{I^*}) \\ &\leq \vartheta I^*(-\frac{V}{V^*} + \frac{I}{I^*} - ln\frac{I}{I^*} + ln\frac{V}{V^*}) + \vartheta(I-I*)(V-V*) \end{aligned}$$

This inequality can be simplified as

$$D_3' \leq a_{31}G_{31} + a_{32}G_{32} \tag{3.30}$$

where $a_{31} = \vartheta I^*$ and $a_{32} = \vartheta$. The required Lyapunov function is defined as

$$D = c_1 D_1 + c_2 D_2 + c_3 D_3$$

which returns that $D' \leq 0$, using 3.28, 3.29 and 3.30, for the choice $c_1 = \vartheta I^*$, $c_2 = \alpha\frac{S^*V^*}{U*}$ and $c_3 = \alpha S^* V^*$. Even though in this case it is evident that $D' \leq 0$, without going deeper into the very the general setting of the graph-theoretical results used in [47], we see that the matrix $A = [a_{ij}]$ forms a weighted directed graph containing three nodes and two cycles which could be used in Theorem 3.5 of [47]. The cycle comprising of nodes 1 and 3 holds that the associated functions G_{13} and G_{31} add up to zero. The same holds for functions associated with nodes 3 and 2. In the current setting, we need not use many details of the graph-theoretic method as it is evident that $D' <\leq 0$ in $int(\Gamma)$, though we acknowledge the fact that this simplified approach was obtained in an attempt to apply the graph-theoretic method in [47].

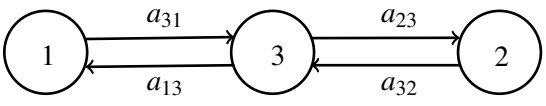

Since D is not a strict Lyapunov function, we need to utilize the Lasalle Invariance Principle to obtain global asymptotic stability of the endemic equilibrium. Since the largest invariant set in which $D' = 0$ is $W = \{X^*\}$, we conclude that X^* is *globally asymptotically stable*(GAS)using the Lasalle Invariance Principle[31]. ■

To conclude with the discussion of global asymptotic stability, we summarize that when $R_0 \leq 1$, DFE is the only equilibrium for the system 3.6 and it is GAS in the positively invariant set of model 3.6, namely $\Gamma = \{X = (S,I,R,U,V) : 0 \leq X(i) \leq 1, S+I+R \leq 1, U+V \leq 1\}$ and when $R_0 > 1$ there also exists a unique endemic equilibrium in the interior of Γ. Then we have that in the interior of Γ the endemic equilibrium is GAS.

Remark 3.17 In the case, $R_0 = 1$, we see that $Q' = 0$ implies $W(S,I,V) = 0$ and it is true if and only if, $(S,U) = (1,1)$ or $(I,V) = (0,0)$. In both cases, we can verify that the largest invariant set for 3.6 where $(S,U) = (1,1)$ or $(I,V) = (0,0)$ is the singleton set with DFE.

Remark 3.18 The threshold point $R_0 = 1$ corresponds to a transcritical bifurcation[20, 55] for model 3.6. There is an exchange of stability occurring at $R_0 = 1$.

3.3 Numerical Results

For numerical studies, we have used model 3.7 in this section. Firstly we have set the parameters to certain values for which the model exhibits the scenario of disease dying out or the DFE is asymptotically stable, and another set of parameters for which the endemic equilibrium being asymptotically stable. An exemplary scenario is simulated with the choice of parameters as per Table 3.1. The death rate(birth rate) of hosts and vectors is taken as the reciprocal of the average life expectancy. Here we use the value 65 years as the life expectancy of humans and 10 days as that of vectors, as per [45]. The population size of hosts is fixed as $N = 7000$ and the vector population's size is fixed as $M = 10^5$. The proportion of initial susceptible hosts, infected hosts and infected vectors are taken as $[S,I,V] = [0.2032, 0.0142, 0.0617]$. For this initial condition and the set of parameters, the two scenarios are obtained by varying the rate of recovery, γ. In figure 3.2,

Parameter	value	units
μ	$1/(65*365)$	$[days^{-1}]$
ν	$1/10$	$[days^{-1}]$
α	0.008	$[days^{-1}]$
β	0.01	$[days^{-1}]$
ϑ	0.4	$[days^{-1}]$

Table 3.1 – Parameters are fixed except the recovery rate

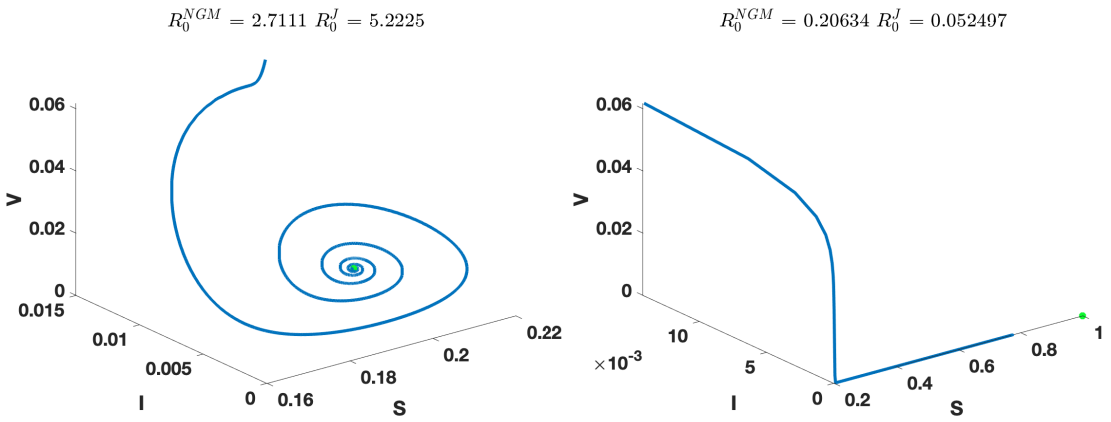

(a) For $R_0 > 1$ Endemic equilibrium EE is asymptotically stable

(b) For $R_0 < 1$ disease-free equilibrium DFE is asymptotically stable

Figure 3.2 – Both figures have a final time $t = 30000$ days. The figures are plotted for the parameters defined above in Table 3.1. The first case is for the choice of $\gamma = 0.008$. In Figure (a) we can see that a spiral is formed and as time tends to ∞ the solution curve is approaching the endemic equilibrium. In the title of the figure, the two reproduction numbers can be seen as greater than 1. At the same time for the choice of $\gamma = 0.8$, we can see that the solution curve is approaching the disease-free equilibrium $[1,0,0]$ and the reproduction numbers are less than 1 for this case.

part (a) we can see that, for the choice of $\gamma = 0.008$ we obtained the endemic equilibrium to be asymptotically stable. At equilibrium the proportions are given by $S^* = 0.1939$, $I^* = 0.0042$ and $V^* = 0.0166$. The number of infected (i^*) hosts can be deduced as $i^* = N * I^* \approx 29$. Similarly s^* and v^* can be obtained from S^* and V^*. Then the recovered number of people at equilibrium can be obtained using $r^* = N - s^* - i^*$. Similarly, the number of susceptible mosquitoes at equilibrium can be obtained as $M - V^*$. In Figure 3.2, part (b), we see that for the choice of $\gamma = 0.8$, the disease-free equilibrium is asymptotically stable. The phase portraits are given in Figure 3.2.

It is also interesting to see that for the case $R_0 > 1$, however close the initial condition is to the DFE, the trajectory goes asymptotically towards the equilibrium point. To exhibit this property we use the same set of parameters as in [35] which is used for simulations of a $SIRUV$-vector model. The set of parameters is as given in Table 3.2. The population size of hosts is fixed as $N = 10^5$ and the vector population's size is fixed as $M = 10 * N = 10^6$. The only parameter that has to be chosen is the host-host transmission rate β. This is chosen as $\beta = 1/7$. The sizes of host and vector populations are the same as in the previous simulation study. The simulation results can be seen in the phase portraits given in Figure 3.3.

Parameter	value	units
μ	$1/(72*365)$	$[days^-1]$
ν	$1/10$	$[days^-1]$
α	$1/7$	$[days^-1]$
ϑ	5ν	$[days^-1]$
γ	$1/14$	$[days^-1]$

Table 3.2 – Parameters in [35] are defined per year, which we have converted to parameters per day

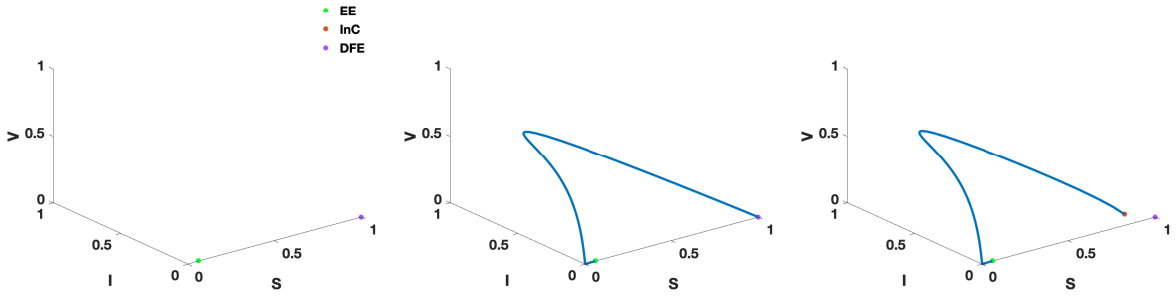

(a) $I_0 = 0$ **(b)** $I_0 = 0.001$ **(c)** $I_0 = 0.1$

(d) $I_0 = 0.3$ **(e)** $I_0 = 0.7$ **(f)** $I_0 = 1$

Figure 3.3 – In fig (a) the initial condition InC(red) being $(1,0,0)$ the trajectory is not seen because DFE(violet) is an equilibrium. In Fig (b) it can be seen that the disease-free equilibrium (DFE) is very close to the initial point. Even then the trajectory is moving towards the endemic equilibrium(green). The same does the trajectory for any other initial condition in the interior of Γ as seen in Figures(c), (d), (e) and (f). All plots are made for a final time of 5 years.

The simulations are done for initial conditions where the number of infected vectors always remains zero initially. The initial infected proportion of hosts I_0 is varied within the set of values $\{0\%,0.1\%,10\%,30\%,70\%,100\%\}$. The susceptible proportion of hosts is taken as $1-I_0$. For the chosen set of parameters, the reproduction numbers are $\mathcal{R}_0^{NGM} = 2.5021$ and $\mathcal{R}_0^{J} = 5.7085$. The endemic equilibrium is

$$EE = (0.0683, 4.9605 * 10^{-4}, 0.0024).$$

3.3.1 Parameter Analysis

For studying the dependence of $\mathcal{R}_0^{NGM}$ on the recovery rate(γ) and the transmission rates among humans(β) and that from vectors to humans(α) we have plotted in Figure 3.4, the reproduction number $\mathcal{R}_0^{NGM}$, as a function of α and β for different values of γ ranging between 0.25, 1 and 2.5. All other parameters and population sizes are fixed to the constants as per the following table.

μ	ν	ϑ
10/(1000*365)	1/14	0.4

Even though the host population and vector population sizes do not play any role in the formulation of reproduction number, we have taken the case that $N = 5000$ and $M = 10000$. Within the surface plot itself the lighter-colored region represents the case where $\mathcal{R}_0^{NGM} < 1$ and the darker part represents the values for which $\mathcal{R}_0^{NGM} > 1$. In the 2D view in Figure 3.4, the function $\mathcal{R}_0^{NGM}$ is plotted for three different cases by varying the recovery rate and below each line representing γ value we can see the darker region(including the regions for the smaller values of γ) which represents the area where $\mathcal{R}_0^{NGM} < 1$ and the whole region above this line is representing the case when $\mathcal{R}_0^{NGM} > 1$. We see that, as the recovery rate increases the chances of $\mathcal{R}_0^{NGM} < 1$ increase and thus the disease free equilibrium is globally asymptotically stable for more combinations of β and α.

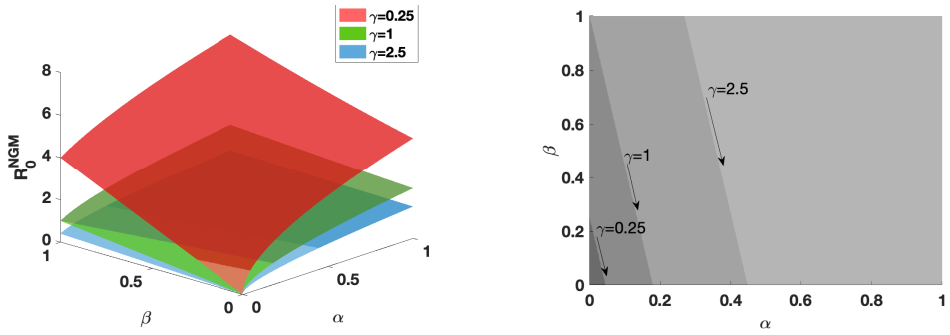

Figure 3.4 – For different values of the recovery rate γ, the reproduction number $\mathcal{R}_0^{NGM}$ is plotted as a function of the vector-host transmission rate α and host-host transmission rate β. In the first figure, a 3-dimensional view can be seen, where the lighter region represents the values of α and β for which $\mathcal{R}_0^{NGM} < 1$ and the whole darker region represents the case when $\mathcal{R}_0^{NGM} > 1$. For the vector-host transmission rate α and host-host transmission rate β for $\gamma = 0.25$ the set of parameters for which $\mathcal{R}_0^{NGM} < 1$ is smaller compared to a possible combination of α and β, for which the reproduction number is greater than 1. As γ gets larger the set of values α and β for which $\mathcal{R}_0^{NGM} < 1$ is increasing. In the second figure we have a 2-dimensional view of this, where for each γ the region below each line represents the case $\mathcal{R}_0^{NGM} < 1$, and that above the line represents the case in which $\mathcal{R}_0^{NGM} > 1$. A similar trend is seen in this 2-dimensional view as well, that as γ increases the range of the set of α and β values for which $\mathcal{R}_0^{NGM} < 1$ is also getting bigger in size.

4 Vector-host SIRUV model- A different scaling

In Chapter 3, we have seen how the *SIRUV* model is derived for diseases that involve a transmission due to an interaction between vectors and hosts and also due to a host-host interaction. We have done the mathematical analysis on the normalized model 3.6. In this chapter we redefine the parameters and obtain a similar model but with a different set of coefficients. Unlike model 3.6, a major difference is that the ratio of sizes of the vector as well as host populations directly appears in the normalized system of differential equations and we would see the differences in both models through the parameters. The mathematical analysis of the new model would be similar to the model 3.6.

4.1 Model Formulation and Analysis

As in Chapter 3, we have the host and vector populations divided into mutually exclusive compartments namely, s, i, r, u and v which represent the size of each compartment in numbers. The total number of hosts(N) and vectors(M) in the system is assumed to remain constant. All parameters like recovery rate, birth rate and death rate of hosts and vectors are defined the same as that of the model in Chapter 3. We consider the vital dynamics due to birth and death as well in this model and make an assumption that the populations under consideration have constant birth and death rates. The birth rate and death rate are assumed to be equal respectively for the host and vector populations. For the host population, we assume that after being infected they get recovered permanently and enter into the compartment r at a constant rate γ.

4.1.1 Redefining the Transmission Parameters

In this section, we propose a different definition for the transmission rates from that of Chapter 3. This also brings a difference in the way the incidence terms are formulated in the new model. The disease transmission parameters are defined as follows,

- The parameter corresponding to host-host interaction, β is defined as the average number of adequate contacts that is happening per infected host with hosts per unit time. The dimension of β is $[time^{-1}]$.
- The parameter corresponding to vector to host incidence, α is defined as the average number of adequate contacts that is happening per infected mosquito with hosts per unit time. The dimension of α is $[time^{-1}][mosquito population^{-1}][host population]$.

- The parameter corresponding to host to vector incidence, ϑ is defined as the average number of adequate contacts that is happening per infected host with mosquitoes per unit time. The dimension of ϑ is $[time^{-1}][hostpopulation^{-1}][mosquitopopulation]$.

The incidence terms appearing in the new model are described as follows,

Host to Host incidence: If unit time is a day, the total number of contacts that an infected host has with hosts in a day is given by β, out of which $\beta\frac{i}{N}$ or $\beta\frac{r}{N}$ does not result in an infection. The proportion of all adequate contacts of this infected host with hosts that lead to an infection is therefore those with the susceptible fraction of the host population, given by $\beta\frac{s}{N}$. So the total number of infections as a whole would be $\beta\frac{s}{N}i$.

Vector to Host incidence: By its definition, α is from the perspective of an infected mosquito. In a day it has α contacts with hosts and the proportion of these contacts with infected or recovered individuals does not lead to an infection. As above, the average number of adequate contacts this mosquito has with susceptible proportion, given by $\alpha\frac{s}{N}$ only leads to incidence from vector to host. The total number of such incidences is given by $\alpha\frac{s}{N}v$.

Host to Vector incidence: The host to vector incidence is through the parameter ϑ, which is seen from the perspective of an infected host, where this individual has ϑ adequate contacts with mosquitoes in a day, out of which, only $\vartheta\frac{u}{M}$ contacts lead the infection to pass from this infected host to the vector population. And $\vartheta\frac{u}{M}i$ is the total number of such incidences.

The dynamics of change in the population size of each compartment is thereby described by the following *SIRUV* model.

$$\begin{aligned}
\frac{ds}{dt} &= \mu(N-s) - \frac{\alpha}{N}sv - \frac{\beta}{N}si \\
\frac{di}{dt} &= \frac{\alpha}{N}sv + \frac{\beta}{N}si - (\gamma+\mu)i \\
\frac{dr}{dt} &= \gamma i - \mu r \\
\frac{du}{dt} &= \nu M - \nu u - \frac{\vartheta}{M}ui \\
\frac{dv}{dt} &= \frac{\vartheta}{M}ui - \nu v
\end{aligned} \tag{4.1}$$

The normalized variables $S=\frac{s}{N}$, $I=\frac{i}{N}$, $R=\frac{r}{N}$, $U=\frac{u}{M}$ and $V=\frac{v}{M}$, gives us the normalized system of differential equations which will be analyzed throughout this chapter. The system is given by,

$$\begin{aligned}
\frac{dS}{dt} &= \mu(1-S) - \frac{\alpha M}{N}SV - \beta IS \\
\frac{dI}{dt} &= -(\gamma+\mu)I + \frac{\alpha M}{N}SV + \beta IS \\
\frac{dR}{dt} &= \gamma I - \mu R \\
\frac{dU}{dt} &= \nu(1-U) - \frac{\vartheta N}{M}UI \\
\frac{dV}{dt} &= -\nu V + \frac{\vartheta N}{M}UI
\end{aligned} \tag{4.2}$$

Structurally model 4.2 is same as the model 3.6. The coefficients are only different. So the majority of the analysis results of 4.2 are the same as that of 3.6. To avoid confusion for the reader the transmission coefficients α, β and ϑ from model 3.6 will be further referred to as α_0, β_0 and ϑ_0. The feasible region is the same for both models, which is given in Theorem 4.1.

Theorem 4.1 The region Γ is a positively invariant set for system 4.2 where the trajectory of an IVP involving system 4.2 and an initial condition from a region satisfying the following conditions will remain in this region for all points in time.

$$\Gamma = \{X = (S,I,R,U,V); 0 \leq S,I,R,U,V \leq 1, S+I+R = 1, U+V = 1\}$$

Proof for this is not given as it is very similar to the proof of the same theorem for model 3.6. Even though we need to get the values of all compartments we need not use all the equations in model 3.6 to find out the values. As we have the properties $S+I+R = 1$ and $U+V = 1$ we need to find the values of S,I and V to get the solution for model 3.6. Also, we may notice that if we add up the first and second equations in 3.6 we get the third equation. Similarly, equations 4 and 5 are simply negations of each other. So we may disregard the two redundant equations in the further study. The sufficient and necessary equations form the new system

$$\begin{aligned}
\frac{dS}{dt} &= \mu(1-S) - \frac{\alpha M}{N} SV - \beta IS \\
\frac{dI}{dt} &= -(\gamma+\mu)I + \frac{\alpha M}{N} SV + \beta IS \\
\frac{dV}{dt} &= -\nu V + \frac{\vartheta N}{M}(1-V)I
\end{aligned} \tag{4.3}$$

4.1.2 Equilibrium points

Model 4.2 also has the two fates asymptotically, either the disease dying out or it prevailing. The disease-free equilibrium(DFE) is $(1,0,0,1,0)$ in this case as well. We are looking for that equilibrium for which $(S,I,R,U,V)(t) \to (S^*,I^*,R^*,U^*,V^*)$ such that $I^* > 0$.

Theorem 4.2 The endemic equilibrium for model 4.2 is

$$(S^*,I^*,R^*,U^*,V^*) = (1 - \frac{(\gamma+\mu)}{\mu} I^*, I^*, \frac{\gamma}{\mu} I^*, \frac{\nu M}{M\nu + \vartheta I^* N}, \frac{\vartheta I^* N}{M\nu + \vartheta I^* N})$$

where I^* is the solution of the quadratic polynomial in the unknown x given by $ax^2 + bx + c = 0$

$$\begin{aligned}
a &= \beta \frac{\vartheta N(\gamma+\mu)}{\mu M} \\
b &= -(\frac{\beta\vartheta N}{M} - \frac{\beta\nu(\gamma+\mu)}{\mu} - \frac{\alpha\vartheta(\gamma+\mu)}{\mu} - (\gamma+\mu)\frac{\vartheta N}{M}) \\
c &= (\gamma+\mu)\nu - \alpha\vartheta - \beta\nu.
\end{aligned}$$

The endemic equilibrium exists in the int(Γ) and is unique provided

$$c = \nu(\gamma+\mu-\beta)-\alpha\vartheta < 0$$

Even though the threshold property for the uniqueness of endemic equilibrium is the same as that of model 3.6, the endemic equilibrium is different here.

4.1.3 The linearized system and Jacobian

Let $X(t) = (S(t), I(t), R(t), U(t), V(t))^T$ be the 5-dimensional variable whose change with respect to time is represented by the system of equations 4.2, which can be simply written as

$$X' = F(X(t)) = \begin{pmatrix} \mu(1-S) - \frac{\alpha M}{N} SV - \beta IS \\ -(\gamma+\mu)I + \frac{\alpha M}{N} SV + \beta IS \\ \gamma I - \mu R \\ \nu(1-U) - \frac{\vartheta N}{M} UI \\ -\nu V + \frac{\vartheta N}{M} UI \end{pmatrix} \tag{4.4}$$

where X' denotes $\frac{d}{dt}X$. The jacobian of the flux part is given by

$$J = \frac{\partial F}{\partial X} = \begin{pmatrix} -\mu - \frac{\alpha M}{N} V - \beta I & -\beta S & 0 & 0 & -\alpha \frac{M}{N} S \\ \frac{\alpha M}{N} V + \beta I & -(\gamma+\mu) + \beta S & 0 & 0 & \alpha \frac{M}{N} S \\ 0 & \gamma & -\mu & 0 & 0 \\ 0 & -\vartheta \frac{N}{M} U & 0 & -\nu & 0 \\ 0 & \vartheta \frac{N}{M} U & 0 & 0 & -\nu \end{pmatrix} \tag{4.5}$$

The ratio of the size of the mosquito population to that of the host population, $c = M/N$ is having an impact on the Jacobian here. For c and $1/c$ appearing in the Jacobian at the same time, we should focus on the condition number of the Jacobian.

4.1.4 Basic reproduction number

In this case, also we analyze the two methods available in the literature to deduce the two reproduction numbers. We see that in this case also the two reproduction numbers can be used interchangeably from a mathematical point of view. However the biological definition of a reproduction number is satisfied for the one deduced through the Jacobian method.

Jacobian matrix approach

To analyse the behaviour of the dynamics locally near the disease-free equilibrium(DFE) we focus on the linearized system at this point, which is given by the variational equation along the solution of 4.4 with initial state X_0 being the DFE. This autonomous linear system[31] is given by

$$W' = DF_{X_0} W$$

where DF_{X_0} denotes the Jacobian matrix of F evaluated at X_0 and $W = X - X_0$. The Jacobian evaluated at the disease free equilibrium is given by,

$$J = \frac{\partial F}{\partial X}|_{(1,0,0,1,0)} = \begin{pmatrix} -\mu & -\beta & 0 & 0 & -\alpha\frac{M}{N} \\ 0 & -(\gamma+\mu)+\beta & 0 & 0 & \alpha\frac{M}{N} \\ 0 & \gamma & -\mu & 0 & 0 \\ 0 & -\vartheta\frac{N}{M} & 0 & -\nu & 0 \\ 0 & \vartheta\frac{N}{M} & 0 & 0 & -\nu \end{pmatrix} \tag{4.6}$$

The characteristic polynomial given by $|J - \lambda I| = 0$ is expressed as

$$[-\mu-\lambda][-\mu-\lambda][-\nu-\lambda][\lambda^2+\lambda(\nu+\gamma+\mu-\beta)+\nu(\gamma+\mu-\beta)-\alpha\vartheta] = 0$$

Even though the Jacobian at DFE is different from that of model 3.6, structurally the characteristic polynomials are the same for both models. So it can be deduced that the reproduction number obtained from the Jacobian is also structurally the same here which is given by

$$\mathcal{R}_0^J = \frac{\beta}{\gamma+\mu} + \frac{\alpha\vartheta}{\nu(\gamma+\mu)} \tag{4.7}$$

Theorem 4.3 $\mathcal{R}_0^J > 1 \iff \nu(\gamma+\mu-\beta)-\alpha\vartheta < 0$. The endemic equilibrium exists and is unique provided $\mathcal{R}_0^J > 1$

Proof. Since we have that $\nu(\gamma+\mu-\beta)-\alpha\vartheta < 0$ is the threshold condition to be satisfied by the parameters to ensure the existence and uniqueness of model 4.2 and this is the same condition for the existence and uniqueness of the endemic equilibrium for the model 3.6. Also, the reproduction number $\mathcal{R}_0^J$ is structurally the same. So we can use the proof of 3.10 here as well to prove that when $\mathcal{R}_0^J > 1$, the endemic equilibrium exists and is unique. ■

Next-generation-matrix approach

For finding the reproduction number using the next generation matrix approach given in [20, 21], we choose the disease compartments vector $x = [I,V]^T$ and the non-disease compartment vector $y = [S,R,U]^T$. The disease incidence part of the flux $\mathcal{F}$ and the vital transition part of the flux function $\mathcal{V}$ of the equations involving x are as given below

$$\mathcal{F} = \begin{pmatrix} \alpha\frac{M}{N}VS + \beta IS \\ \frac{\vartheta N}{M}UI \end{pmatrix} \quad \text{and} \quad \mathcal{V} = \begin{pmatrix} (\gamma+\mu)I \\ \nu V \end{pmatrix}$$

In this case the next generation matrix is given by $K = \hat{F}\hat{V}^{-1}$ and the basic reproduction number($\mathcal{R}_0^{NGM}$) is the spectral radius of this matrix, where

$$\hat{F} = \frac{\partial\mathcal{F}}{\partial x}|_{DFE} = \begin{pmatrix} \beta & \alpha\frac{M}{N} \\ \vartheta\frac{N}{M} & 0 \end{pmatrix} \quad \text{and} \quad \hat{V} = \frac{\partial\mathcal{V}}{\partial x}|_{DFE} = \begin{pmatrix} \gamma+\mu & 0 \\ 0 & \nu \end{pmatrix}$$

We deduce that

$$\mathcal{R}_0^{NGM} = \rho(K) = \frac{\beta}{2(\gamma+\mu)} + \left[\left(\frac{\beta}{2(\gamma+\mu)}\right)^2 + \frac{\alpha\vartheta}{\nu(\gamma+\mu)}\right]^{\frac{1}{2}} \tag{4.8}$$

which is also structurally the same as that of the $\mathcal{R}_0^{NGM}$ of model 3.6. It directly follows $\mathcal{R}_0^{NGM}$ and $\mathcal{R}_0^J$ for the newly formulated model is also related by

$$\mathcal{R}_0^J = \mathcal{R}_0^{NGM^2} + 2a(1 - \mathcal{R}_0^{NGM}) \tag{4.9}$$

where $2a = \frac{\beta}{\gamma+\mu}$. We also have that the threshold condition is simultaneously holding for $\mathcal{R}_0^{NGM}$ and $\mathcal{R}_0^J$, for a given set of parameters.

Theorem 4.4 For $\mathcal{R}_0^{NGM}$ and $\mathcal{R}_0^J$ we have

(a) $\mathcal{R}_0^{NGM} \leq 1 \iff \mathcal{R}_0^J \leq 1$

(b) $\mathcal{R}_0^{NGM} > 1 \iff \mathcal{R}_0^J > 1$

For proof see theorem 3.13

4.1.5 Global Stability of Equilibria

As we have seen previously the reproduction numbers for both models 4.2 and 3.6 are the same, we will now see how they are connected in the case of global stability of the two equilibria.

Theorem 4.5 The SIRUV model 3.6 holds the sharp threshold property.

Proof. The reproduction number $R_0 = \mathcal{R}_0^{NGM}$ is structurally the same as that of model 3.6. So the derivation of the Lyapunov functions is almost the same as in the proof of Theorem 3.16. The Lyapunov function for the disease-free equilibrium is obtained using the matrix theoretic method given in [47].

The Lyapunov funcion is given by $Q = w^T \hat{V}^{-1} x$.

$$= \frac{R_0 I}{\alpha} + \frac{V}{\nu}$$

where

$$w = \begin{pmatrix} \frac{R_0(\gamma+\mu)}{\alpha} \\ 0 \\ 1 \end{pmatrix}$$

is the left eigenvector of $\hat{V}^{-1}\hat{F}$. (where $\hat{F}$ and $\hat{V}$ are coming from the derivation of $\mathcal{R}_0^{NGM}$). We see that structurally, the Lyapunov function for disease-free equilibrium is also the same as in model 3.6. From theorem 3.15 we have that, $Q' = \omega^T \hat{V}^{-1} x' \leq 0$ when $R_0 \leq 1$. Again by Lasalle Invariance principle, we see that the disease-free equilibrium is GAS when $R_0 \leq 1$.

Now using the graph-theoretic method suggested in [47] we have deduced the Lyapunov function for the endemic equilibrium for model 3.6. Using the same method we can deduce that, D_1, D_2, and D_3 defined as

$$D_1 = S - S^* - S^* ln\frac{S}{S^*} + I - I^* - I^* ln\frac{I}{I^*}$$
$$D_2 = \frac{1}{2}(U - U^*)^2$$
$$D_3 = V - V^* - V^* ln\frac{V}{V^*}$$

we have that

$$D = c_1 D_1 + c_2 D_2 + c_3 D_3$$

is the Lyapunov function for the endemic equilibrium, where $(S^*, I^*, R^*, U^*, V^*)$ denotes the endemic equilibria of model 4.2 and for this model we need to choose $c_1 = \frac{\vartheta N I^*}{M}$, $c_2 = \frac{\alpha M}{N}\frac{S^* V^*}{U*}$ and $c_3 = \frac{\alpha M}{N} S^* V^*$. Again by the Lasalle Invariance Principle, we can conclude that the endemic equilibrium is not only existing and is unique when $R_0 > 1$, but is also globally asymptotically stable in the int(Γ). ■

4.2 Numerical Results

We have seen that the *SIRUV* model given by 3.6 and 4.2 shows structural similarities in terms of the reproduction number and further stability analysis. However, we have already stated that the endemic equilibrium is not the same. This difference in the models leads to the fact that for both the models to reach the same endemic equilibrium we should start the different initial conditions. But how does this make sense when it comes to real-time application? Before answering this question, we give a numerical example to show that the endemic equilibria for both models are distinct.

4.2.1 Distinct endemic equilibrium

We have only stated that the endemic equilibrium is different for the two models. An explicit expression of the endemic equilibrium for both models was not given. To exhibit the distinction of the two endemic equilibria we have done a numerical experiment. For the set of parameters given in Table 4.1, with the number of hosts as $N = 100000$, we simulate the values of S^*, $I*$ and V^* as a function of the M/N, which is the ratio of the population size of mosquitoes to that of the hosts. For model 3.6 we use the polynomial given in theorem 3.5 and for model 4.2 we used the expressions in theorem 4.2 to obtain both the equilibrium. It is seen that the expression of endemic equilibrium is different for both models. For the choice of M/N values ranging from 1 to 100, we have plotted the susceptible host, infected host and infected vector proportions in Figure 4.1. The relation between M/N and endemic equilibrium for model 4.2 is shown in a log-log plot. Here the ratio M/N is varied from 10^{-10} to 10^{10} and the value of V^* is plotted in a log-log plot for each choice of M/N. For the case, when the population size of vectors M is more than the host population size(N), the endemic proportion of infected vectors of model 4.2 decreases from the

value of V^* of model 3.6 as M/N increases. For $M < N$, the endemic proportion of infected vectors V^* of model 4.2 increases from the value of V^* of model 3.6 until it reaches the value of $V^* = 1$. We observe that, for the model 4.2, when the value of M/N is too small, we get $V^* = 1$. This is reasonable that if the population size of mosquitoes is too small compared to the population size of hosts then at endemic equilibrium all mosquitoes end up in the infected compartment.

Parameter	value	time unit
μ	$1/(72*365)$	$[day]$
ν	$1/10$	$[day]$
β	$1/7$	$[day]$
α	$1/7$	$[day]$
ϑ	5ν	$[day]$
γ	$1/14$	$[day]$

(a) All the parameters except β are taken from [35] which are defined per year. We have converted these parameters to values per day. Also for the host-host transmission rate(β) we chose $\beta = 1/7$.

Parameter	value	time unit
μ	$1/(72*365)$	$[day]$
ν	$1/10$	$[day]$
α	0.008	$[day]$
β	0.01	$[day]$
ϑ	0.4	$[day]$
γ	0.0008	$[day]$

(b) For the given set of parameters we have plotted a log-log plot of V^* as a function of M/N.

Table 4.1 – The set of parameters in (a) is used for plotting S^*, I^* and V^* as a function of M/N in Figure 4.1. For the set of parameters in (a) and (b), a log-log plot in Figure 4.2 compares the endemic infected vector proportion V^* as a function of M/N.

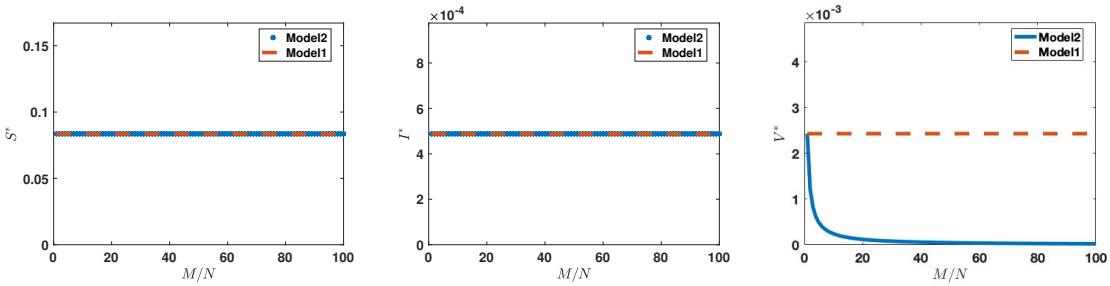

(a) Endemic proportion of susceptible hosts S^*

(b) Endemic proportion of infected hosts I^*

(c) Endemic proportion of infected vectors V^*

Figure 4.1 – For the set of parameters in Table 4.1 we have calculated the endemic proportions S^*, I^* and V^* of model 3.7 (referred to as model 1) and model 4.3 (referred to as model 2) as a function of the ratio of the population size of mosquitoes to that of hosts(M/N). We see that the endemic equilibrium for model 2 is different from that of model 1 for the endemic proportion of infected vectors alone. For susceptible and infected host proportion at endemic equilibrium, there is no impact of the fraction M/N on model 4.3

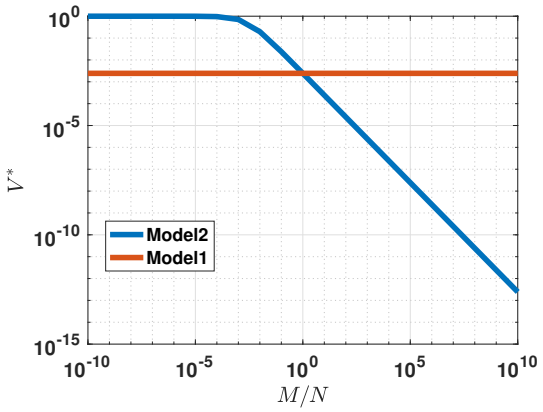

(a) Endemic proportion of infected vectors as a function of M/N, for the set of parameters in Table 4.1 (a)

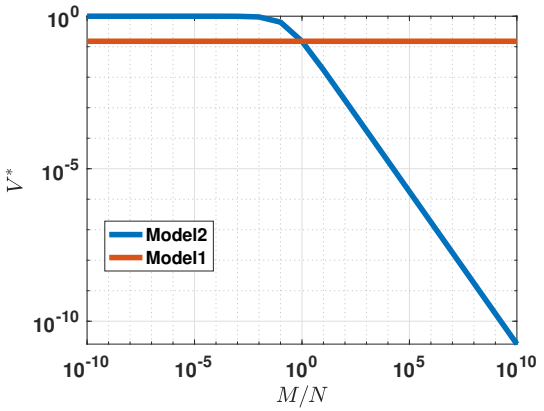

(b) Endemic proportion of infected vectors as a function of M/N, for the set of parameters in Table 4.1 (b)

Figure 4.2 – For the set of parameters in Table 4.1 we have calculated the endemic proportions V^* of model 3.7 (referred to as model 1) and model 4.3 (referred to as model 2) as a function of the ratio of the population size of mosquitoes to that of hosts(M/N) in a log-log plot. The values of M/N is ranging from 10^{-10} to 10^{10}. For $M > N$, the value of V^* of model 4.3 decreases as M/N increases. For $N > M$, the value of V^* increases as M/N decreases and for $N >> M$, the value of V^* is 1.

M/N	10^{-10}	10^{-9}	10^{-8}	10^{-7}	10^{-6}	10^{-5}	10^{-4}
V	1	1	1	1	0.99999	0.99994	0.99944
M/N	10^{-3}	10^{-2}	10^{-1}	10^{0}	10^{1}	10^{2}	10^{3}
V	0.9944	0.94667	0.63967	0.15076	0.017443	0.0017721	0.00017749
M/N	10^{4}	10^{5}	10^{6}	10^{7}	10^{8}	10^{9}	10^{10}
V	1.7752e-05	1.7753e-06	1.7753e-07	1.7753e-08	1.7753e-09	1.7753e-10	1.7753e-11

Table 4.3 – For the set of parameters in Table 4.1 (b) for model 3.6 the endemic proportion of infected vectors is given by $V_2^* = 0.15076$. For the same set of parameters, the values of V^* of model 4.2 depending on the choice of M/N are given here.

The values of V^* of model 4.2 for different choices of M/N for the set of parameters in Table 4.1 (a) is given in Table 4.2, and the values of V^* of model 4.2 for the set of parameters in Table 4.1(b) is given in Table 4.3. The value of V^* for model 3.6 for the set of parameters given in Table 4.1 (a) are given by $V_1^* = 0.0024338$ and for Table 4.1 (b) are given by $V_2^* = 0.15076$. From this study, we conclude that the endemic equilibrium is structurally not the same for both model 4.2 and model 3.6. for the same set of parameters, the value of endemic equilibrium changes for the value of V^* and the value of V^* in model 4.2, decreasing exponentially when $M/N >> 1$.

4.2.2 Dependence of disease dynamics on the initial condition

For the set of parameters as in Table 4.1, except for the host-host transmission rate β, we have done the numerical study for analyzing the dependence of the profile of infected hosts on the initial num-

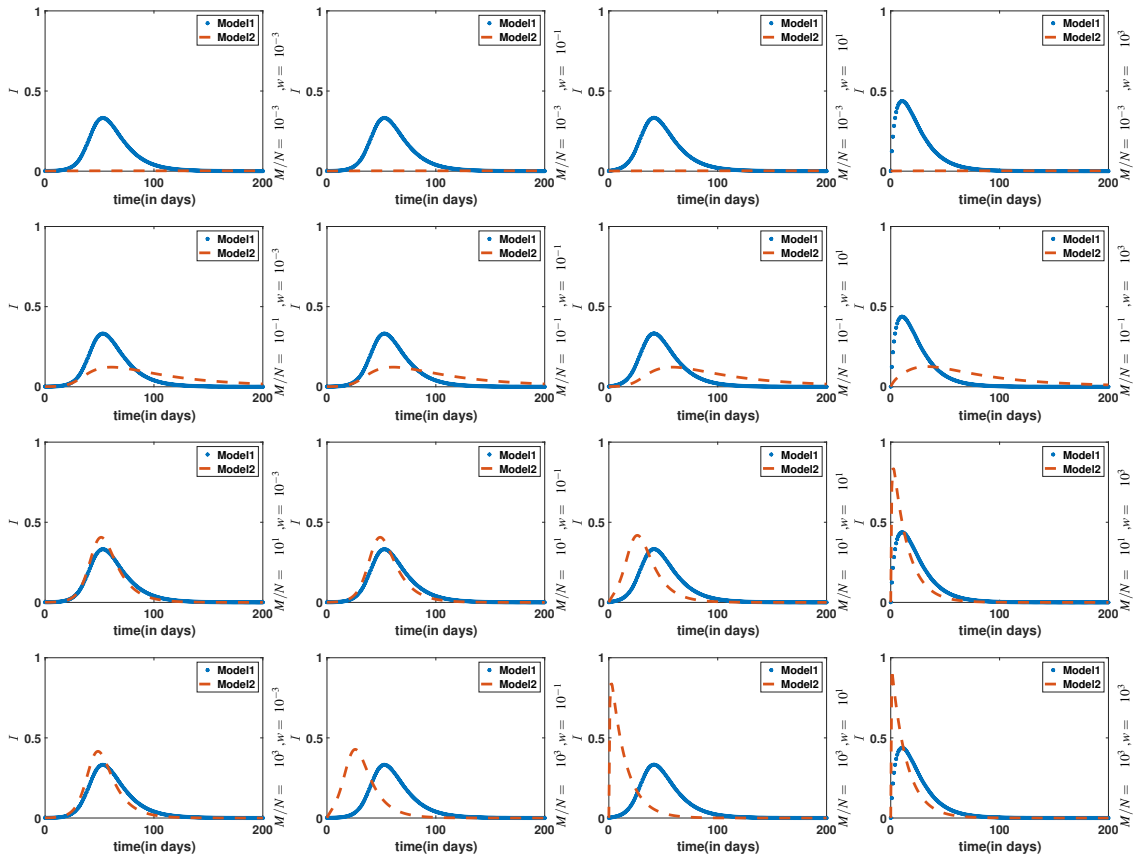

Figure 4.3 – For the host-host transmission rate $\beta = 0.1/7$, the figures show the disease propagation in infected hosts for various choices of M/N, which is the ratio of population sizes of vector to host. For each choice of M/N, the temporal dynamics of the proportion of infected hosts is plotted as the initial proportion of infected vectors(V_{init}) is varied by defining $V_{init} = w * I_{init}$.

M/N	10^{-10}	10^{-9}	10^{-8}	10^{-7}	10^{-6}	10^{-5}	10^{-4}
V	1	1	1	0.99996	0.99959	0.99592	0.96063
M/N	10^{-3}	10^{-2}	10^{-1}	10^{0}	10^{1}	10^{2}	10^{3}
V	0.70928	0.19613	0.023817	0.0024338	0.00024392	2.4397e-05	2.4398e-06
M/N	10^{4}	10^{5}	10^{6}	10^{7}	10^{8}	10^{9}	10^{10}
V	2.4398e-07	2.4398e-08	2.4398e-09	2.4398e-10	2.4398e-11	2.4398e-12	2.4398e-13

Table 4.2 – For the set of parameters in Table 4.1 (a) for model 3.6, the endemic proportion of infected vectors is given by $V_1^* = 0.0024338$. For the same set of parameters, the values of V^* of model 4.2 depending on the choice of M/N are given here.

ber of infected vectors. We assume that for a given number of initially infected hosts, I_{init}, the initial condition is $(S_{init}, I_{init}, V_{init}) = (1 - I_{init}, I_{init}, w * I_{init})$, range$(w)$ is $W = \{10^{-3}, 10^{-1}, 10^{1}, 10^{3}, 10^{5}\}$. The profile of infected hosts proportion is plotted for different values of M/N in the range of W, when $\beta = 0.1/7$ and $\beta = 2/7$, for various choices of initial conditions obtained by varying the value of w. The results for $\beta = 0.1/7$ are shown in Figure 4.3 and that for $\beta = 2/7$ is given in Figure 4.4.

For model 3.6, the disease profile gets significantly faster for $V_{init} > 10^3 I_{init}$ for all choices of M/N and for all choices of β. For model 4.2(referred to as Model 2 in figures) when $M/N = 10^{-3}$ and 10^{-1}, the change in initial conditions does not show any significant change in the profile of the proportion of infected hosts. For $M/N = 10^1$ and 10^3 as the number of initially infected vectors increases the infection process in hosts gets faster. Moreover,

- For $M/N = 10^1$, the disease process is changing for the choice of the proportion of initially infected vectors, V_{init} is greater than 10 times the proportion of initially infected hosts.
- For $M/N = 10^3$, the change in the disease dynamics is visible for the choice of initially infected vector proportion greater than 0.1 times the proportion of infected hosts.

Model 4.2 shows a trend that for both cases of host-host transmission rates, the disease propagation within hosts is impacted by the ratio of the population size of vectors to that of hosts(M/N) and as this ratio increases, the proportion of initially infected vectors required to increase the speed of disease progression is getting smaller. In model 3.6, irrespective of the increase in the ratio of M/N, the initial proportion of infected vectors impacts the disease dynamics only when it is 1000 times that of the proportion of initially infected hosts. By the definition of α and ϑ in model 3.6, in application to real-life scenarios, the effect of M/N is expected to appear through these parameters.

4.3 Data fitting and parameter estimation

In this section, we work on the data from the Zika Virus outbreak which began in Brazil and prevailed throughout the nearby countries during 2015 and 2016. We use weekly data of confirmed infected cases of the year 2016 for different provinces or states of Brazil. Using this data set we have

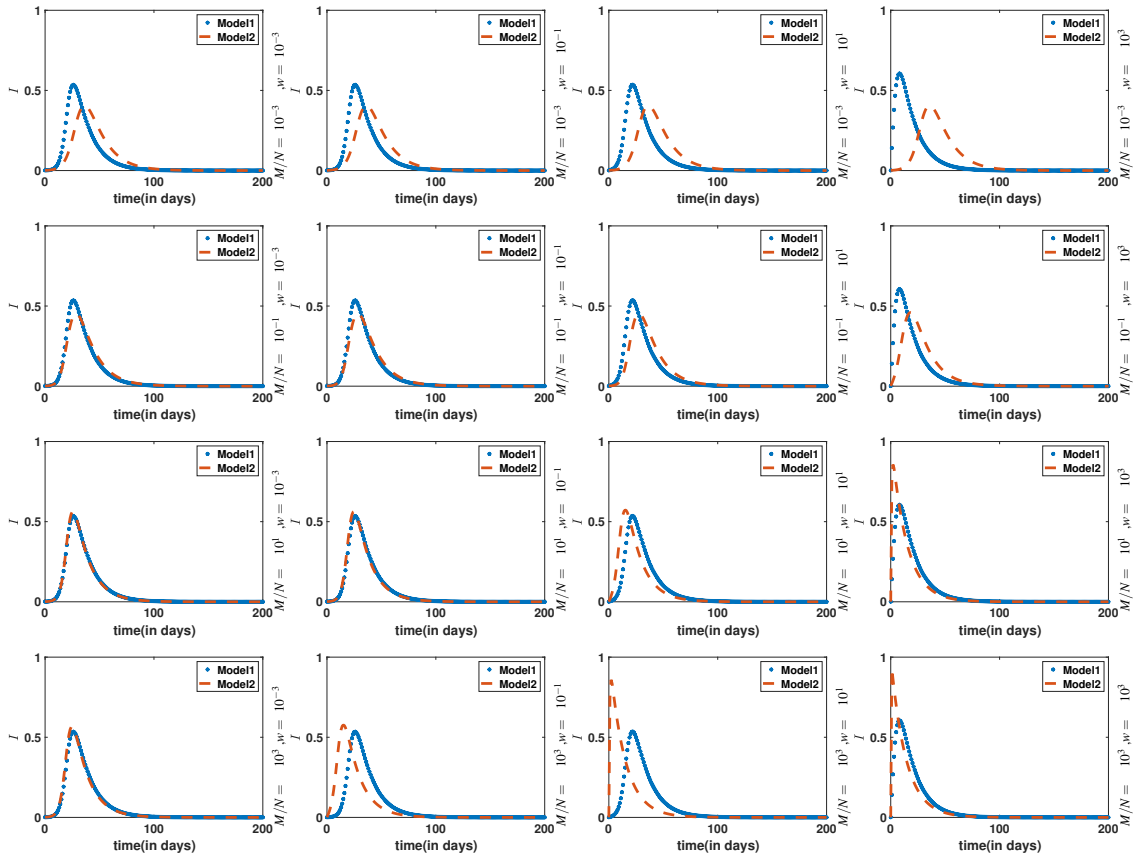

Figure 4.4 – For the host-host transmission rate $\beta = 2/7$, the figures show the disease propagation in infected hosts for various choices of M/N, which is the ratio of population sizes of vector to host. For each choice of M/N, the temporal dynamics of the proportion of infected hosts is plotted as the initial proportion of infected vectors(V_{init}) is varied by defining $V_{init} = w * I_{init}$.

done a least squares fit for models 3.6 and 4.2. For data fitting, we keep certain parameters fixed. These are the birth/death rate μ, which is taken as the reciprocal of the average life expectancy of Brazil for the year 2016. The average life expectancy of Brazil for the year 2016 was obtained from the World Bank data[51] and is fixed as, $1/\mu = 75$ years. The population size of Brazil and its federative units for the year 2016 was not obtained. So we used the data for the year 2015, obtained from [33]. The estimated parameters are β, α, ϑ and γ. The parameter estimation was done by using the inbuilt routine 'fmincon' from the optimization toolbox of MATLAB. We solve a constrained minimization problem which involves a quadratic cost functional given by

$$J(u) = \sum_{i=1}^{n} (I(t_i) - I_i)^2 \tag{4.10}$$

where $u = [\beta, \gamma, \alpha, \theta]$. The fitted parameters are found by solving the minimization problem given by $\min_u J(u), u \geq 0$. To understand the dynamics and data fitting we start with the classical *SIR* model and analyse if the estimated parameters are in a range of the desirable values. In the classical *SIR* model, we fix the birth rate(death rate) μ and the population size(N), and the infection rate β

and recovery rate γ are estimated using data-fitting. The optimal parameter vector $u = [\beta, \gamma, \alpha, \theta]$ that minimizes the cost functional J is sought. The raw data for the Zika outbreak in Brazil was used initially and we were not able to obtain a good fit for the chosen scenario. After many attempts to find a proper fit, the data was scaled up and using the scaled data we tried to fit for the *SIR* model. The results are shown in Figure 4.5. It can be seen that the attempt to find the best fit to the raw data failed and the parameters for which the given fit is obtained are $\beta = 1.9944$ and $\gamma = 2.0100$. The data was scaled by a factor of $\tau = 30$ and using the scaled data the fitted parameters are $\beta = 3.4204$ and $\gamma = 3.2317$. The scaling factor was obtained by a trial and error method. The scale was fixed for that value for which we get a recovery rate in the range $[1, 3.5]$. The recovery rate is defined as the reciprocal of the number of days taken for recovery in classical compartmental models. In this case, for Zika disease, the number of days for recovery is 2 to 7 days according to WHO[54]. The recovery rate is defined per week and thereby the given range was chosen. The infection rate β and recovery rate γ fitted for the *SIR* model, for different choices of the scale for the raw data, is given in Table 4.4.

τ	10	20	30	40
β	27.4720	4.4774	3.5401	2.9961
γ	27.4960	4.2705	3.3420	2.8043

Table 4.4 – For $\tau < 30$, we got the fitted γ value out of the desired range.

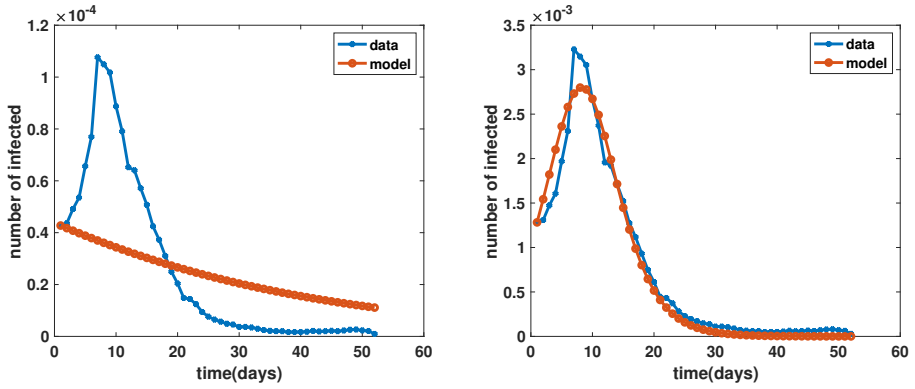

(a) Raw data fit **(b)** Scaled-data fit

Figure 4.5 – The fitted parameters for the raw data did not give a proper fit. The maximum proportion of infected people in the real data is around $1.1 * 10^{-4}$. In the second figure we have used the scaled data to find the fitting parameters for the model and in this case, we could obtain a proper fit.

By choosing the same scaling for the data, we have done the parameter fitting for models 3.7 and 4.3. In this case, we assumed that the birth/death rate of hosts and vectors are fixed as $\frac{1}{\mu} = 75$ years and $\frac{1}{\nu} = 10$ days. The population size of mosquitoes is fixed as $M = 100 * N$. The parameters estimated using data fitting are the recovery rate γ, human-human infection rate β, vector-human

infection rate α and human-vector infection rate ϑ. The initial values of the estimated parameters are as follows. $\beta = 2$, $\gamma = 0$, $\alpha = 0$ and $\theta = 0$.The results are given in Figure 4.6. The estimated parameters for the two models are given in Table 4.5. Without the box-constraints, the optimal parameters were either out of the desired range or gave a bad fit.

Parameter	γ	β	α	ϑ
Model 1[3.7]	3.3466	3.4825	0.2380	0.2205
Model 2[4.3]	3.3463	3.4813	0.2302	0.2300

Table 4.5 – When the range of gamma is given as $[1, 3.5]$ and that of other parameters is kept between $[0, 20]$, the estimated values of all parameters for both models are given.

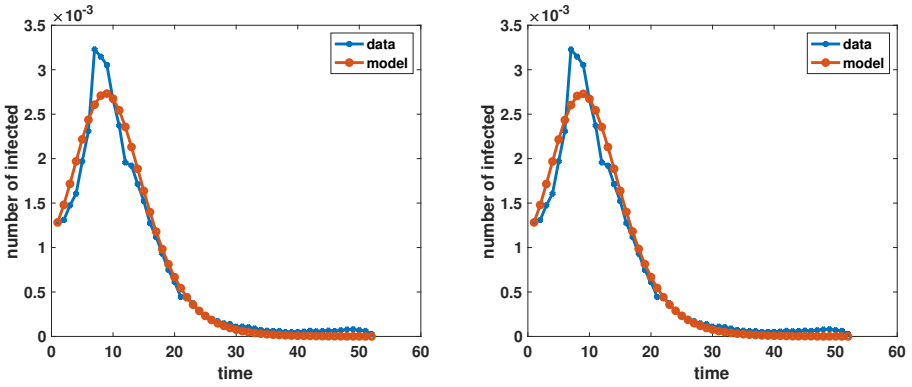

(a) Data fit of model 1 **(b)** Data fit of Model 2

Figure 4.6 – The data fit for both models gave good fit for the scaled data when the scaling factor $\tau = 30$ provided the box constraints are applied for the parameters to be estimated. The range of γ was given as $[1, 3.5]$. For all other parameters, it was given as $[0, 20]$

5 Multipatch model

In Chapters 3 and 4, we have discussed models that are helpful in studying the temporal dynamics of the proportion of individuals in various stages of a disease. In this chapter, we propose a model that incorporates spatial heterogeneity into the model developed in Chapter 4. Hosts(humans) can be moving from one place to another thereby mixing among different populations and transmitting diseases. The spatial movement of hosts can be a long-term movement, like migration and short-term movement, like daily or weekly commuting between cities. In epidemiological terms, these short-term movements are called Lagrangian-type movements and the long-term movements are referred to as Eulerian[15]. Multi-patch models are one method used for studying disease transmission by involving temporal and spatial dynamics. We have chosen a multi-patch modelling method in this chapter majorly to incorporate the effect of short-term movements or commuting behaviour of hosts, in the disease dynamics. To mathematically model this scenario, we divide the space under consideration into different patches and model them to form a network. Each patch has a population that originally belongs to it and corresponding to each patch we have a respective set of parameters. Multi-patch modelling for various important epidemic models is proposed and studied in the literature[5, 10, 12, 15, 19, 28, 30].

5.1 Model Formulation

Each patch i is assumed to have a homogeneous intrinsic population of hosts of size N_i and a homogeneous vector population of size M_i. In patch i, the vector and host population consists of the different compartments namely, the number of susceptible($\mathscr{S}_i$), infected($\mathscr{I}_i$) and recovered($\mathscr{R}_i$) hosts and the number of susceptible($\mathscr{U}_i$) and infected($\mathscr{V}_i$) vectors. We assume that the host population are moving to the other patches and people in each compartment are getting involved with the vectors and hosts there. The vectors are assumed to remain in the respective patches without directly moving to the other patches. The heterogeneous movement of hosts is happening at a respective rate among each pair of patches. These short-term movements are incorporated using a residence time budgeting matrix $P = (p_{ij})_{nxn}$[9–11, 39], where p_{ij} denotes the time fraction that an average person in patch i has spent in patch j in unit time. For example on average if a person in patch i spent 8 hours in patch j, then $p_{ij} = \frac{8}{24}$, provided that unit time is one day. By the definition of this matrix, we also have that, for each patch i and j, $0 \leq p_{ij} \leq 1$, and the sum of all column entries of the ith row of P, $\sum_{j=1}^{n} p_{ij} = 1$. Following some insights from [10] and [30] we have developed a multi-patch model as an extension of the model given by system 4.2 in Chapter 4. We refer to this as the multi-patch $SIRUV - ZIKV$ model. In [30] a term called contact rate is clearly defined, which is the average number of adequate contacts per day of an infected person from patch

j with any individuals in patch i by which we have decided to set the parameters as a property of the respective patch. The parameters are defined for each patch as follows,
α_j = number of adequate contacts that are happening per infected mosquito per unit of time with the people present in patch j,
β_j= number of adequate contacts that are happening per infected host per unit of time with the people present in patch j,
ϑ_j = number of adequate contacts that are happening per infected human with mosquitoes in patch j in unit time,
γ_j = number of recoveries that are happening per unit time in patch j,
μ_j = birth rate/death rate of the intrinsic host population of patch j and
ν_j = birth rate/death rate of the intrinsic vector population of patch j.
Now the incidences in patch j can be understood in the following manner. Let us focus on patch j and see how many susceptibles from patch i get infected in patch j. If N_j inhabitants are residing in patch j, they commute to other patches in unit time. So the effective population in patch j is given by $N^j_{eff} = \sum_{k=1}^n p_{kj}N_k$. By the definition of α_j, the number of adequate contacts the infected mosquitoes in patch j has with the people in patch j is given by $\alpha_j\mathscr{V}_j$. The effective population of susceptibles in patch j is $\sum_{k=1}^n p_{kj}\mathscr{S}_k$ among which $p_{ij}\mathscr{S}_i$ are coming from patch i. Finally, the number of susceptibles from patch i who get infected in patch j due to mosquitoes is given by

$$\alpha_j\mathscr{V}_j\frac{p_{ij}\mathscr{S}_i}{\sum_{k=1}^n p_{kj}N_k}.$$

Now we focus on infections between humans. The number of adequate contacts the infected people present in patch j has with other humans in unit time is given by $\beta_j I^j_{eff}$, where I^j_{eff} is the effective number of infected people who came to patch j in unit time which is given by $I^j_{eff} = \sum_{k=1}^n p_{kj}\mathscr{I}_k$. Out of these $\beta_j\sum_{k=1}^n p_{kj}\mathscr{I}_k$ host-host interactions in patch j, the number of infections happened to the susceptible people of patch i is

$$\beta_j\sum_{k=1}^n p_{kj}\mathscr{I}_k\frac{p_{ij}\mathscr{S}_i}{\sum_{k=1}^n p_{kj}N_k}.$$

Now we normalize each compartmental value same as in Chapters 3 and 4. For example, we define $S_i = \frac{\mathscr{S}_i}{N_i}$ or as in the vector population we have $U_i = \frac{\mathscr{U}_i}{M_i}$, where M_i is the number of vectors present in patch i.

Remark 5.1 For U_i the normalisation yields,

$$\begin{aligned}
&\frac{d\mathscr{U}_i}{dt} &&= \nu_i(M_i-\mathscr{U}_i) - \vartheta_i\frac{\mathscr{U}_i}{M_i}\sum_{k=1}^n p_{ki}N_kI_k\\
\Leftrightarrow\quad &\frac{M_idU_i}{dt} &&= \nu_i(M_i-M_iU_i) - \vartheta_iU_i\sum_{k=1}^n p_{ki}N_kI_k\\
\Leftrightarrow\quad &\frac{dU_i}{dt} &&= \nu_i(1-U_i) - \vartheta_i\frac{U_i}{M_i}\sum_{k=1}^n p_{ki}N_kI_k.
\end{aligned}$$

The following system of ODEs describes disease spread in each patch i

$$\begin{aligned}
\frac{dS_i}{dt} &= \mu_i(1-S_i) - \sum_{j=1}^{n} \alpha_j M_j V_j \frac{p_{ij}S_i}{\sum_{k=1}^{n} p_{kj}N_k} - \sum_{j=1}^{n} \beta_j \sum_{k=1}^{n} p_{kj}N_k I_k \frac{p_{ij}S_i}{\sum_{k=1}^{n} p_{kj}N_k} \\
\frac{dI_i}{dt} &= -(\gamma_i+\mu_i)I_i + \sum_{j=1}^{n} \alpha_j M_j V_j \frac{p_{ij}S_i}{\sum_{k=1}^{n} p_{kj}N_k} + \sum_{j=1}^{n} \beta_j \sum_{k=1}^{n} p_{kj}N_k I_k \frac{p_{ij}S_i}{\sum_{k=1}^{n} p_{kj}N_k} \\
\frac{dR_i}{dt} &= \gamma_i I_i - \mu_i R_i \\
\frac{dU_i}{dt} &= \nu_i(1-U_i) - \vartheta_i \frac{U_i}{M_i} \sum_{k=1}^{n} p_{ki}N_k I_k \\
\frac{dV_i}{dt} &= -\nu_i V_i + \vartheta_i \frac{U_i}{M_i} \sum_{k=1}^{n} p_{ki}N_k I_k.
\end{aligned} \tag{5.1}$$

Remark 5.2 Like in the single-patch model 4.2, we have $S_i + I_i + R_i = 1$ and $U_i + V_i = 1$ for each compartmental value in patch i. We can neglect the two sets of redundant equations on R_i and U_i on each patch i and solve for S_i, I_i and V_i using the set of equations as given below and solve for R_i and U_i using the equations $R_i = 1 - S_i - I_i$ and $U_i = 1 - V_i$.

$$\begin{aligned}
\frac{dS_i}{dt} &= \mu_i(1-S_i) - \sum_{j=1}^{n} \alpha_j M_j V_j \frac{p_{ij}S_i}{\sum_{k=1}^{n} p_{kj}N_k} - \sum_{j=1}^{n} \beta_j \sum_{k=1}^{n} p_{kj}N_k I_k \frac{p_{ij}S_i}{\sum_{k=1}^{n} p_{kj}N_k} \\
\frac{dI_i}{dt} &= -(\gamma_i+\mu_i)I_i + \sum_{j=1}^{n} \alpha_j M_j V_j \frac{p_{ij}S_i}{\sum_{k=1}^{n} p_{kj}N_k} + \sum_{j=1}^{n} \beta_j \sum_{k=1}^{n} p_{kj}N_k I_k \frac{p_{ij}S_i}{\sum_{k=1}^{n} p_{kj}N_k} \\
\frac{dV_i}{dt} &= -\nu_i V_i + \vartheta_i \frac{U_i}{M_i} \sum_{k=1}^{n} p_{ki}N_k I_k.
\end{aligned} \tag{5.2}$$

The feasibility region is also analogous to the model 4.2.

Theorem 5.3 The region Γ is a positively invariant set for system 5.1 where the trajectory of an IVP involving system 5.1 and an initial condition from a region satisfying the following conditions will remain in this region for all points in time.

$$\Gamma = \{\mathbf{X} = (\mathbf{S},\mathbf{I},\mathbf{R},\mathbf{U},\mathbf{V}); 0 \leq S_i, I_i, R_i, U_i, V_i \leq 1, S_i + I_i + R_i = 1, U_i + V_i = 1\}$$

where the ith component of $\mathbf{S}$ is given by S_i and correspondingly for the other terms as well.

5.2 Equilibrium points of the multi-patch model

The multi-patch $SIRUV - ZIKV$ model also has a disease-free equilibrium which is given by $(\mathbf{S}_0, \mathbf{I}_0, \mathbf{R}_0, \mathbf{U}_0, \mathbf{V}_0)$, where $\mathbf{S}_0 = (S_1, S_2, S_3 ..., S_n)_0 = (1,1,1,...,1) = \mathbb{1}_n$ and $\mathbf{I}_0 = (I_1, I_2, I_3 ..., I_n)_0 = (0,0,0,...,0) = \mathbb{0}_n$. Similarly, $\mathbf{R}_0 = \mathbf{V}_0 = \mathbb{0}_n$ and $\mathbf{U}_0 = \mathbb{1}_n$. The endemic equilibrium is deduced for the system of equations of patch i. Let $(S_i^*, I_i^*, R_i^*, U_i^*, V_i^*)$ be such that it satisfies the following

$$\mu_i(1-S_i^*) - \sum_{j=1}^{n} \alpha_j M_j V_j^* \frac{p_{ij}S_i^*}{\sum_{k=1}^{n} p_{kj}N_k} - \sum_{j=1}^{n} \beta_j \sum_{k=1}^{n} p_{kj}N_k I_k^* \frac{p_{ij}S_i^*}{\sum_{k=1}^{n} p_{kj}N_k} = 0 \tag{5.3}$$

$$-(\gamma_i+\mu_i)I_i^* + \sum_{j=1}^{n} \alpha_j M_j V_j^* \frac{p_{ij}S_i^*}{\sum_{k=1}^{n} p_{kj}N_k} + \sum_{j=1}^{n} \beta_j \sum_{k=1}^{n} p_{kj}N_k I_k^* \frac{p_{ij}S_i^*}{\sum_{k=1}^{n} p_{kj}N_k} = 0 \tag{5.4}$$

$$\gamma_i I_i^* - \mu_i R_i^* = 0 \tag{5.5}$$

$$\nu_i(1-U_i^*) - \vartheta_i \frac{U_i^*}{M_i} \sum_{k=1}^{n} p_{ki}N_k I_k^* = 0 \tag{5.6}$$

$$-\nu_i V_i^* + \vartheta_i \frac{U_i^*}{M_i} \sum_{k=1}^{n} p_{ki}N_k I_k^* = 0. \tag{5.7}$$

We may deduce a simplified set of equations for the compartmental values at endemic equilibrium from 5.3 to 5.7. Adding equations 5.3 and 5.4 we get

$$\mu_i(1-S_i^*) - (\gamma_i+\mu_i)I_i^* = 0$$

which in turn gives us that

$$S_i^* = 1 - \frac{\gamma_i+\mu_i}{\mu_i} I_i^* \tag{5.8}$$

We know that $U_i^* = 1 - V_i^*$. Using this in 5.7 we get

$$\vartheta_i \frac{1-V_i^*}{M_i} \sum_{k=1}^{n} p_{ki}N_k I_k^* - \nu_i V_i^* = 0 \tag{5.9}$$

which implies that

$$\sum_{k=1}^{n} p_{ki}N_k I_k^* = \frac{\nu_i M_i V_i^*}{\vartheta_i(1-V_i^*)} \tag{5.10}$$

Using equation 5.8 and 5.10 in 5.4 gives

$$-(\gamma_i+\mu_i)I_i^* + \sum_{j=1}^{n} \alpha_j M_j V_j^* \frac{p_{ij}(1-\frac{\gamma_i+\mu_i}{\mu_i}I_i^*)}{\sum_{k=1}^{n} p_{kj}N_k} + \sum_{j=1}^{n} \beta_j \frac{\nu_j M_j V_j^*}{\vartheta_j(1-V_j^*)} \frac{p_{ij}(1-\frac{\gamma_i+\mu_i}{\mu_i}I_i^*)}{\sum_{k=1}^{n} p_{kj}N_k} = 0$$

which can be simplified to get

$$-(\gamma_i+\mu_i)I_i^* + (1-\frac{\gamma_i+\mu_i}{\mu_i}I_i^*) \left[\sum_{j=1}^{n} \left(\alpha_j + \frac{\beta_j \nu_j}{\vartheta_j(1-V_j^*)} \right) \frac{M_j V_j^* p_{ij}}{\sum_{k=1}^{n} p_{kj}N_k} \right] = 0 \tag{5.11}$$

Using 5.10 we get

$$-(\gamma_i+\mu_i)I_i^* + (1-\frac{\gamma_i+\mu_i}{\mu_i}I_i^*) \left[\sum_{j=1}^{n} \alpha_j \frac{M_j V_j^* p_{ij}}{\sum_{k=1}^{n} p_{kj}N_k} + \sum_{j=1}^{n} \beta_j \frac{p_{ij}\sum_{k=1}^{n} p_{kj}N_k I_k^*}{\sum_{k=1}^{n} p_{kj}N_k} \right] = 0 \tag{5.12}$$

To obtain the endemic equilibrium, we have to solve the system of non-linear polynomials formed by combining the system of equations given by 5.9 and 5.12. We get a system of $2n$ equations in $2n$ variables I_i^* and V_i^*. Even though we have simplified the quest of finding the endemic equilibrium until this point where we are seeking the root of a system of $2n$ non-linear polynomial equations in $2n$ unknowns, the complexity of solving this system analytically hinders us from obtaining an explicit expression of endemic equilibrium for the multi-patch model. Further, we can solve this system of equations numerically to find the endemic equilibrium.

5.3 Reproduction number of the multi-patch Zika model

As discussed in Chapter 3, the reproduction number can be deduced using the next-generation matrix approach, by finding the spectral radius of the next-generation matrix[21, 47]. For this, we first divide the compartmental variables from each patch namely S_i, I_i, R_i, U_i, and V_i into disease and non-disease compartments. In this setting, we denote $\mathbf{S} = (S_1, S_2 \dots S_n)^T$ and its counterparts $\mathbf{I}$, $\mathbf{R}$, $\mathbf{U}$, $\mathbf{V}$ for the other compartmental variables. The compartments can be partitioned as disease and non-disease terms by appending these vector forms. Let $\mathbf{x} = [\mathbf{I}, \mathbf{V}]^T \in \mathbb{R}^{2n}$ denote the disease and $\mathbf{y} = [\mathbf{S}, \mathbf{R}, \mathbf{U}]^T \in \mathbb{R}^{3n}$ the non-disease compartments respectively. The model can now be represented as

$$\mathbf{x}' = \mathcal{F}(\mathbf{x}, \mathbf{y}) - \mathcal{V}(\mathbf{x}, \mathbf{y}), \qquad \mathbf{y}' = g(\mathbf{x}, \mathbf{y}),$$

where $\mathcal{F} = (\mathcal{F}_1, \mathcal{F}_2, \dots, \mathcal{F}_{2n})$ and $\mathcal{V} = (\mathcal{V}_1, \mathcal{V}_2, \dots, \mathcal{V}_{2n})$, where $\mathcal{F}_i$ represents the rate of appearance of new infection in the i th disease compartment and $\mathcal{V}_i$ represents the rate of change in i th patch apart from that represents vital dynamics, for example, birth, death, recovery etc. These transition rates can be expressed explicitly in the multi-patch model and these expressions can be used further to deduce the next generation matrix. In model 5.1 we denote $A1 = (\mathcal{F}_1, \mathcal{F}_2, \dots, \mathcal{F}_n)^T$, where

$$A1_i = \sum_{j=1}^{n} \alpha_j M_j V_j \frac{p_{ij} S_i}{\sum_{k=1}^{n} p_{kj} N_k} + \sum_{j=1}^{n} \beta_j \sum_{k=1}^{n} p_{kj} N_k I_k \frac{p_{ij} S_i}{\sum_{k=1}^{n} p_{kj} N_k}$$

and $A2 = (\mathcal{F}_{n+1}, \mathcal{F}_{n+2}, \dots, \mathcal{F}_{2n})^T$ where

$$A2_i = \vartheta_i \frac{U_i}{M_i} \sum_{k=1}^{n} p_{ki} N_k I_k$$

On the other hand $\mathcal{V} = (B1, B2)^T$ where $B1_i = (\gamma_i + \mu_i) I_i$ and $B2_i = \nu_i V_i$. Using the same approach as in [21], two $2n * 2n$ matrices are defined as follows,

$$\hat{F} = \left[\frac{\partial \mathcal{F}_i}{\partial x_j} \right]_{|DFE} \tag{5.13}$$

$$\hat{V} = \left[\frac{\partial \mathcal{V}_i}{\partial x_j} \right]_{|DFE} \tag{5.14}$$

In this case we get

$$\hat{F} = \begin{bmatrix} \frac{\partial A1}{\partial I} |DFE & \frac{\partial A1}{\partial V} |DFE \\ \frac{\partial A2}{\partial I} |DFE & \frac{\partial A2}{\partial V} |DFE \end{bmatrix} = \begin{bmatrix} J_{11} & J_{12} \\ J_{21} & J_{22} \end{bmatrix} \tag{5.15}$$

where the element in row l and column m of the $n * n$ matrices J_{11}, J_{12}, J_{21} and J_{22} are given by,

$$J_{11}(l, m) = \frac{\partial A1_l}{\partial I_m}_{|DFE} = \sum_{j=1}^{n} \frac{\beta_j P_{mj} N_m P_{lj}}{\sum_{k=1}^{n} P_{kj} N_k}$$

$$J_{12}(l,m) = \frac{\partial A1_l}{\partial V_m}_{|DFE} = \frac{\alpha_m M_m P_{lm}}{\sum_{k=1}^{n} P_{km} N_k}$$

$$J_{21}(l,m) = \frac{\partial A2_l}{\partial I_m}_{|DFE} = \frac{\vartheta_l P_{ml} N_m}{M_m}$$

$$J_{22}(l,m) = \frac{\partial A2_l}{\partial V_m}_{|DFE} = \left[\frac{\vartheta_m}{M_m}\sum_{k=1}^{n} P_{km} N_k I_k\right]_{|DFE} = 0$$

Similarly we get that

$$\hat{V}^{-1} = \begin{pmatrix} G_{11} & \mathbf{0} \\ \mathbf{0} & G_{22} \end{pmatrix}$$

where $G_{11}(l,l) = \frac{1}{\gamma_l+\mu_l}$, $G_{22}(l,l) = \frac{1}{\nu_l}$ which in turn gives us the next generation matrix

$$K = \hat{F}\hat{V}^{-1} = \begin{pmatrix} J_{11}G_{11} & J_{12}G_{22} \\ J_{21}G_{11} & \mathbf{0} \end{pmatrix} \tag{5.16}$$

The spectral radius of matrix K is the reproduction number of model 5.1. A general expression of the reproduction number for the case of n patches is not deduced here due to the fact that in the matrix K, except the last one, all other block matrices that constitute K are full matrices. To find an explicit expression for the spectral radius of this complex matrix is tedious. But numerically, this can be achieved and approximate values of the reproduction number can be found.

Remark 5.4 It is to be noted that a similar approach can be used to derive a multi-patch model from the *SIRUV* model 3 given in Chapter 3. Without going further into the elaborate model description we would present this model and examine the important aspects of this model.

$$\begin{aligned}
\frac{dS_i}{dt} &= \mu_i(1-S_i) - \sum_{j=1}^{n}\alpha_j V_j p_{ij} S_i - \sum_{j=1}^{n}\beta_j \sum_{k=1}^{n} p_{kj} N_k I_k \frac{p_{ij}S_i}{\sum_{k=1}^{n} p_{kj}N_k} \\
\frac{dI_i}{dt} &= -(\gamma_i+\mu_i)I_i + \sum_{j=1}^{n}\alpha_j V_j p_{ij} S_i + \sum_{j=1}^{n}\beta_j \sum_{k=1}^{n} p_{kj} N_k I_k \frac{p_{ij}S_i}{\sum_{k=1}^{n} p_{kj}N_k} \\
\frac{dR_i}{dt} &= \gamma_i I_i - \mu_i R_i \\
\frac{dU_i}{dt} &= \nu_i(1-U_i) - \vartheta_i U_i \frac{\sum_{k=1}^{n} p_{ki} N_k I_k}{\sum_{k=1}^{n} p_{ki} N_k} \\
\frac{dV_i}{dt} &= -\nu_i V_i + \vartheta_i U_i \frac{\sum_{k=1}^{n} p_{ki} N_k I_k}{\sum_{k=1}^{n} p_{ki} N_k}.
\end{aligned} \tag{5.17}$$

Here the parameters α_j, β_j and ϑ_j are defined in a slightly different manner. It is to be noted that α_j is the number of adequate contacts that a susceptible person present in patch j has with mosquitoes, ϑ_j is the number of adequate contacts that a susceptible vector has with hosts present in patch j and β_j is the contact rate of an average susceptible person in patch j with people present in patch j. By mixing the definition of parameters in the two models we can also have further combinations of the set of equations. For eg: the first three equations of system 5.1 combined with the last two equations of model 5.2 will give us a new system with the respective definitions for the parameters.

5.4 Numerical Results

5.4.1 Endemic equilibrium and Reproduction number

In this section, we would like to first exhibit the endemic equilibrium and reproduction number of a two-patch model which are both obtained numerically. The endemic equilibrium is obtained by solving the system of equations as per equations 5.9 and 5.12. In an example, we consider two patches as in the first numerical example of Chapter 3. In the single-patch example, we saw that the choice of $\gamma = 0.008$ gave us the scenario that the disease pertains and when $\gamma = 0.8$ is chosen, the disease dies out. Here, we consider that patch 1 and patch 2 have all other parameters same as in Table 3.1. But patch 1 is assumed to have a recovery rate $\gamma_1 = 0.008$ and patch 2 has a recovery rate $\gamma_2 = 0.8$. Both patches are assumed to have the same initial conditions given by $(S_i, I_i, V_i) = [0.2032, 0.0142, 0.0617]$. We assume that the two patches are connected using the commuting matrix, $P = \begin{pmatrix} 0.1 & 0.9 \\ 0.01 & 0.99 \end{pmatrix}$ by which it is assumed that people from patch 1 mostly go to patch 2 and people in patch 2 spend only some time in patch 1. The solution is given as in Figure 5.1(a). The endemic equilibrium is given by $(S_1^*, I_1^*, V_1^*) = (0.3673, 0.0033, 0.0009)$ and $(S_2^*, I_2^*, V_2^*) = (0.3854, 3.237 * 10^{-5}, 0.0084)$. It can be seen that the solution curve in patch 2 also goes to an endemic equilibrium unlike in the single patch case where the DFE was asymptotically stable. The reproduction number was calculated by using the *eig* function in MATLAB by giving the matrix as in equation 5.16. At the same time, in an example where patch 1 was also assumed to have a recovery rate $\gamma_1 = 0.8$, both patches showed the asymptotic stability of the DFE.

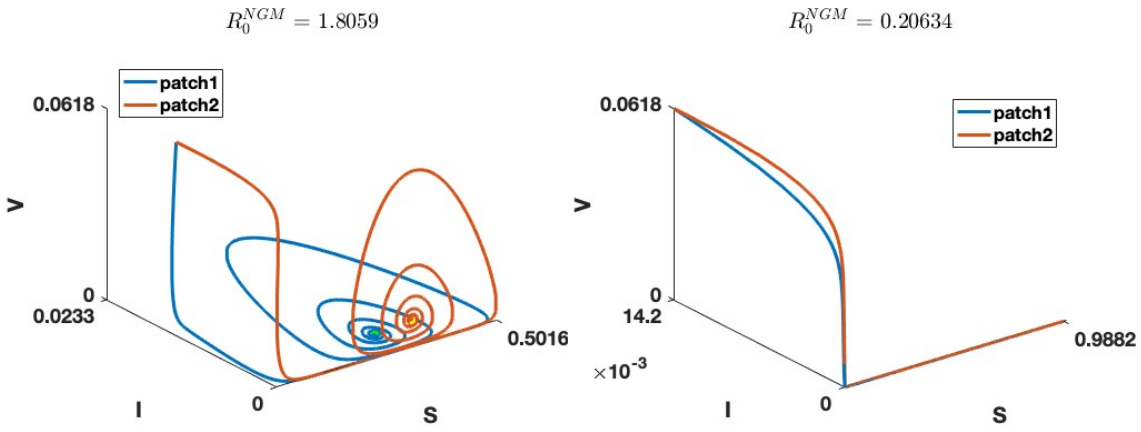

(a) For $R_0 > 1$ Endemic equilibrium EE is asymptotically stable

(b) For $R_0 < 1$ disease free equilibrium DFE is asymptotically stable

Figure 5.1 – Both figures have a final time $t = 100000$ days. The figures are plotted for the parameters defined above in Table 3.1. The first case is for the choice of $\gamma_1 = 0.008$ and $\gamma_2 = 0.8$. In Figure (a) we can see that a spiral is formed and as time tends to ∞ the solution curve is approaching the endemic equilibrium. In the title of the figure, the reproduction number can be seen as greater than 1. At the same time for the choice of $\gamma_1 = 0.8$ and $\gamma_2 = 0.8$, we can see that the solution curve is approaching the disease-free equilibrium $[1, 0, 0]$ and the reproduction number is less than 1 for this case.

5.4.2 Studying the influence of mobility matrix P through parameter fitting

This chapter focuses on the importance of commuting in disease spread models. The temporal dynamics of the disease are captured in most of the compartmental models. At the same time, we try to incorporate the spatial dependence of the disease dynamics through the commuting matrix. We show in an exemplary scenario that the *SIRUV* model may not be enough in some cases where hosts exhibit short-term movements. The multi-patch model is developed from an underlying single-patch model by incorporating a matrix that defines the fraction of time that the average person of each patch spends in other patches in unit time. How does mobility affect the disease dynamics? This in turn answers the question of the need for a multi-patch model as well. Is it not sufficient to have a single patch model? To answer this question we are doing a numerical experiment. The experimental setup is as follows. We simulate the scenario where we have a multi-patch model and all patches have identical behaviour in terms of the disease and non-disease parameters. In terms of the mobility matrix, we incorporate the spatial movement across patches by using a non-identical residence time budgeting matrix to represent the commuting between patches. In such a scenario we simulate the multi-patch system, average out the values of all the compartments and use this as the data to fit for the parameter β of the single patch model 4 which assumes the collection of patches involved as a single entity. As one can easily assume we have the result that when $P = I$ the fitted parameter values in the single-patch model coincide with the β value for each of the patches in the multi-patch scenario. The multi-patch model is numerically simulated for the set of parameters given in Table 5.1.

μ_i	α_i	γ_i	ν_i	ϑ_i	N_i	M_i
10/(1000*365)	0.08	0.08	1/14	0.1	5000	10000

Table 5.1 – Parameters in each patch

In this section, we show how different P matrices influence the dynamics of the disease spread and how much the dynamics vary from that of the single patch model. For this, we choose P matrices of different patterns and study the influence of P on the disease dynamics. The central point of interest is how much does the disease dynamics perturb from the single patch *SIRUV* model with the introduction of P. The experimental setup is as follows. All patches are assumed to have the same set of parameters and identical initial proportions of susceptible and infected hosts and infected vectors. By assuming this we establish that all the patches are identical. We choose a particular P matrix and simulate the multi-patch model for a given set of parameters as in Table 5.1. Now we take the average of this solution with respect to the number of patches and use this as data to fit the parameter β in the single-patch model, provided all other parameters of the single-patch model, except the host-to-host transmission rate β is fixed and is equal to the parameters given as in Table 5.1. We have used a data fitting algorithm fminsearch in MATLAB to find the closest β value that suits the model. The study is done for three different choices of P.

Case 1 : $P = I_n$

Taking an average of the *SIRUV* multi-patch model across the patches, provided $P = I_n$ is supposed to result in the single patch model. For the scenario under consideration, we have validated this by choosing $P = I_n$ and simulating the model to get solutions for S, I and V. The simulations are

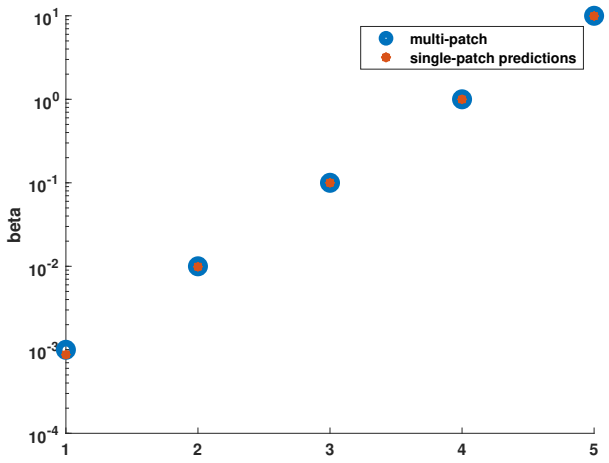

Figure 5.2 – For the case of residence time budgeting matrix $P = I_n$, for the value of β_i = 0.001, 0.01, 0.1, 1 and 10 we have simulated the multi-patch model for $n = 30$ patches. An average of the simulated values of susceptible and infected hosts and infected vectors were used as data in the single patch model and is used to fit for the parameter β. Fitted β values turned out to be 0.0009, 0.0099, 0.0999, 0.9988, 9.9413. Logarithmic values are plotted here for each case. The fitted values were close to the β_i values used in the multi-patch model simulation. The x-axis does not signify much but the five different experimental setup with different β values.

done in a setting of n = 30 patches. The set of parameters in Table 5.1 was used and for identical initial conditions, the values of S_i, I_i, and V_i for each patch are simulated using the multi-patch model, by which we establish that all patches are identical. We take the average of the solution of the multi-patch model for all compartments S_i, I_i, and V_i across the patches and use this data for fitting the parameter β in the single-patch model for the set of values of all other parameters kept the same as in Table 5.1. In this case, we have tested for five different choices of β. For all five cases, we have found out that the β values fitted for the single-patch model were the same as in the multi-patch model. Results are plotted in Figure 5.2

Case 2: P being non-identity

In this case, we chose a non-identity matrix for P and examined the impact of this residence time budgeting matrix on the disease dynamics. The setting is the same as case 1. The only change is that in the place of $P = I$ we have a non-identity P matrix which is constructed as follows. We start with the numbering of the patches. The numbered patches are then mapped to the points in the coordinate system. A patch with number i is mapped to a point in the coordinate system through

the mapping q which is defined as follows,

$$q(i) = (\lceil i/p \rceil - 1, i - 1 \pmod p)$$

where the total number of patches is given by $n = p^2$, $\lceil x \rceil$ represents the largest integer close to the real number x and $k \pmod p$ denotes the remainder when k is divided by p. To understand the pattern in which the patches are numbered and the mapping to the points in the coordinate system defined by

$$q(i) = (\lceil i/p \rceil - 1, i - 1 \pmod p),$$

a simple example of the case where $n = 4^2$ is given in Figure 5.3.

1	5	9	13
2	6	10	14
3	7	11	15
4	8	12	16

$\longleftrightarrow$

(0,0)	(0,1)	(0,2)	(0,3)
(1,0)	(1,1)	(1,2)	(1,3)
(2,0)	(2,1)	(2,2)	(2,3)
(3,0)	(3,1)	(3,2)	(3,3)

Figure 5.3 – Mapping between the numbering of patches and the coordinate representation

The P matrix is defined using the Euclidean norm between the coordinate representation of these patches. The definition of the residence time budgeting matrix goes as follows:

$$\begin{aligned} P(i,i) &= \frac{1}{p^2} \\ P(i,j) &= \left(1 - \frac{1}{p^2}\right) \frac{A(i,j)}{\sum_{k \neq i} A(i,k)} \text{ for } i \neq j \end{aligned} \tag{5.18}$$

where

$$A(i,i) = 0; \quad A(i,j) = \frac{1}{\|(q(i) - q(j)\|^\eta} \tag{5.19}$$

The construction of the matrix given by equation 5.18 is also satisfying the property that the row sum of the matrix P is 1. We have done a similar study on fitting the parameter β for the single-patch model by using the data from the multi-patch model involving the new P matrix. The results can be seen in Figure 5.4. As expected the fitted β values are distorted, unlike the first case where P is the identity matrix. For this choice of P matrix, it should be noted that, for larger values of the choice of β_i, the value of β from the data fitting is close to the desired values. For the same residence time budgeting matrix, we have examined the dependence of the predicted β on the value η. For a fixed value of β_i, we generated the data for a set of η values ranging from 0 to 5, by simulating the multi-patch model for different P matrices in connection with the choice of α. For each generated data, β value was fitted for the single patch model and the difference of the fitted β value from β_i

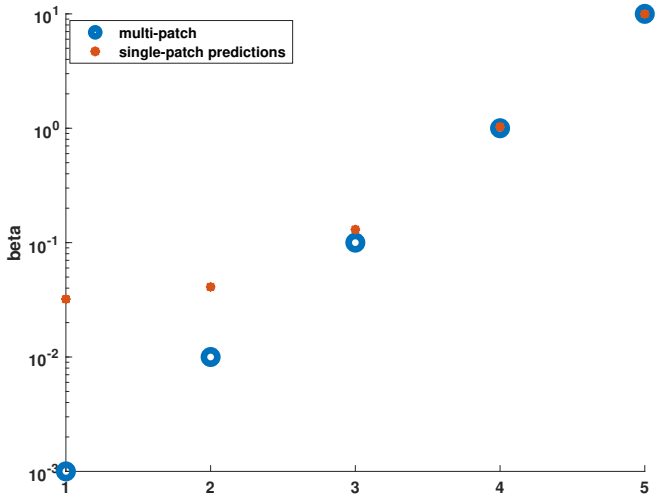

Figure 5.4 – For the choice of $\eta = 0.1$, fitted beta values turned out to be 0.0321, 0.0410, 0.1301, 1.0287, and 9.9751. Logarithmic values are plotted here for each case. The x-axis of the figure shows the 5 different experimental setups with the 5 distinct choices of β

value is shown in Figure 5.5. Another study using the same P matrix is done, where the number of patches is varied and the dependence of the predicted host-host transmission rate β for the single patch model on the value of η is plotted in Figure 5.6. The total number of patches $n = p^2$ is varied by making a choice of $p = 3, 5, 10, 15$. For a number of patches being small, the deviation of the host-host transmission rate of the single-patch model from that of the multi-patch model is large. As p increases

Case 3: Another non-trivial choice of P

For academic purposes, we have developed a P that increases the value of p_{ij} as the number of columns increases. For this P matrix, we have easily verified that the sum of each row is 1 and that each element has a value between 0 and 1. The matrix is defined as follows

$$P(i, j) = (2 * j - 1)/n^2$$

5.4.3 Numerical simulation for local and non-local spread

We have simulated two scenarios each for the multi-patch model where the number of patches is 50*50. The first case is where we choose a P matrix that exhibits the mobility between the nearest neighbouring patches alone. For understanding how non-local transport is achieved by the choice of P we have given another example.

Nearest neighbor coupling

The movement between patches is given in Figure 5.8. The chosen P matrix for incorporating a movement between the nearest neighbour patches is as follows

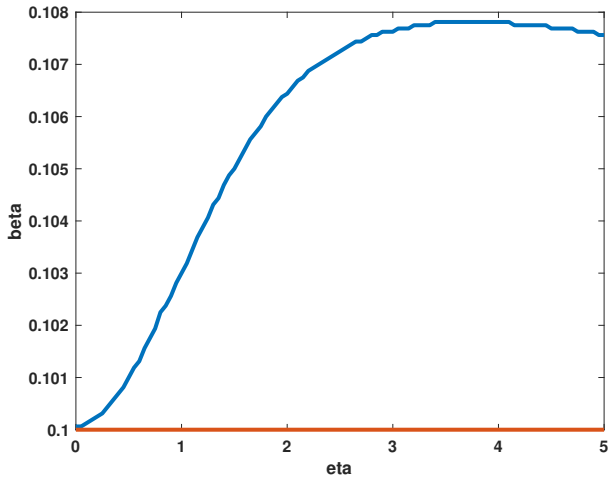

Figure 5.5 – Using the data generated for $\beta = 0.1$ and different choices of η ranging from 0 to 5, the fitted β for the single patch model is distorted from the value 0.1. The dependence of these predicted β values on η is shown in this figure

$$\begin{aligned} P(i,j_i) &= \frac{1}{b_i} - \frac{1}{n} \\ P(i,i) &= \frac{b_i}{n} \\ P(i,j) &= 0 \text{ for } j \neq i, j_i \end{aligned} \tag{5.20}$$

where b_i is the number of nearest neighbours and these neighbours of patch i are represented by j_i. For this case it is to be noticed that the two required conditions are satisfied for the P matrix.

- $0 < P(i,j) < 1$ for all $1 \leq i, j \leq n$.
- The row sum equals 1. This is shown in theorem 5.5

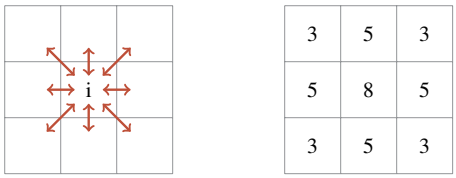

Figure 5.8 – The number of nearest neighbours b_i for each patch i in the case of $n = 9$ is shown in the second grid. The corners have 3 neighbours, inner patches have 8 neighbours and the other boundary patches have 5 neighbours each

Theorem 5.5 The P matrix defined by 5.20 satisfies the condition that $\sum_{j=1}^{n} P(i,j) = 1$

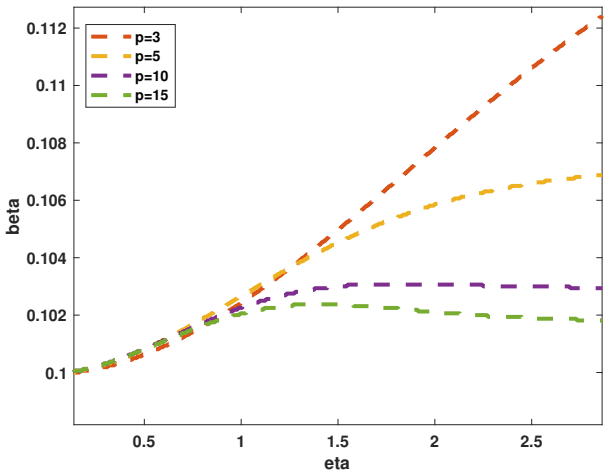

Figure 5.6

Proof.

$$\begin{aligned}\sum_{j=1}^{n} P(i,j) &= P(i,i) + \sum_{j=j_i} P(i,j) \\ &= \frac{b_i}{n} + b_i\left(\frac{1}{b_i} - \frac{1}{n}\right) \\ &= 1\end{aligned}$$

■

For the numerical simulation using nearest neighbour coupling, we take $b_i = 8$ for the internal patches. The number of neighbours is counted in the same way as in an exemplary case of $n = 3^2$ as in Figure 5.8. For a choice of $p = 50$, we have worked on a setting of 50*50 = 2500 patches and have done a simulation of the disease spread model 5.1. The disease is spread across other patches which is incorporated in the model using the residence time budgeting matrix described in 5.20, which exhibits only a movement from each patch to its nearest neighbours. We assume that initially, all the patches are at a state where the infected number of people is zero and the whole population in these patches is susceptible. The only exceptions are the corners of the grid. On these patches the infected number of people is non-zero. With this as the initial condition, the evolution of disease across patches connected using the nearest neighbour residence time budgeting matrix P has been simulated. In this setting, we assume that all the patches have an identical set of parameters and all four corners have identical initial conditions given as in Table 5.2. The people from corner patches are moving to other patches and infecting them. The results are plotted in Figure 5.9. From the solution, we can see that the disease transmission across patches is showing a diffusive behaviour.

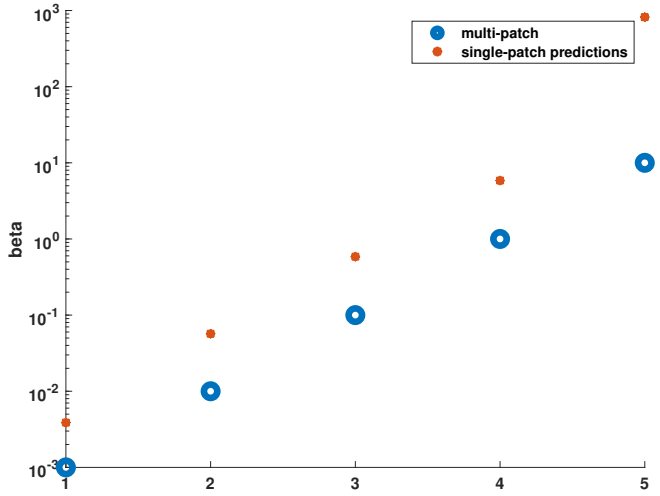

Figure 5.7 – For $\beta = 0.001, 0.01, 0.1, 1, 10$, fitted beta values turned out to be 0.0041, 0.0571, 0.5844, 5.8336, 262.0286. Logarithmic values are plotted here for each case. The x-axis signifies the five different experimental setups with five distinct β values.

μ_i	β_i	α_i	γ_i	ν_i	ϑ_i	N_i	M_i	S_{i_c}	I_{i_c}	V_{i_c}
1/(71*365)	1/7	1/7	1/14	1/10	$5\nu_i$	1000	5000	0.7	0.3	0.1

Table 5.2 – Parameters in each patch

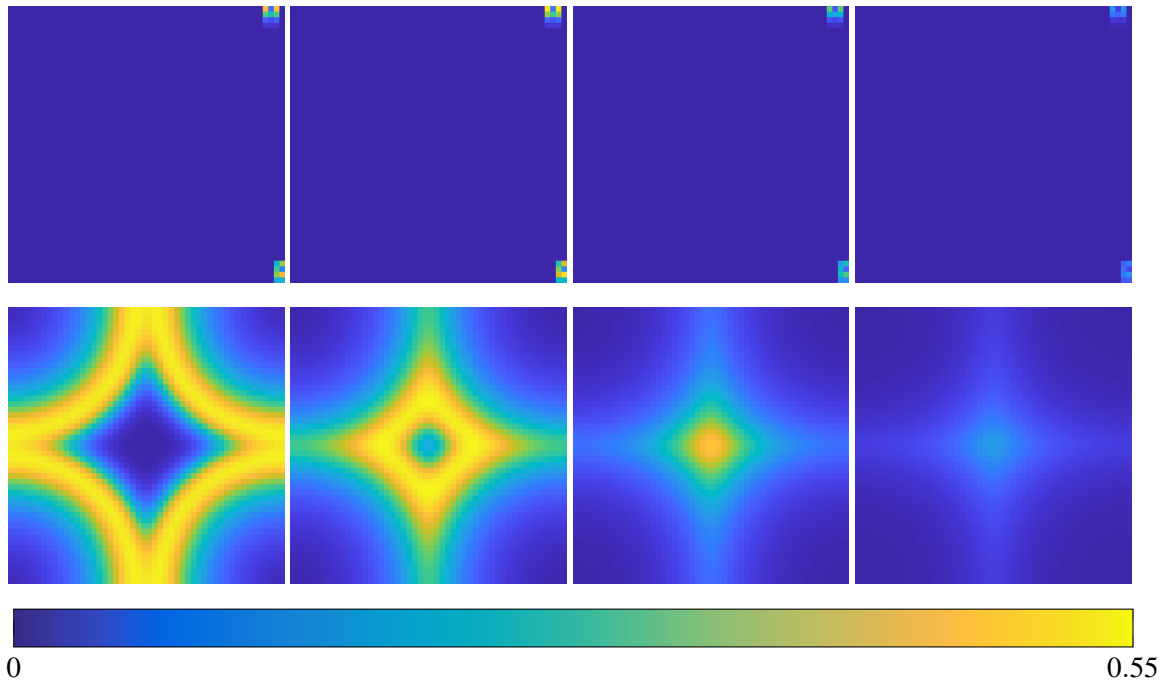

Figure 5.9 – The figure depicts the size of the infected compartment $I_i(t)$ for each patch i at time t, where the colour blue depicts the infected proportion to be zero and yellow represents the scenario when 55 percent of the total population is infected. The simulation is done for a time span of four months with an assumption that the disease outbreak happened initially in the four outer corner patches. The nearest neighbour coupling has resulted in the disease spreading in a diffusive manner from the initially infected corner patches towards the inner ones. The simulation results of the time instances at the end of every two weeks shown in the figure.

An example of non-local disease spread

In this section, we are modelling a scenario in which the commuting happens between patches that are not the nearest neighbours so that the disease is spreading to a patch from another patch that is not its nearest neighbour. This is achieved by constructing a residence time budget matrix that exhibits commuting behaviour between patches that are not geographically close. The P matrix is constructed as follows. We assume three separate geographical entities that are formed by a collection of nearby patches. In this scenario, we refer to these geographical entities as cities and name them city1, city2 and city3. An average person is assumed to be moving from patch any to its nearest neighbours as well and the patches in the cities are connected among each other due to the non-local commuting of hosts between them. The P matrix should also maintain the sum of each row as 1.

We refer to the residence time budget matrix given in 5.20 by P_{loc} and use this in the construction of the new matrix, which we refer to as P_{nonloc}. Let i^1 be a patch which belongs to city1. In a given unit of time, the hosts that are intrinsically belonging to patch i^1, on average spends $k1$ percent of the time in the nearest neighbouring patches. The rest of the $(1-k1)$ percent of the time people spend in the city2. Similarly, $k2$ is the fraction of time spent by people of city2 in its nearest neighbours and $(1-k2)$ percent of the time is spent in city3. Collectively, let i^k denote patches in cityk, the time budgets of an average host in patch i^k is given by,

$$\begin{aligned}
P_{nonloc}(i^1,j) &= k1P_{loc}(i^1,j) + \frac{(1-k1)}{\#city2} && \text{for } j \in \text{city2} \\
P_{nonloc}(i^1,j) &= k1P_{loc}(i^1,j) && \text{for } j \notin \text{city2} \\
P_{nonloc}(i^2,j) &= k2P_{loc}(i^2,j) + \frac{(1-k2)}{\#city3} && \text{for } j \in \text{city3} \\
P_{nonloc}(i^2,j) &= k2P_{loc}(i^2,j) && \text{for } j \notin \text{city3}
\end{aligned} \tag{5.21}$$

where $\#cityk$ shows the number of patches in cityk. For a patch i that does not belong to city 1 and city 2, the entries of the i-th row of the commuting matrix $P_{nonloc}(i,:)$ is the same as that of the nearest neighbour commuting matrix given by, $P_{loc}(i,:)$ which indicates the situation that people from patch i are only moving to its nearest neighbours. It is to be noted that, by the construction of P_{loc}, we have that each row of P_{loc} has row-sum 1. Now the sum of a row corresponding to patches that belong to city 1 in P_{nonloc} is given by

$$\begin{aligned}
\sum_{j=1}^{n} P_{nonloc}(i^1,j) &= k1 \sum_{j\notin city2} P_{loc}(i,j) + \sum_{j\in city2} k1P_{loc}(i^1,j) + \frac{(1-k1)}{\#city2} \\
&= k1\sum_{j} P_{loc}(i,j) + \sum_{j\in city2} \frac{(1-k1)}{\#city2} \\
&= 1
\end{aligned}$$

Similarly, for those patches i^2 in city 2 as well we have that $\sum_{j=1}^{n} P_{nonloc}(i^2,j) = 1$. Collectively, the new commuting matrix does the following,

- People from all patches follow the nearest neighbour commuting as given in example 5.8.

- People from any patch in city 1 spend k1 percent of the unit time in the nearest neighbours and the rest of the time in city 2. Similarly, the hosts in city 2 spend k2 percent of their time in the nearest neighbours and the rest of the time in city 3.

Using this new P matrix we have simulated the scenario of city 1 being affected initially and see how does the commuting hosts take the disease to the second region. For this simulation, we consider the scenario, where the total number of patches is given by $n = p^2$ where $p = 50$. The number of patches of cities is 5^2 each and they are distinct apart so that they both do not share any patches that are nearest neighbours to each city. In principle, the people of city 1 and city 3 are not moving to each other. When a disease outbreak happens in the city1 it is spread to its nearest neighbours as well as to city 2. And later the disease is taken to city3 as the people of patches of city2 are transmitting the disease to the city3. The simulations are done for the set of identical parameters for each patch given in Table 5.3. The initial conditions of the city1 are also given in this table. The simulation results are given in Figure 5.12 for the scenario where $k_1 = 20\%$ and $k_2 = 99\%$, which means people in city 1 spend 80% of their time in city 2 and people in city 2 spend 1% time in city 3.

μ_i	β_i	α_i	γ_i	ν_i	ϑ_i	N_i	M_i	S_{i^1}	I_{i^1}	V_{i^1}
1/(71*365)	0.8/7	0.5/7	1/14	1/10	$5\nu_i$	5000	10000	0.9	0.1	0.1

Table 5.3 – Parameters in each patch

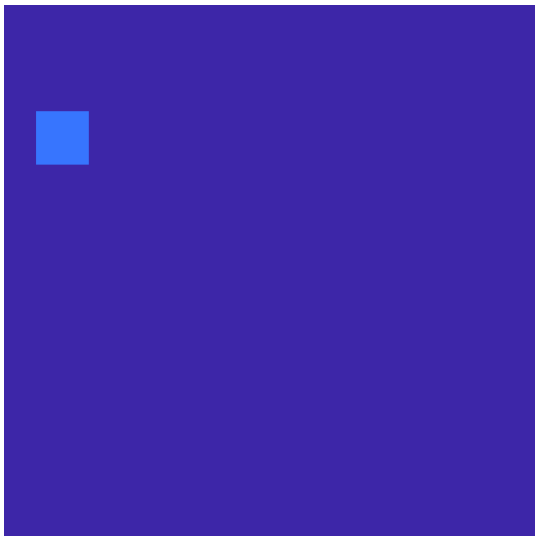

Figure 5.10 – Figure shows the initial condition where there are only infected hosts in city 1

The average number of infected people in all three cities is given in Figure 5.11. It can be seen that city 2 is infected in the first week itself and city 3 is infected in the third week. The infection dynamics in cities 1 and 2 reach its peak in the third week and that of city 3 reaches its peak in the

end of the eighth week.

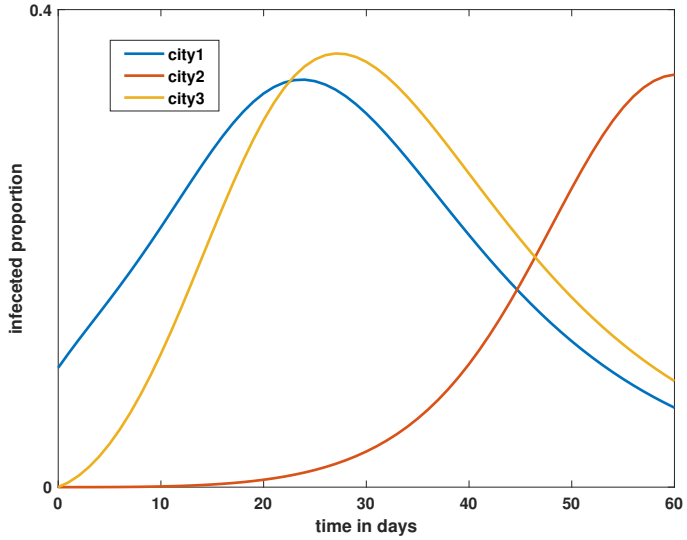

Figure 5.11 – The average proportion of infected hosts in all three cities is plotted for the period of two months. It can be seen that the disease is transmitted to city 3 roughly close to the fourth week.

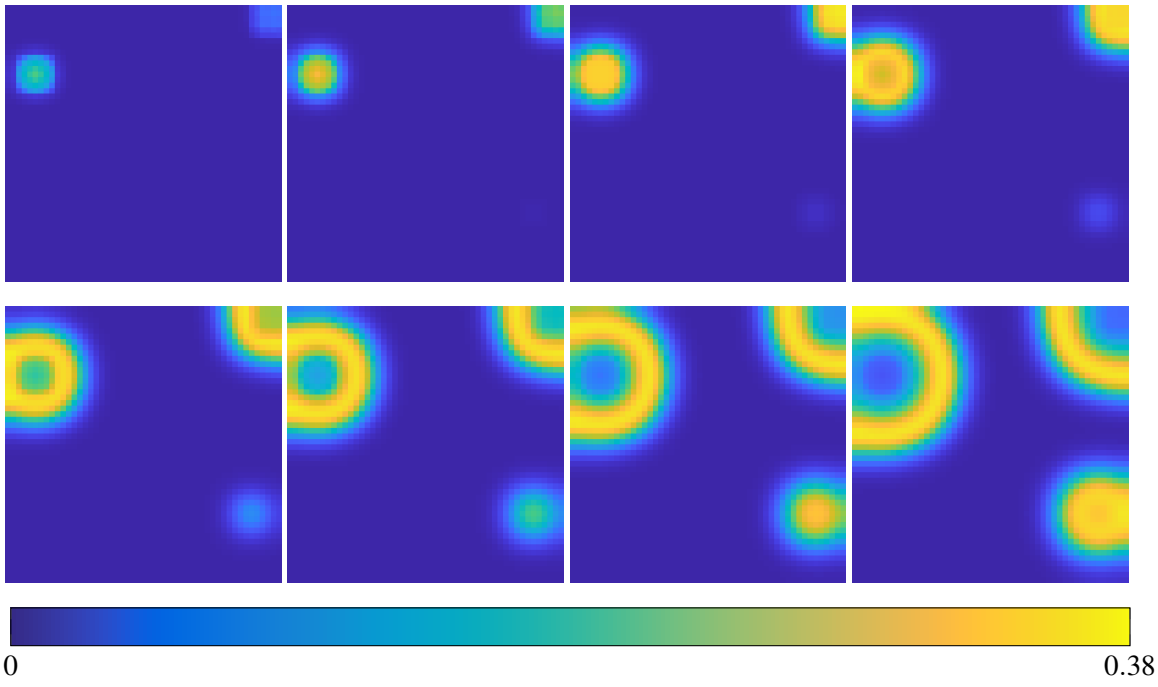

Figure 5.12 – The dynamics of the disease spread across patches is given for every week up to two months. The disease outbreak in city 1 is transmitted to its nearest neighbors as well as to city 2. Slowly the disease is taken from city 2 to city 3 and each city spread the disease to its nearest neighbours in a diffusive manner

6 Developing a PDE Model

In this chapter, we show that the multi-patch model with nearest neighbour-like coupling converges to a system of partial differential equations. The nearest-neighbour coupling defined in the section 5.4.3 is different from the residence time budget matrix that is used in this chapter. Here, we just assume four patches as the nearest neighbours. Firstly, we rewrite the multi-patch ODE model given in 5.1 with double indices. This is done to assign each patch to a Cartesian-coordinate-like system. We are focusing on a two-dimensional space domain and thereby use double indices (i, j) to denote a patch, where $1 \leq i, j \leq n$ and they count to a total of n^2 in number. We use either a subscript or superscript ij to distinguish the compartments, parameters etc. patch-wise. The elements of the residence time budgeting matrix is updated as p_{ij}^{rs}, which gives the rate of commuting from (i, j) to (r, s).

$$
\begin{aligned}
\frac{dS_{ij}}{dt} =& \mu_{ij}(1 - S_{ij}) - S_{ij}\left(\sum_{1\leq r,s\leq n} \alpha_{rs} V_{rs} M_{rs} \frac{p_{ij}^{rs}}{\sum_{1\leq l,q\leq n} p_{lq}^{rs} N_{lq}} + \left(\sum_{1\leq r,s\leq n} \beta_{rs} p_{ij}^{rs} \sum_{1\leq l,q\leq n} \frac{p_{lq}^{rs} N_{lq} I_{lq}}{\sum_{1\leq l,q\leq n} p_{lq}^{rs} N_{lq}}\right)\right) \\
\frac{dI_{ij}}{dt} =& S_{ij}\left(\sum_{1\leq r,s\leq n} \alpha_{rs} V_{rs} M_{rs} \frac{p_{ij}^{rs}}{\sum_{1\leq l,q\leq n} p_{lq}^{rs} N_{lq}} + \left(\sum_{1\leq r,s\leq n} \beta_{rs} p_{ij}^{rs} \sum_{1\leq l,q\leq n} \frac{p_{lq}^{rs} N_{lq} I_{lq}}{\sum_{1\leq l,q\leq n} p_{lq}^{rs} N_{lq}}\right)\right) - (\gamma_{ij} + \mu_{ij}) I_{ij} \\
\frac{dR_{ij}}{dt} =& \gamma_{ij} I_{ij} - \mu_{ij} R_{ij} \\
\frac{dU_{ij}}{dt} =& \nu_{ij}(1 - U_{ij}) - \vartheta_{ij} \frac{U_{ij}}{M_{ij}} \sum_{1\leq r,s\leq n} p_{rs}^{ij} N_{rs} I_{rs} \\
\frac{dV_{ij}}{dt} =& -\nu_{ij} V_{ij} + \vartheta_{ij} \frac{U_{ij}}{M_{ij}} \sum_{1\leq r,s\leq n} p_{rs}^{ij} N_{rs} I_{rs}
\end{aligned}
$$

Now we focus on the specific case where the movement from each patch is either to the nearest neighbours to which horizontal or vertical movement is admissible. Diagonally close neighbours are not considered. The values of p_{ij}^{rs} would look like this,

$$
\begin{aligned}
p_{ij}^{ij} =& \frac{b_{ij}}{n} \\
p_{ij}^{ij\pm 1} =& \frac{1}{b_{ij}} - \frac{1}{n} \\
p_{ij}^{i\pm 1 j} =& \frac{1}{b_{ij}} - \frac{1}{n} \\
p_{ij}^{rs} =& 0 \text{ for } r \in I_0, s \in J_0
\end{aligned}
\tag{6.1}
$$

where b_{ij} is the number of neighbours to which people of patch ij have admissible movement. Also, $I_0 = \{1, 2, \ldots t\} - \{i-1, i, i+1\}$ and $J_0 = \{1, 2, \ldots t\} - \{j-1, j, j+1\}$. In this setting, for internal patches $b_{ij} = 4$ and it varies on the boundary patches (see Figure 6.1) For the chosen P

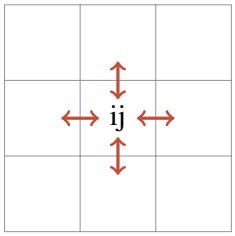

2	3	2
3	4	3
2	3	2

Figure 6.1 – The number of nearest neighbours b_{ij} for each patch ij in the case of $n = 3$ is shown in the second grid. The corners have 2 neighbours, inner patches have 4 neighbours and the other boundary patches have 3 neighbours each

matrix for internal nodes, the first equation of the system can be expanded. For simplicity we define $f_{rs} = \frac{\alpha_{rs} M_{rs} V_{rs}}{N_{eff}^{rs}}$ and $h_{rs} = N_{rs} I_{rs}$ where $N_{eff}^{rs} = \sum_{1 \le l,q \le n} p_{lq}^{rs} N_{lq}$

$$
\begin{aligned}
\frac{dS_{ij}}{dt} =& \mu_{ij}(1 - S_{ij}) - S_{ij}\left((\frac{1}{4} - \frac{1}{n})(f_{ij-1} + f_{ij+1} + f_{i-1j} + f_{i+1j} - f_{ij}) + (\frac{1}{4} - \frac{1}{n}) f_{ij} + \frac{4}{n} f_{ij} \right) \\
& - S_{ij}\Bigg((\frac{1}{4} - \frac{1}{n})(\frac{\beta_{ij-1}}{N_{eff}^{ij-1}}((\frac{1}{4} - \frac{1}{n})(h_{ij-2} + h_{ij} + h_{i-1j-1} + h_{i+1j-1} - h_{ij-1}) + \frac{4}{n} h_{ij-1} + (\frac{1}{4} - \frac{1}{n}) h_{ij-1}) \\
& + \frac{\beta_{ij+1}}{N_{eff}^{ij+1}}((\frac{1}{4} - \frac{1}{n})(h_{ij} + h_{ij+2} + h_{i-1j+1} + h_{i+1j+1} - h_{ij+1}) + \frac{4}{n} h_{ij+1} + (\frac{1}{4} - \frac{1}{n}) h_{ij+1}) \\
& + \frac{\beta_{i-1j}}{N_{eff}^{i-1j}}((\frac{1}{4} - \frac{1}{n})(h_{i-1j-1} + h_{i-1j+1} + h_{i+2j} + h_{ij} - h_{i-1j}) + \frac{4}{n} h_{i-1j} + (\frac{1}{4} - \frac{1}{n}) h_{i-1j}) \\
& + \frac{\beta_{i+1j}}{N_{eff}^{i+1j}}((\frac{1}{4} - \frac{1}{n})(h_{i+1j-1} + h_{i+1j+1} + h_{ij} + h_{i+2j} - h_{i+1j}) + \frac{4}{n} h_{i+1j} + (\frac{1}{4} - \frac{1}{n}) h_{i+1j})) \\
& - \frac{4}{n}\frac{\beta_{ij}}{N_{eff}^{ij}}((\frac{1}{4} - \frac{1}{n})(h_{ij-1} + h_{ij+1} + h_{i-1j} + h_{i+1j} - h_{ij}) + \frac{4}{n} h_{ij} + (\frac{1}{4} - \frac{1}{n}) h_{ij}) \Bigg)
\end{aligned}
\tag{6.2}
$$

Now we rewrite this set of equations by redefining the variables involved to establish a continuous dependence of these equations on the space domain. This is inspired by a similar work where a continuous model(PDE) is derived from a discrete SIR model. A probabilistic equation that connects the current state of the population to a future state is the discrete model used to develop the continuous model in this paper[14]. The probabilistic function involved is varying with respect to time t and the number of susceptible n and infected people(m) in the population. The limiting behaviour of this probabilistic function is studied as the population size tends to infinity and the time step tends to zero. Asymptotically, for large population size a PDE whose characteristics are the classical SIR model is obtained. We define the coordinates of space domain as, $x = \frac{i}{n}$ and $y = \frac{j}{n}$ where n^2 is the total number of patches. Each unknown and parameter involved in 6.2 can be written in the continuous format as follows. Let $U_{ij}(t)$ be an unknown, function or parameter in the

discrete setting. We define $U(t,x,y) = U_{ij}(t)$ So equation 6.2 can be rewritten as follows

$$
\begin{aligned}
\frac{dS_{ij}}{dt} =& \frac{\partial S(t,x,y)}{\partial t} \\
&= \mu(t,x,y)\,(1 - S(t,x,y)) \\
&- S(t,x,y)\Bigg((\frac{1}{4} - \frac{1}{n})(f(t,x,y-\delta) + f(t,x,y+\delta) + f(t,x-\delta,y) + f(t,x+\delta,y) \\
&- f(t,x,y)) + (\frac{1}{4} + \frac{3}{n}) f(t,x,y) \Bigg) \\
&- S(t,x,y)\Bigg((\frac{1}{4} - \frac{1}{n}) \Bigg[\frac{\beta(t,x,y-\delta)}{N_{eff}(t,x,y-\delta)} ((\frac{1}{4} - \frac{1}{n})(h(t,x,y-2\delta) + h(t,x,y) \\
&+ h(t,x-\delta,y-\delta) + h(t,x+\delta,y-\delta) - h(t,x,y-\delta)) + (\frac{1}{4} + \frac{3}{n}) h(t,x,y-\delta)) \\
&+ \frac{\beta(t,x,y+\delta)}{N_{eff}(t,x,y+\delta)} ((\frac{1}{4} - \frac{1}{n})(h(t,x,y) + h(t,x,y+2\delta) + h(t,x-\delta,y+\delta) + h(t,x+\delta,y+\delta) \\
&- h(t,x,y+\delta)) + (\frac{1}{4} + \frac{3}{n}) h(t,x,y+\delta)) \\
&+ \frac{\beta(t,x-\delta,y)}{N_{eff}(t,x-\delta,y)} ((\frac{1}{4} - \frac{1}{n})(h(t,x-\delta,y-\delta) + h(t,x-\delta,y+\delta) + h(t,x+2\delta,y) + h(t,x,y) \\
&- h(t,x-\delta,y)) + (\frac{1}{4} + \frac{3}{n}) h(t,x-\delta,y)) \\
&+ \frac{\beta(t,x+\delta,y)}{N_{eff}(t,x+\delta,y)} ((\frac{1}{4} - \frac{1}{n})(h(t,x+\delta,y-\delta) + h(t,x+\delta,y+\delta) + h(t,x,y) + h(t,x+2\delta,y) \\
&- h(t,x+\delta,y)) + (\frac{1}{4} + \frac{3}{n}) h(t,x+\delta,y)) \Bigg] \\
&- \frac{4}{n} \frac{\beta(t,x,y)}{N_{eff}(t,x,y)} ((\frac{1}{4} - \frac{1}{n})(h(t,x,y-\delta) + h(t,x,y+\delta) + h(t,x-\delta,y) + h(t,x+\delta,y) \\
&- h(t,x,y)) + (\frac{1}{4} + \frac{3}{n}) h(t,x,y)) \Bigg)
\end{aligned}
\tag{6.3}
$$

where $\delta = \frac{1}{n}$.

Remark 6.1 — Taylor expansion in higher dimensions. [Königsberger] Let $U \subset \mathbb{R}^n$ and $f : U \to \mathbb{R}$ be a $\mathcal{C}^{p+1}-$ function. Let us consider points $a, x \in U$ so that the line segment connecting them lies in U, so that

$$f(x) = \sum_{k=0}^{p} \frac{1}{k!} d^{(k)} f(a)(x-a)^k + R_{p+1}(x;a)$$

where the Residual with a given point $\xi \in [a;x]$ can be represented in the form

$$R_{p+1}(x;a) = \frac{1}{(p+1)!} d^{(p+1)} f(\xi)(x-a)^{(p+1)}$$

where

$$d^{(k)}f(a)(x)^k = \sum_{i_1=1}^{n} \cdots \sum_{i_k=1}^{n} \partial_{i_1} \cdots \partial_{i_k} f(a) x_{i_1} \cdots x_{i_k}$$

In 2D we have

$$f(t,x_0+\delta x, y_0+\delta y) = f(t,x_0,y_0) + \frac{\partial f}{\partial x}(x_0,y_0)\delta x + \frac{\partial f}{\partial y}(x_0,y_0)\delta y + \frac{1}{2}\left[\frac{\partial^2 f}{\partial x^2}(x_0,y_0)(\delta x)^2 + 2\frac{\partial^2 f}{\partial x \partial y}(x_0,y_0)\delta x \delta y + \frac{\partial^2 f}{\partial y^2}(x_0,y_0)(\delta y)^2\right] + O(\Delta x^3 + \Delta y^3)$$

Now we make use of Taylor expansion to get all terms in equation 6.3 as a function of t, x and y. For example, let us see how Taylor expansion would simplify a set of functions in the following expression.

$$\begin{aligned}
&\left(\frac{1}{4}-\frac{1}{n}\right)\left[f(t,x,y-\delta)+f(t,x,y+\delta)+f(t,x-\delta,y)+f(t,x+\delta,y)-f(t,x,y)\right]+\left(\frac{1}{4}+\frac{3}{n}\right)f(t,x,y)\\
&=\left(\frac{1}{4}-\frac{1}{n}\right)\left[\left\{f(t,x,y)-\delta\frac{\partial f(t,x,y)}{\partial y}+\frac{\delta^2}{2}\frac{\partial^2 f(t,x,y)}{\partial y^2}\right\}+\left\{f(t,x,y)+\delta\frac{\partial f(t,x,y)}{\partial y}+\frac{\delta^2}{2}\frac{\partial^2 f(t,x,y)}{\partial y^2}\right\}\right.\\
&\quad\left.+\left\{f(t,x,y)-\delta\frac{\partial f(t,x,y)}{\partial x}+\frac{\delta^2}{2}\frac{\partial^2 f(t,x,y)}{\partial x^2}\right\}+\left\{f(t,x,y)+\delta\frac{\partial f(t,x,y)}{\partial x}+\frac{\delta^2}{2}\frac{\partial^2 f(t,x,y)}{\partial x^2}\right\}\right]\\
&\quad+\frac{4}{n}f(t,x,y)\\
&=\left(\frac{1}{4}-\frac{1}{n}\right)\left[\frac{\delta^2}{2}\frac{\partial^2 f(t,x,y)}{\partial y^2}+\frac{\delta^2}{2}\frac{\partial^2 f(t,x,y)}{\partial y^2}+\frac{\delta^2}{2}\frac{\partial^2 f(t,x,y)}{\partial x^2}+\frac{\delta^2}{2}\frac{\partial^2 f(t,x,y)}{\partial x^2}\right]\\
&\quad(f(t,x,y)-\frac{4}{n}f(t,x,y))+\frac{4}{n}f(t,x,y)\\
&=\left(\frac{1}{4}-\frac{1}{n}\right)\left[\delta^2\Delta f(t,x,y)\right]+f(t,x,y)\\
&=f(t,x,y)+\frac{\delta^2}{4}\Delta f(t,x,y)
\end{aligned} \tag{6.4}$$

As $f(t,x,y) = \frac{\alpha(t,x,y)M(t,x,y)V(t,x,y)}{N_{eff}(t,x,y)}$, we focus on the function $\frac{1}{N_{eff}(t,x,y)}$ to see if this can be further simplified. For this let us focus on the effective population in the discrete setting.

$$\begin{aligned}
N_{eff}^{rs} = \sum_{1\le l,q\le n} p_{lq}^{rs} N_{lq} &= \left(\frac{1}{4}-\frac{1}{n}\right)(N_{r-1s}+N_{rs-1}+N_{r+1s}+N_{rs+1})+\frac{4}{n}N_{rs}\\
&= \left(\frac{1}{4}-\frac{1}{n}\right)(N_{r-1s}+N_{rs-1}+N_{r+1s}+N_{rs+1}-4N_{rs})+N_{rs}
\end{aligned}$$

In the continuous setting, this expression becomes

$$\begin{aligned}
N_{eff}(t,x,y) = \left(\frac{1}{4}-\frac{1}{n}\right)&(N(t,x-\delta,y)+N(t,x,y-\delta)+N(t,x+\delta,y)+N(t,x-\delta,y)\\
&-4N(t,x,y))+N(t,x,y)
\end{aligned}$$

Expanding each term using the Taylor series and keeping only terms of order up to δ^2 gives

$$\begin{aligned} N_{eff}(t,x,y) =& \left(\frac{1}{4}-\frac{1}{n}\right)\left[\delta^2(N_{xx}(t,x,y)+N_{yy}(t,x,y))\right]+N(t,x,y) \\ =& N(t,x,y)+\frac{\delta^2}{4}\Delta N(t,x,y) \end{aligned}$$

So we have,

$$\frac{1}{N_{eff}(t,x,y)} = \frac{1}{N(t,x,y)}\left(\frac{1}{1+\delta^2\frac{\Delta N(t,x,y)}{N(t,x,y)}}\right)$$

For n large enough we have,

$$\left|\delta^2\frac{\Delta N(t,x,y)}{N(t,x,y)}\right| \leq 1$$

Using $\frac{1}{1+x} = 1-x+x^2-x^3+\ldots$ and keeping only terms of order up to δ we get

$$\frac{1}{N_{eff}(t,x,y)} = \frac{1}{N(t,x,y)}$$

So for every term involving $\frac{1}{N_{eff}(t,x,y)}$, asymptotically as $n\to\infty$, it behaves like $\frac{1}{N(t,x,y)}$. So the function $f(t,x,y)$ can be defined as

$$f(t,x,y) = \frac{\alpha(t,x,y)M(t,x,y)V(t,x,y)}{N(t,x,y)}.$$

The same method as in equation 6.4 can be used to simplify the terms involving the function h at different points in the stencil. At the point (x,y) this will be given by the expression $\left(\frac{\delta^2}{4}\right)[\Delta h(t,x,y)]+h(t,x,y)$ Thereby equation 6.3, will be simplified as follows.

$$\begin{aligned} \frac{\partial S(t,x,y)}{\partial t} =& \mu(t,x,y)\,(1-S(t,x,y)) - S(t,x,y)\left(f(t,x,y)+\frac{\delta^2}{4}\Delta f(t,x,y)\right) \\ & - S(t,x,y)\left((\frac{1}{4}-\frac{1}{n})\left[\frac{\beta(t,x,y-\delta)}{N_{eff}(t,x,y-\delta)}(\left(\frac{\delta^2}{4}\right)[\Delta h(t,x,y-\delta)]+h(t,x,y-\delta)\right)\right. \\ & + \frac{\beta(t,x,y+\delta)}{N_{eff}(t,x,y+\delta)}(\left(\frac{\delta^2}{4}\right)[\Delta h(t,x,y+\delta)]+h(t,x,y+\delta)) \\ & + \frac{\beta(t,x-\delta,y)}{N_{eff}(t,x-\delta,y)}(\left(\frac{\delta^2}{4}\right)[\Delta h(t,x-\delta,y)]+h(t,x-\delta,y)) \\ & + \frac{\beta(t,x+\delta,y)}{N_{eff}(t,x+\delta,y)}(\left(\frac{\delta^2}{4}\right)[\Delta h(t,x+\delta,y)]+h(t,x+\delta,y)) \\ & \left. + \frac{4}{n}\frac{\beta(t,x,y)}{N_{eff}(t,x,y)}(\left(\frac{1}{4}-\frac{1}{n}\right)\left[\delta^2\Delta h(t,x,y)\right]+h(t,x,y))\right] \end{aligned} \tag{6.5}$$

For simplification let us define

$$k(t,x,y) = \frac{\beta(t,x,y)}{N_{eff}(t,,x,y)}\Delta h(t,x,y) \qquad g(t,x,y) = \frac{\beta(t,x,y)}{N_{eff}(t,,x,y)}h(t,x,y)$$

Now 6.5 simplifies to

$$\begin{aligned}\frac{\partial S(t,x,y)}{\partial t} =&\mu(t,x,y)\,(1-S(t,x,y))-S(t,x,y)\left(f(t,x,y)+\frac{\delta^2}{4}\Delta f(t,x,y)\right)\\ &-S(t,x,y)\left(\frac{1}{4}-\frac{1}{n}\right)\delta^2\Bigg(\left(\frac{1}{4}-\frac{1}{n}\right)(k(t,x,y-\delta)+k(t,x,y+\delta)+k(t,x-\delta,y)\\ &+k(t,x+\delta,y))+\frac{4}{n}k(t,x,y)\Bigg)\\ &-S(t,x,y)\Bigg(\left(\frac{1}{4}-\frac{1}{n}\right)(g(t,x,y-\delta)+g(t,x,y+\delta)+g(t,x-\delta,y)+g(t,x+\delta,y))\\ &+\frac{4}{n}g(t,x,y)\Bigg)\end{aligned} \tag{6.6}$$

Using the same method as in 6.4

$$\begin{aligned}\frac{\partial S(t,x,y)}{\partial t} =&\mu(t,x,y)\,(1-S(t,x,y))-S(t,x,y)\left(f(t,x,y)+\frac{1}{4}\Delta\tilde{f}(t,x,y)\right)\\ &-S(t,x,y)\left(\frac{1}{4}-\frac{1}{n}\right)\delta^2\left(\left(\frac{1}{4}-\frac{1}{n}\right)\left[\delta^2\Delta k(t,x,y)\right]+k(t,x,y)\right)\\ &-S(t,x,y)\left(\left(\frac{1}{4}-\frac{1}{n}\right)\left[\delta^2\Delta g(t,x,y)\right]+g(t,x,y)\right)\\ =&\mu(t,x,y)\,(1-S(t,x,y))-S(t,x,y)f(t,x,y)\\ &-S(t,x,y)\left(\frac{\delta^2}{4}(\frac{\delta^2}{4}\Delta k(t,x,y)+k(t,x,y))\right)\\ &-S(t,x,y)\left(g(t,x,y)+\frac{\delta^2}{4}\Delta g(t,x,y)\right)\end{aligned} \tag{6.7}$$

Neglecting all terms that have δ or its powers in 6.7 we get,

$$\frac{\partial S(t,x,y)}{\partial t} =\mu(t,x,y)\,(1-S(t,x,y))-S(t,x,y)\,(f(t,x,y)+g(t,x,y))) \tag{6.8}$$

In a similar way, we find out the corresponding partial differential equations for the functions I,R,U and V respectively. Asymptotically assuming that all higher-order terms in the Taylor expansion are infinitesimal we deduce the following system of equations for $n\to\infty$

$$\begin{aligned}\frac{\partial S}{\partial t} &= \mu(1-S)-S(f+g)\\ \frac{\partial I}{\partial t} &= -(\gamma+\mu)I+S(f+g)\\ \frac{\partial R}{\partial t} &= (\gamma+\mu)I\\ \frac{\partial U}{\partial t} &= \nu(1-U)-\frac{\vartheta U}{M}h\\ \frac{\partial V}{\partial t} &= -\nu V+\frac{\vartheta U}{M}h\end{aligned}$$

where

$$f(t,x,y) = \frac{\alpha(t,x,y)M(t,x,y)V(t,x,y)}{N(t,x,y)} \qquad g(t,x,y) = \frac{\beta(t,x,y)}{N(t,x,y)}h(t,x,y), \qquad h(t,x,y) = N(t,x,y)I(t,x,y)$$

7 Conclusion

The main objective of this research work is to formulate models that simulate the spread of diseases that are transmitted directly among humans as well as through mosquitoes. In Chapter 3, a model that has human and mosquito populations is presented, which is a combination of the *SIRUV* model for normal vector-borne diseases like Dengue and the classical *SIR* model. Further, this model was mathematically analyzed. In general compartmental disease models, a threshold value called basic reproduction number is crucial and there are two methods to find an expression of this threshold value. A unique property of our model is that the mathematical expressions of the reproduction numbers that are obtained using these two methods were not identical or did not have an obvious relationship. However, it is proven that the sharp threshold property for the model can be equivalently described using these two reproduction numbers. The global stability of the two equilibrium points of the model is proven by constructing the Lyapunov functions using the matrix-theoretic and graph-theoretic methods available in the literature. Later numerical simulations were seen to be in agreement with the mathematical results. In Chapter 4, a model with a different definition of parameters was formulated, which explicitly incorporated the terms that directly exhibited the ratio of population sizes of humans and mosquitoes. The mathematical expressions for the reproduction numbers, Lyapunov function for the disease-free equilibria and characteristic polynomial of the Jacobian matrix etc were structurally same for the both models whereas the major difference was with the endemic equilibria, which was shown later in the numerical simulations. A comparative numerical study showed the difference between both models for simulations done with the same initial conditions. It is seen that the second model exhibits the variation in the ratio of population sizes of humans and mosquitoes evidently. In Chapter 5, we extended the second model given in Chapter 4, to a multi-patch model to incorporate the spatial dependence of the disease dynamics. In this model, we have used a meta-population modelling approach by dividing the region under consideration into mutually exclusive spatial units called patches. The host and mosquito population under consideration is divided into different compartments depending upon the stage of disease they are in as well as the patches they belong to. Thereby each patch has an intrinsic population of humans and mosquitoes and the model describes the disease spread within and among the patches due to the commuting behavior of humans. The short-term or Lagrangian movement of hosts between these patches is incorporated using the residence-time budgeting matrix. In this study, we have obtained simplified expressions for finding the endemic equilibrium and reproduction number(using next generation matrix approach) for an n-patch scenario. In the numerical simulations, a 2-patch example is given where we can see that the sharp threshold property is holding for the multi-patch model as well. That is when the reproduction number is less

than 1, the disease dies out and if it is greater than 1, the disease becomes endemic. But unlike in the single-patch cases as in Chapters 3 and 4, an explicit mathematical expression for the endemic equilibrium and reproduction number is not derived. However, a simplified method combining the mathematical and numerical toolbox of MATLAB can be used to find the endemic equilibrium and reproduction number for specific cases. This is also shown in the numerical example. Later, using the multi-patch model, we demonstrated the importance of using the meta-population model instead of the single-patch model. In the example cases using different residence-time-budgeting matrices, we have shown the variation in infection rate from the single-patch scenario using the data-fitting method which used the optimization toolbox of MATLAB. We have also presented two examples where the multi-patch model shows the diffusive behaviour of disease spread when a local and non-local residence time budget matrix is respectively used. In Chapter 6, we have derived a system of partial differential equations from the multi-patch model for a given residence-time budgeting matrix.

Bibliography

[1] M. Ali, S. T. H. Shah, M. Imran, **and** A. Khan. *The role of asymptomatic class, quarantine and isolation in the transmission of COVID-19*. *Journal of Biological Dynamics*, 14: 389–408, 2020. DOI: 10.1080/17513758.2020.1773000 (see p. 2)

[2] L. J. Allen. *A primer on stochastic epidemic models: Formulation, numerical simulation, and analysis*. *Infectious Disease Modelling*, 2: 128–142, 2017. DOI: 10.1016/j.idm.2017.03.001 (see p. 3)

[3] R. M. Anderson. *Discussion: the Kermack-McKendrick epidemic threshold theorem*. *Bulletin of mathematical biology*, 53: 1–32, 1991. (see p. 12)

[4] R. M. Anderson **and** R. M. May. *Infectious diseases of humans: dynamics and control*. Oxford university press, 1992. (see p. 3)

[5] J. Arino, J. R. Davis, D. Hartley, R. Jordan, J. M. Miller, **and** P Van Den Driessche. *A multi-species epidemic model with spatial dynamics*. *Mathematical Medicine and Biology*, 22: 129–142, 2005. (see p. 50)

[6] M. Aronna, R. Guglielmi, **and** L. Moschen. *A model for COVID-19 with isolation, quarantine and testing as control measures*. *Epidemics*, 34: 100437, 2021. DOI: 10.1016/j.epidem.2021.100437 (see p. 2)

[7] J. Beattie, S. Parajuli, M. Sanger, G. Lee, P. Pleninger, G. Crowley, S. Kwon, V. Murthy, J. A. Manko, A. Caplan, E. Dufort, D. M. Pastula, **and** A. Nolan. *Zika Virus–Associated Guillain-Barré Syndrome in a Returning US Traveler*. *Infectious Diseases in Clinical Practice*, 26: e80–e84, 2018. DOI: 10.1097/ipc.0000000000000654 (see p. 1)

[8] M Besnard, S Lastère, A Teissier, V. M. Cao-Lormeau, **and** D Musso. *Evidence of perinatal transmission of Zika virus, French Polynesia, December 2013 and February 2014*. *Eurosurveillance*, 19: 2014. DOI: 10.2807/1560-7917.es2014.19.13.20751 (see p. 1)

[9] D. Bichara **and** C. Castillo-Chavez. *Vector-borne diseases models with residence times – A Lagrangian perspective*. *Mathematical Biosciences*, 281: 128–138, 2016. DOI: https://doi.org/10.1016/j.mbs.2016.09.006 (see p. 50)

[10] D. Bichara **and** A. Iggidr. *Multi-patch and multi-group epidemic models: a new framework*. *Journal of Mathematical Biology*, 77: 107–134, 2018. (see p. 50)

[11] D. Bichara, Y. Kang, C. Castillo-Chavez, R. Horan, **and** C. Perrings. *SIS and SIR Epidemic Models Under Virtual Dispersal*. *Bulletin of Mathematical Biology*, 77: 2004–2034, 2015. DOI: 10.1007/s11538-015-0113-5 (see p. 50)

[12] W. Bock **and** Y. Jayathunga. *Optimal control and basic reproduction numbers for a compartmental spatial multipatch dengue model*. *Mathematical Methods in the Applied Sciences*, 41: 3231–3245, 2018. (see p. 50)

[13] A. F. de Brito, I. P. Ribeiro, R. M. de Miranda, R. S. Fernandes, S. S. Campos, K. A. B. da Silva, M. G. de Castro, M. C. Bonaldo, P. Brasil, **and** R. L. de Oliveira. *First detection of natural infection of Aedes aegypti with Zika virus in Brazil and throughout South America*. *Memórias do Instituto Oswaldo Cruz*, 111: 655–658, 2016. DOI: 10.1590/0074-02760160332 (see p. 1)

[14] F. A. Chalub **and** M. O. Souza. *The SIR epidemic model from a PDE point of view*. *Mathematical and Computer Modelling*, 53: Mathematical Methods and Modelling of Biophysical Phenomena, 1568 –1574, 2011. DOI: https://doi.org/10.1016/j.mcm.2010.05.036 (see p. 68)

[15] C. Cosner, J. Beier, R. Cantrell, D. Impoinvil, L. Kapitanski, M. Potts, A. Troyo, **and** S. Ruan. *The effects of human movement on the persistence of vector-borne diseases*. *Journal of Theoretical Biology*, 258: 550–560, 2009. DOI: 10.1016/j.jtbi.2009.02.016 (see pp. 3, 50)

[16] G. Dick. *Zika virus (II). Pathogenicity and physical properties*. *Transactions of the Royal Society of Tropical Medicine and Hygiene*, 46: 521–534, 1952. DOI: https://doi.org/10.1016/0035-9203(52)90043-6 (see p. 1)

[17] G. Dick, S. Kitchen, **and** A. Haddow. *Zika Virus (I). Isolations and serological specificity*. *Transactions of the Royal Society of Tropical Medicine and Hygiene*, 46: 509–520, 1952. DOI: https://doi.org/10.1016/0035-9203(52)90042-4 (see p. 1)

[18] J. Dormand **and** P. Prince. *A family of embedded Runge-Kutta formulae*. *Journal of Computational and Applied Mathematics*, 6: 19–26, 1980. DOI: 10.1016/0771-050x(80)90013-3 (see p. 11)

[19] P Van den Driessche. *Spatial structure: patch models*. **in**: *Mathematical epidemiology*. Springer, 2008. 179–189 (see p. 50)

[20] P Van den Driessche **and** J. Watmough. *Further notes on the basic reproduction number*. *Mathematical epidemiology*, 159–178, 2008. (see pp. 9, 23, 24, 32, 40)

[21] P van den Driessche **and** J. Watmough. *Reproduction numbers and sub-threshold endemic equilibria for compartmental models of disease transmission*. *Mathematical biosciences*, 180: 29–48, 2002. DOI: 10.1016/s0025-5564(02)00108-6 (see pp. 9, 23, 24, 40, 54)

[22] M. R. Duffy, T.-H. Chen, W. T. Hancock, A. M. Powers, J. L. Kool, R. S. Lanciotti, M. Pretrick, M. Marfel, S. Holzbauer, C. Dubray, L. Guillaumot, A. Griggs, M. Bel, A. J. Lambert, J. Laven, O. Kosoy, A. Panella, B. J. Biggerstaff, M. Fischer, **and** E. B. Hayes. *Zika Virus Outbreak on Yap Island, Federated States of Micronesia*. *New England Journal of Medicine*, 360: 2536–2543, 2009. DOI: 10.1056/nejmoa0805715 (see p. 1)

[23] O. Faye, O. Faye, D. Diallo, M. Diallo, M. Weidmann, **and** A. A. Sall. *Quantitative real-time PCR detection of Zika virus and evaluation with field-caught Mosquitoes*. *Virology Journal*, 10: 311, 2013. DOI: 10.1186/1743-422X-10-311 (see p. 1)

[24] M. Fošnarič, T. Kamenšek, J. Ž. Gros, **and** J. Žibert. *Extended compartmental model for modeling COVID-19 epidemic in Slovenia*. *Scientific Reports*, 12: 2022. DOI: 10.1038/s41598-022-21612-7 (see p. 2)

[25] B. D. Foy, K. C. Kobylinski, J. L. C. Foy, B. J. Blitvich, A. T. da Rosa, A. D. Haddow, R. S. Lanciotti, **and** R. B. Tesh. *Probable Non–Vector-borne Transmission of Zika Virus, Colorado, USA*. *Emerging Infectious Diseases*, 17: 880–882, 2011. DOI: 10.3201/eid1705.101939 (see p. 1)

[26] P. Girardi **and** C. Gaetan. *An SEIR Model with Time-Varying Coefficients for Analyzing the SARS-CoV-2 Epidemic*. *Risk Analysis*, 2021. DOI: 10.1111/risa.13858 (see p. 3)

[27] V. Grimm, F. Mengel, **and** M. Schmidt. *Extensions of the SEIR model for the analysis of tailored social distancing and tracing approaches to cope with COVID-19*. *Scientific Reports*, 11: 2021. DOI: 10.1038/s41598-021-83540-2 (see p. 2)

[28] P. Heidrich, Y. Jayathunga, W. Bock, **and** T. Götz. *Prediction of dengue cases based on human mobility and seasonality—An example for the city of Jakarta*. *Mathematical Methods in the Applied Sciences*, n/a: 2021. (see p. 50)

[29] H. W. Hethcote. *The mathematics of infectious diseases*. *SIAM review*, 42: 599–653, 2000. (see pp. 12, 13, 22, 24)

[30] H. W. Hethcote **and** J. W. Van Ark. *Epidemiological models for heterogeneous populations: proportionate mixing, parameter estimation, and immunization programs*. *Mathematical Biosciences*, 84: 85–118, 1987. (see p. 50)

[31] M. W. Hirsch, S. Smale, **and** R. L. Devaney. *Differential equations, dynamical systems, and an introduction to chaos*. Academic press, 2012. (see pp. 7, 8, 20, 32, 39)

[32] N. A. Honório, W. da Costa Silva, P. J. Leite, J. M. Gonçalves, L. P. Lounibos, **and** R. L. de Oliveira. *Dispersal of Aedes aegypti and Aedes albopictus (Diptera: Culicidae) in an urban endemic dengue area in the State of Rio de Janeiro, Brazil*. *Memórias do Instituto Oswaldo Cruz*, 98: 191–198, 2003. DOI: 10.1590/s0074-02762003000200005 (see p. 4)

[33] INSTITUTO BRASILEIRO DE GEOGRAFIA E ESTATÍSTICA *Population size* data retrieved from Instituto Brasileiro de Geografia e Estatística, https://ftp.ibge.gov.br/Estimativas_de_Populacao/Estimativas_2015/serie_2001_2015_TCU.pdf 2015 (see p. 47)

[34] S. IOOS, H.-P. MALLET, I. LEPARC GOFFART, V. GAUTHIER, T. CARDOSO, **and** M. HERIDA. *Current Zika virus epidemiology and recent epidemics*. *Médecine et Maladies Infectieuses*, 44: 302–307, 2014. DOI: https://doi.org/10.1016/j.medmal.2014.04.008 (see p. 1)

[35] Y. JAYATHUNGA. *Mult-patch Dengue Models*. Ph.D. Thesis, Technische Üniversität Kaiserslautern, 2019. (see pp. 3, 33, 34, 43)

[36] W. O. KERMACK **and** A. G. MCKENDRICK. *A contribution to the mathematical theory of epidemics*. *Proceedings of the royal society of london. Series A, Containing papers of a mathematical and physical character*, 115: 700–721, 1927. (see p. 12)

[37] J. P. LA SALLE. *The stability of dynamical systems*. SIAM, 1976. (see p. 29)

[38] M. L. LANDRY **and** K. ST. GEORGE. *Laboratory diagnosis of Zika virus infection*. *Archives of pathology & laboratory medicine*, 141: 60–67, 2017. (see p. 1)

[39] S. LEE **and** C. CASTILLO-CHAVEZ. *The role of residence times in two-patch dengue transmission dynamics and optimal strategies*. *Journal of Theoretical Biology*, 374: 152–164, 2015. DOI: https://doi.org/10.1016/j.jtbi.2015.03.005 (see p. 50)

[40] R. LOWE, C. BARCELLOS, P. BRASIL, O. CRUZ, N. HONÓRIO, H. KUPER, **and** M. CARVALHO. *The Zika Virus Epidemic in Brazil: From Discovery to Future Implications*. *International Journal of Environmental Research and Public Health*, 15: 96, 2018. DOI: 10.3390/ijerph15010096 (see p. 1)

[41] M. MARTCHEVA. *An introduction to mathematical epidemiology*. **volume** 61 Springer, 2015. (see pp. 21, 23, 25)

[42] J. MLAKAR, M. KORVA, N. TUL, M. POPOVIĆ, M. POLJŠAK-PRIJATELJ, J. MRAZ, M. KOLENC, K. R. RUS, T. V. VIPOTNIK, V. F. VODUŠEK, A. VIZJAK, J. PIŽEM, M. PETROVEC, **and** T. A. ŽUPANC. *Zika Virus Associated with Microcephaly*. *New England Journal of Medicine*, 374: 951–958, 2016. DOI: 10.1056/nejmoa1600651 (see p. 1)

[43] D. MUSSO, C. ROCHE, E. ROBIN, T. NHAN, A. TEISSIER, **and** V.-M. CAO-LORMEAU. *Potential Sexual Transmission of Zika Virus*. *Emerging Infectious Diseases*, 21: 359–361, 2015. DOI: 10.3201/eid2102.141363 (see p. 1)

[44] V. RAM **and** L. P. SCHAPOSNIK. *A modified age-structured SIR model for COVID-19 type viruses*. *Scientific Reports*, 11: 2021. DOI: 10.1038/s41598-021-94609-3 (see p. 3)

[45] F. ROCHA, L. MATEUS, U. SKWARA, M. AGUIAR, **and** N. STOLLENWERK. *Understanding dengue fever dynamics: a study of seasonality in vector-borne disease models*. *International Journal of Computer Mathematics*, 93: 1405–1422, 2016. DOI: 10.1080/00207160.2015.1050961 eprint: https://doi.org/10.1080/00207160.2015.1050961 (see pp. 3, 14, 32)

[46] A. SHERLY **and** W. BOCK. *Multipatch ZIKV Model and Simulations*. **in**: *Mathematics in Industry*. Springer International Publishing, 2022. 433–438 DOI: 10.1007/978-3-031-11818-0_56

[47] Z. SHUAI **and** P. VAN DEN DRIESSCHE. *Global Stability of Infectious Disease Models Using Lyapunov Functions*. *SIAM Journal on Applied Mathematics*, 73: 1513–1532, 2013. DOI: 10.1137/120876642 (see pp. 27, 29, 31, 41, 42, 54)

[48] C. I. SIETTOS **and** L. RUSSO. *Mathematical modeling of infectious disease dynamics*. *Virulence*, 4: PMID: 23552814, 295–306, 2013. DOI: 10.4161/viru.24041 eprint: https://doi.org/10.4161/viru.24041 (see p. 2)

[49] D. L. SMITH, K. E. BATTLE, S. I. HAY, C. M. BARKER, T. W. SCOTT, **and** F. E. MCKENZIE. *Ross, Macdonald, and a Theory for the Dynamics and Control of Mosquito-Transmitted Pathogens*. *PLoS Pathogens*, 8: e1002588, 2012. DOI: 10.1371/journal.ppat.1002588 (see p. 3)

[50] S. H. STROGATZ. *Nonlinear dynamics and chaos: with applications to physics, biology, chemistry, and engineering*. CRC press, 2018. (see p. 20)

[51] THE WORLD BANK *Life expectancy* data retrieved from World Development Indicators, https://data.worldbank.org/indicator/SP.DYN.LE00.FE.IN?end=2016&locations=BR&start=1960 2016 (see p. 47)

[52] S. J. THOMAS, T. P. ENDY, A. L. ROTHMAN, **and** A. D. BARRETT. *155 - Flaviviruses (Dengue, Yellow Fever, Japanese Encephalitis, West Nile Encephalitis, St. Louis Encephalitis, Tick-Borne Encephalitis, Kyasanur Forest Disease, Alkhurma Hemorrhagic Fever, Zika)*. **in**: *Mandell, Douglas, and Bennett's Principles and Practice of Infectious Diseases (Eighth Edition)* **byeditor**J. E. BENNETT, R. DOLIN, **and** M. J. BLASER. Eighth Edition Philadelphia: W.B. Saunders, 2015. 1881–1903.e6 DOI: https://doi.org/10.1016/B978-1-4557-4801-3.00155-7 (see p. 1)

[53] T. M. WATSON, A. SAUL, **and** B. H. KAY. *Aedes notoscriptus(Diptera: Culicidae) Survival and Dispersal Estimated by Mark-Release-Recapture in Brisbane, Queensland, Australia*. *Journal of Medical Entomology*, 37: 380–384, 2000. DOI: 10.1093/jmedent/37.3.380 (see p. 4)

[54] WHO *Zika Virus-Key Facts* https://www.who.int/news-room/fact-sheets/detail/zika-virus [Online; accessed 14. December. 2022] 2022 (see p. 48)

[55] S. WIGGINS. *Introduction to applied nonlinear dynamical systems and chaos*. English **volume** 2 Texts Appl. Math. New York etc.: Springer-Verlag, 1990. (see pp. 9, 32)

Akademischer Lebenslauf

2022 Wissenschaftlicher Mitarbeiterin am Fraunhofer ITWM, Kaiserslautern

2018 Beginn des Doktorats in Mathematik Technische Universität Kaiserslautern unter Prof. Dr. Axel Klar.

2018 M.Sc. Mathematics International, Fachbereich Mathematik, Technische Universität Kaiserslautern.
Thesis: A Nonlinear Multi-lane Traffic Flow Model.

2016 M.Sc. Mathematik, National Institute of Technology Calicut, Indien.
Thesis: Multigrid approach for the human tear film equations

2014 B.Sc. Mathematik, University of Kerala, Indien.

Academic curriculum vitae

2022 Scientific employee at Fraunhofer ITWM, Kaiserslautern.

2018 Acceptance as PhD student at the Department of Mathematics, Technische Universität Kaiserslautern under Prof. Dr. Axel Klar.

2018 M.Sc. Mathematics International, Department of Mathematics, Technische Universität Kaiserslautern.
Thesis: A Nonlinear Multi-lane Traffic Flow Model.

2016 M.Sc. Mathematics, National Institute of Technology Calicut, India.
Thesis: Multigrid approach for the human tear film equations

2014 B.Sc. Mathematics, University of Kerala, India.